

**EXPERIMENTAL INVESTIGATION ON PREDICTION  
OF PHYSICO-MECHANICAL PROPERTIES OF  
SEDIMENTARY ROCKS USING MECHANICAL  
PARAMETERS OBTAINED DURING ROTARY  
DRILLING**

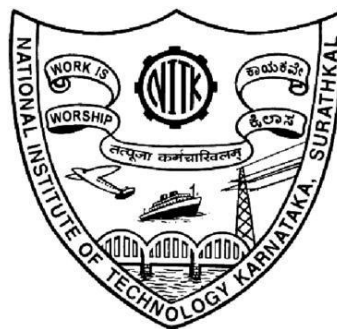
Thesis

Submitted in partial fulfillment of the requirements for the degree of

DOCTOR OF PHILOSOPHY

by

LAKSHMINARAYANA C.R.



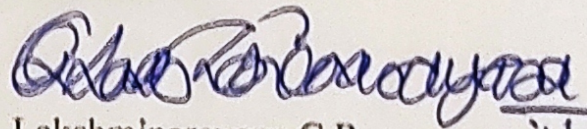
DEPARTMENT OF MINING ENGINEERING  
NATIONAL INSTITUTE OF TECHNOLOGY KARNATAKA,  
SURATHKAL, MANGALORE-575025

November, 2021

## DECLARATION

*by the Ph.D. Research Scholar*

I hereby declare that the Research Thesis entitled "**Experimental investigation of prediction of physico-mechanical properties of sedimentary rocks using mechanical parameters obtained during rotary drilling**", which is being submitted to the National Institute of Technology Karnataka, Surathkal in partial fulfillment of the requirements for the award of the Degree of Doctor of Philosophy in the Department of **Mining Engineering** is a *bonafide report of the research work carried out by me*. The material contained in this Research Thesis has not been submitted to any University or Institution for the award of any degree.



Lakshminarayana C.R.

Reg.No: 158006MN15F08

Department of Mining Engineering

Place: NITK, Surathkal

Date: 03/11/21

## CERTIFICATE

This is to certify that the Research Thesis entitled “**Experimental Investigation on Prediction of Physico-Mechanical Properties of Rocks Using Mechanical Parameters Obtained During Rotary Drilling**”, submitted by **Mr. Lakshminarayana C.R. (Register Number: 158006MN15F08)** as the record of the research work carried out by him, is *accepted as the Research Thesis submission* in partial fulfillment of the requirements for the award of the degree of Doctor of Philosophy.

Research Guide(s)

Anup Kumar Tripathi 03/11/2021

**Dr. Anup Kumar Tripathi**

Research Guide(s)

Department of Mining Engineering

03/11/2021

**Dr. M. Aruna**

Chairman -DRPC

Department of Mining Engineering

**Chairman - DRPC**

Department of Mining Engineering

National Institute of Technology Karnataka, Surathkal.

P.O. Srinivasnagar-575 025, Mangalore.

Karnataka State, India.

*Dedicated to my Beloved Family*

## ACKNOWLEDGEMENTS

At the outset, I would like to express my appreciation to my supervisor **Dr. Anup Kumar Tripathi**, Assistant Professor, Department of Mining Engineering, N.I.T.K., Surathkal, for his excellent guidance and moral support throughout the research work. His constant encouragement, help and review of the entire work during the investigation are invaluable.

Further, I am thankful to **Dr. Samir Kumar Pal**, Professor and Head of the Department, Department of Mining Engineering, IIT, Kharagpur, for his valuable guidance and support throughout the research work.

I wish to thank all the research program assessment committee members, including **Dr. Govindaraj M.**, Professor, Department of Mining Engineering, N.I.T.K., Surathkal, and **Dr. Kumar G.N.**, Associate Professor, Department of Mechanical Engineering, N.I.T.K., Surathkal, for their valuable guidance, unbiased appreciation, and criticism all through this research work.

I am thankful to **Dr. M. Aruna**, Associate professor and Head of the Department of Mining Engineering, N.I.T.K., Surathkal, for encouraging me constantly to accelerate my research work, and often provided the valuable suggestions.

I am thankful to **Dr. K. Ram Chandar**, Associate professor and then Head of the Department of Mining Engineering, N.I.T.K., Surathkal, for extending the departmental facilities, which ensured the satisfactory progress of my research work.

I would like to thank all the Teaching and Non-teaching staff members of the Department of Mining Engineering, NITK, Surathkal, for their continuous help and support throughout the research work.

Finally, I would like to offer a special note of appreciation to my parents, my wife and my son and my little daughter for all the sacrifices and compromises they have made during the tenure of my Ph.D. work.

**Lakshminarayana C.R.**

# ***ABSTRACT***

## **ABSTRACT**

The strength properties of rocks are frequently required during the introductory phase of rock engineering projects, including rock excavation, tunneling, designing of supports at underground mines, blast hole designs, etc. For the determination of rock strength properties like uniaxial compressive strength, tensile strength etc., at the laboratory, several rock core samples with high-grade quality is the prerequisites. Coring is an expensive process, and it is not always possible, particularly for weak and highly fractured, thinly bedded, foliated, and block-in-matrix rock mass. In addition, converting the core samples into test specimens as per the established standard is a tedious and time-consuming process. With all these constraints and problems, many times, the determination of strength or other rock properties may not be feasible in the direct method. Therefore, the subject of the indirect method used for approximation of rock properties has a wide scope.

The main aim of this research study is to estimate the physico-mechanical properties of rock using the selected mechanical parameters obtained during the rotary-type rock drilling. In several rock engineering projects, either in construction or mining environments, rotary drilling operation is often widely used. If an estimation of some vital rock properties is possible during the rock drilling process, it may be a great advantage for engineers and geologists.

In this experimental investigation, during the drilling of several rock blocks with different physico-mechanical properties, the mechanical drilling responses, such as thrust and torque at the bit-rock interface, are collected considering various drill operating parameters using a drill tool dynamometer. Similarly, at the same time, an acoustic parameter such as vibration data is also collected at the drill head using a sound/vibration data acquisition system (DAQ) with an accelerometer sensor. The response of these mechanical parameters collected during the drilling of various rocks was then analyzed and correlated with physico-mechanical rock properties.

Prediction models (Type-I) for physico-mechanical rock properties such as UCS, BTS, SRN and density were developed using thrust, torque, including vibration data, using single order multiple regression methods. Similarly, prediction models (Type-II) were also developed using thrust and torque and excluding the vibration data, using second-order multiple regression methods. The prediction performance and validation of Type-I and Type-II are checked. The results showed that the Type-II model would predict the rock properties, i.e., UCS, BTS, SRN and density with less NRMSE than the Type-I model by 2.58%, 0.56%, 4.3%, and 3.17%, respectively. Similarly, compared to the Type-I models, the Type-II model would decrease the MAPE by 1.33%, 1.4%, 2.72%, and 0.24%, respectively.

However, both types, i.e., Type-I and Type-II, could estimate the rock properties within 15% or acceptable errors. Due to the high sensitivity of vibration data to the spindle speed rather than by the UCS or other properties of rocks, and its high cost, it could conclude that the Type-II model might be useful, especially for estimating UCS and BTS at laboratory capacity without core samples.

Besides, ANN models are developed for the prediction of rock properties. It was observed from the ANN models' prediction performance that the ANN models could estimate the physico-mechanical rock properties comparatively better than the Type-II model. In this case, NRSME of UCS, BTS, SRN, and density were reduced by 1.97%, 7.38%, 1.74%, and 3.49 %, respectively. The results concluded the superiority of soft-computing models over the statistical models.

In this study, strength the relationship between considered rock properties and drilling specific energy is also investigated. Initially, the average drilling specific energy is calculated for each rock type using Teale's equation. The average specific energy was 24.20 MJ/m<sup>3</sup>, 28.78 MJ/m<sup>3</sup>, 35.68 MJ/m<sup>3</sup>, 36.09 MJ/m<sup>3</sup>, 38.40 MJ/m<sup>3</sup>, and 42.12 MJ/m<sup>3</sup> for shale (UCS=19.6MPa), sandstone-1 (UCS =37.5MPa), sandstone-2 (UCS=65.1MPa), sandstone-3 (UCS=72.4 MPa), limestone-1 (UCS=95.3 MPa), and limestone-2 (UCS=119.2MPa), respectively. The drilling specific energy of each rock type was then correlated with their physico-mechanical rock properties. The results



showed that the strength of the relationship of UCS, BTS, SRN and density with drilling specific energy is good with  $R = 0.948, 0.892, 0.859,$  and  $0.908,$  respectively.

*Key words:* Drill thrust, torque, vibration frequency, drill tool dynamometer, accelerometer, multiple regression models.



## NOMENCLATURE

ADC	Analog to digital converter
AI	Artificial Intelligence
ANN	Artificial Neural Network
ANOVA	Analysis of Variance
ASTM	American Society for Testing and Materials
BL	Bit load
BPI	Block Punch Index
BR	Bit rotation
BTS	Brazilian tensile strength
CAI	Cerchar abrasive index
CC	Cubic centimetre
CNC	Computerised numerical control
DAQ	Data Acquisition System
DD	Drill diameter
DPM	Drilling process monitoring apparatus
DSE	Drilling Specific Energy
DV	Dependent Variable
FFT	Fast Fourier Transformation
gm	Gram
GPa	Giga Pascal
ISRM	International Society for Rock Mechanics
KS	Kilo samples

LS-1	Limestone-1
m	Meter
MAPE	Mean Absolute Percentage Error
MHz	Mega Hertz
MLP	Multi Layer Perceptron
MLPNN	Multilayer Perceptron Neural Network
MLR	Multiple linear regression
mm	Millimetre
MPa	Mega Pascal
MSE	Mean square error
MWD	Measurement while drilling
N	Newton
NC	Numerical control
NPT	Nail penetration test
NRMSE	Normalized Root Mean Square Error
PLSI	Point load strength index
PR	Penetration rate
R.P.M	Revolutions per minute
RMSE	Root mean square error
ROP	Rate of penetration
SH	Schmidt hammers
SRN	Schmidt Rebound Number
SS-1	Sandstone-1
SS	Spindle speed

T	Thrust
TQ	Torque
Trainlm	Levenberg–Marquardt
Trainrp	Resilient back propagation
Trainscg	Scaled conjugate gradient back propagation
UCS	Uniaxial compressive strength
USBM	United States Bureau of Mines
VAF	Value account for
VMC	Vertical milling center
Z	Vibration frequency



## TABLE OF CONTENTS

ABSTRACT.....	i
NOMENCLATURE .....	v
TABLE OF CONTENTS.....	ix
LIST OF FIGURES .....	xv
LIST OF TABLES .....	xix
CHAPTER 1 .....	1
INTRODUCTION .....	1
1.1 Background of the Study .....	1
1.2 Measurement of Rock Properties.....	1
1.3 Measurement While Drilling (MWD) Technique for rock characterization .....	2
1.4 Concept of Specific Energy in Drilling .....	3
1.5 Problem Statement .....	4
1.6 Research Objectives.....	4
1.7 Thesis Outline .....	5
1.8 Closure .....	6
CHAPTER 2 .....	9
LITERATURE REVIEW .....	9
2.1 General.....	9
2.2 Indirect Measurement of Uniaxial Compressive Strength (UCS) .....	9
2.3 Application of Measurement While Drilling Technique (MWD) in the Geotechnical Field .....	12
2.4 Application of Multiple Regression Models in Geotechnical Field .....	22

2.5 Applications of Artificial Neural Networking (ANN) Techniques .....	25
2.6 Relationship between Drilling Specific Energy and Rock Properties .....	29
2.7 Summary .....	32
CHAPTER 3 .....	33
METHODOLOGY, EXPERIMENTAL SETUP AND ROCK PROPERTIES .....	35
3.1 Introduction.....	35
3.2 Methodology .....	35
3.2.1 Details of parametric variations .....	38
3.3 Experimental Setup.....	38
3.3.1 CNC–vertical milling center (VMC) .....	41
3.3.2 Diamond core drill bits .....	43
3.3.3 Digital type drill tool Dynamometer .....	44
3.3.4 NI-9234 Data Acquisition System (DAQ).....	45
3.4 Determination of Vibration Frequency at Drill Head during the Drilling .....	46
3.5 Experimental Procedure.....	48
3.6 Determination of Actual Properties of Rocks at Laboratory .....	50
3.6.1 Uniaxial compressive strength (UCS) .....	51
3.6.2 Brazilian tensile Strength (BTS) .....	52
3.6.3 Schmidt rebound number (SRN) .....	54
3.6.4 Dry density of rock ( $\rho$ ).....	55
3.7 Summary .....	56
CHAPTER 4 .....	57
RESULTS OF EXPERIMENTAL INVESTIGATION .....	57
4.1 Importance of Drilling Responses Produced during the Rock Drilling Process ...	57



4.2 Influence of Drill Operating Parameters and UCS on Drilling Responses .....	57
4.3 Influence of penetration rate on drill thrust and torque at bit-rock interface during the drilling of different rocks .....	60
4.4 Influence of spindle speed on drill thrust and torque at bit-rock interface during the drilling of different rocks .....	62
4.5 Influence of drill diameter on drill thrust and torque at bit-rock interface during the drilling of different rocks .....	65
4.6 Influence of drill diameter on bit-pressure during the drilling of different rocks .	68
4.7 Influence of spindle speed on vibration frequency during the drilling of different rocks.....	69
4.8 Summary .....	71
CHAPTER 5 .....	73
STATISTICAL AND ANN MODELLING .....	73
5.1 Introduction.....	73
5.2 Multiple Linear Regression Analysis.....	73
5.3 Analysis of Variance (ANOVA) .....	75
5.4 Development of Multiple Regression Model for Physico-Mechanical Properties of Rocks including vibration parameter (Type-I) .....	75
5.4.1 Development of regression model for prediction of UCS .....	76
5.4.2 Development of regression model for prediction of BTS.....	78
5.4.3 Development of regression model for prediction of SRN .....	80
5.4.4 Development of regression model for prediction of density .....	82
5.5 Evaluation of Prediction Performance of Type-I Models .....	84
5.6 Correlations Strength between UCS and Drilling Responses .....	85

5.7 Development of Multiple Regression Model for Physico-Mechanical Properties of Rocks Excluding Vibration Parameter (Type-II).....	87
5.7.1 Type-II UCS model.....	87
5.7.2 Type-II BTS model.....	88
5.7.3 Type-II SRN model.....	89
5.7.2 Type-II Density model.....	90
5.8 Validation of Type-I and Type-II UCS models. ....	92
5.9 ANN Modeling .....	92
5.9.1 Multilayer perceptron neural network (MLPNN) .....	96
5.9.2 Development of ANN models for prediction of physico-mechanical properties.....	98
5.9.3 Comparative Performance of Multiple Linear Regressions (MLR) and Artificial Neural Network (ANN) Model.....	102
5.10 Summary .....	105
CHAPTER 6 .....	107
DRILLING SPECIFIC ENERGY AND ANALYSIS .....	107
6.1 Introduction.....	107
6.2 Computation of Drilling Specific Energy .....	107
6.3 Correlation of Drilling Specific Energy (DSE) with Rock Properties.....	108
6.4 Influence of Weight on Bit or Drilling Thrust on DSE .....	110
CHAPTER 7 .....	115
CONCLUSIONS AND SCOPE FOR FUTURE WORK .....	115
7.1 Conclusions.....	115
7.2 Scope for Future Work.....	119

REFERNCES .....	121
ANNEXURE-I .....	139
LIST OF PUBLICATIONS BASED ON PH.D. RESEARCH WORK .....	145
BIO-DATA .....	147



## LIST OF FIGURES

Fig.1.1 An overview of the drilling process monitoring apparatus (DPM) .....	3
Fig.3.1 Flow chart of research methodology .....	37
Fig. 3.2 Schematic diagram of the experimental setup .....	39
Fig. 3.3 Experimental setup .....	40
Fig. 3.4 BMV 45 T20 CNC vertical milling center .....	41
Fig. 3.5 Closed loop control system .....	43
Fig. 3.6 Diamond core drill bits .....	43
Fig. 3.7 Drill tool dynamometer .....	44
Fig. 3.8 Accelerometer sensor with magnetic base .....	45
Fig. 3.9 NI-DAQ hardware .....	46
Fig. 3.10 Time-domain vibration signal .....	47
Fig. 3.11 Frequency-domain vibration data (sandstone-2, $Z = 337$ Hz).....	47
Fig. 3.12 Frequency-domain vibration data (sandstone-3, $Z = 340$ Hz).....	47
Fig. 3.13 FFT algorithm .....	48
Fig. 3.14 UCS testing machine .....	51
Fig. 3.15 Brazilian indirect tensile strength testing .....	53
Fig. 3.16 Schmidt hardness tester .....	54
Fig. 4.1 Main effect plots (Thrust).....	58
Fig. 4.2 Incremental impact of variables on thrust .....	58
Fig. 4.3 Main effect plots (Torque).....	58
Fig. 4.4 Incremental impact of variables on torque .....	59
Fig. 4.5 Main effect plots (Vibration frequency) .....	59

Fig. 4.6 Incremental impact of variables on vibration frequency at drill head .....	59
Fig. 4.7 Influence of penetration rate and rock properties on drill thrust .....	60
Fig. 4.8 Influence of penetration rate and rock properties on torque .....	61
Fig. 4.9 Influence of spindle speed and rock properties on drill thrust .....	63
Fig. 4.10 Influence of spindle speed and rock properties on torque.....	64
Fig. 4.11 Influence of drill diameter and rock properties on drill thrust .....	66
Fig. 4.12 Influence of drill diameter and rock properties on torque .....	67
Fig. 4.13 Influence of drill diameter and rock properties on bit-pressure .....	68
Fig: 4.14 Influence of spindle speed and rock properties on vibration frequency .....	70
Fig: 5.1 Comparisons of actual and predicted values of Type-I UCS model .....	77
Fig: 5.2 Comparisons of actual and predicted values of Type-I BTS model .....	79
Fig. 5.3 Comparisons of actual and predicted values of Type-I SRN model .....	81
Fig. 5.4 Comparisons of actual and predicted values of Type-I density model .....	83
Fig. 5.5 Variations of thrust and torque .....	86
Fig: 5.6 Comparisons of actual and predicted values of Type-II UCS model.....	88
Fig. 5.7 Comparisons of actual and predicted values of Type-II BTS model .....	89
Fig. 5.8 Comparisons of actual and predicted values of Type-II SRN model.....	90
Fig. 5.9 Comparisons of actual and predicted values of Type-II density model .....	91
Fig. 5.10 A biological neuron .....	93
Fig. 5.11 ANN Neuron connection .....	94
Fig. 5.12 Multi-layered ANN structure .....	94
Fig. 5.13 A learning cycle in an ANN model .....	95
Fig. 5.14 Information processing through a neuron.....	96
Fig. 5.15 ANN model of the physico-mechanical properties of rocks. ....	98

Fig. 5.16 Adaptation of VAF with number of neurons for trainlm algorithm (UCS) .	99
Fig. 5.17 Adaptation of RMSE by number of neuron for trainlm algorithm (UCS)	100
Fig. 5.18 Adaptation of MAPE by number of neuron for trainlm algorithm (UCS)	100
Fig. 5.19 Example of prediction of UCS using ANN model (Trainlm). .....	101
Fig. 5.20 Comparison of MLR and ANN model for $R^2$ (VAF).....	103
Fig. 5.21 Comparison of MLR and ANN model for RMSE .....	103
Fig. 5.22 Comparison of MLR and ANN model for MAPE .....	104
Fig. 5.23 Comparison of MLR and ANN model for percentage error .....	105
Fig. 6.1 Correlation of specific energy with UCS .....	109
Fig. 6.2 Correlation of specific energy with BTS .....	109
Fig. 6.3 Correlation of specific energy with SRN .....	110
Fig. 6.4 Correlation of specific energy with density .....	110
Fig. 6.5 Influence of thrust on specific energy during the drilling of shale .....	111
Fig. 6.6 Influence of thrust on specific energy during the drilling of sandstone-1 ...	112
Fig. 6.7 Influence of thrust on specific energy during the drilling of sandstone-2....	112
Fig. 6.8 Influence of thrust on specific energy during the drilling of sandstone-3....	113
Fig. 6.9 Influence of thrust on specific energy during the drilling of limestone-1 ...	113
Fig. 6.10 Influence of thrust on specific energy during the drilling of limestone-2..	114





## LIST OF TABLES

Table 3.1 Details of parameteric variations .....	38
Table 3.2 Laboratory test results of UCS.....	52
Table 3.3 Laboratory test results of BTS .....	53
Table 3.4 Laboratory test results of SRN.....	54
Table 3.5 Laboratory test results of density .....	55
Table 4.1 Mean thrust at different penetration rate of drilling .....	61
Table 4.2 Mean torque at different penetration rate of drilling .....	62
Table 4.3 Mean thrust at different spindle speed of drilling.....	64
Table 4.4 Mean torque at different spindle speed of drilling.....	65
Table 4.5 Mean thrust at different drill diameters of drilling .....	66
Table 4.6 Mean torque at different drill diameters of drilling .....	67
Table 4.7 Mean bit-pressure at different drill diameters of drilling .....	69
Table 4.8 Mean vibration frequency at different spindle speeds of drilling.....	70
Table 5.1 Statistical results of UCS model .....	76
Table 5.2 Actual and predicted values of Type-I UCS model.....	77
Table 5.3 Statistical results of BTS model.....	78
Table 5.4 Actual and predicted values of Type-I BTS model .....	79
Table 5.5 Statistical results of SRN model .....	80
Table 5.6 Actual and predicted values of Type-I SRN model.....	81
Table 5.7 Statistical results of Density model .....	82
Table 5.8 Actual and predicted values of Type-I Density model .....	82

Table 5.9 Performance indices of Type-I models .....	84
Table 5.10 Cross correlation matrix.....	86
Table 5.11 Standard statistical table for strength of correlation .....	86
Table 5.12 Actual and predicted values of Type-II UCS model.....	87
Table 5.13 Actual and predicted values of Type-II BTS model .....	88
Table 5.14 Actual and predicted values of Type-II SRN model.....	89
Table 5.15 Actual and predicted values of Type-II Density model .....	90
Table 5.16 Performance indices of the Type-II models.....	91
Table 5.17 Validation of UCS model .....	92
Table 5.18 Performance of training and testing data using trainlm algorithm .....	101
Table 5.11 Performance of training and testing data using trainrp algorithm .....	102
Table 5.12 Performance of training and testing data using trainscg algorithm .....	102
Table 6.1 Average specific energy of different physico-mechanical properties .....	108

# ***CHAPTER-1***

# CHAPTER 1

## 1. INTRODUCTION

This chapter deals with a brief introduction about the essentials of rock properties for engineering projects, the significance of "Measurement while drilling" techniques in estimation of rock properties, the relationship of drilling specific energy with rock properties, problems associated with direct measurement of rock properties along with research objectives.

### 1.1 Background of the Study

Rocks are geological materials and an integral part of our nature. They have been an important construction material since the rise of civilization. Rock masses support large structures such as foundations for buildings and dams, tunnels, shafts, underground installations, etc. In many rock engineering projects, it is observed that the rocks are subjected to either compression or tensile loading or both. Therefore the strength properties of rocks, such as uniaxial compressive strength (UCS) and tensile strength (TS), are the most important data often used for such projects (Kumar et al., 2012). Also, UCS is an important strength property to be considered in a popular rock mass classification system (Bieniawski.1976).

However, the rock materials vary from most other engineering materials as it comprises discontinuities such as joints, bedding planes, folds, sheared zones, faults, etc. Hence, the investigation of the physico-mechanical properties of rocks may be useful for rock engineering applications.

### 1.2 Measurement of Rock Properties

For the determination of rock properties, various methods are available. It could be categorized broadly into two types, namely, direct and indirect methods. The direct

methods include laboratory and in situ tests. A particular test in the laboratory requires a specific testing machine and test samples. American Society for Testing and Materials (ASTM) and International Society for Rock Mechanics (ISRM) furnish the procedures for conducting the actual laboratory and in situ tests.

In the direct method, to obtain better and reliable results, meticulous preparation of rock samples is needed. For example, a standard UCS test required quality specimens of minimum size, i.e., diameter = 54.7 mm, with a diameter to length ratios of 1:2.5 and 1:2 with both ends ground and polished up to some standard limits as per the specifications of ISRM (2007) and ASTM D4543 (2008), respectively. During the diamond core drilling operation, particularly for weak and highly fractured, thinly bedded, foliated, and block-in-matrix rock mass, it may not be possible to obtain a proper and quality core sample required for such laboratory testing (Gokceoglu et al. 2002; Gokceoglu and Zorlu. 2004; Minaeian and Ahangari.2013). Preparation of samples as per standards instituted by ISRM and ASTM may be tedious, time-consuming, and expensive. Due to the limitations in the direct method, geologists, geophysicists, and engineers are interested in using indirect methods, including empirical or theoretical correlations (Zhang 2005).

The main attraction towards the indirect methods may be that the rock properties can determine quickly without using the core samples. Also, many properties could approximate from the single main property.

### **1.3 Measurement While Drilling (MWD) Technique for rock characterization**

Measurement while drilling (MWD) is the process in which specific parameters are measured near the bit and transferred to the surface without disturbing normal drilling operations. The type of information may be (a) Data related to the drilling direction (tool angle, azimuth, tool face). (b) Drilling parameters (weight on bit, torque, rpm, and rate of penetration). (c) Formation characteristics ( $\gamma$ -ray, resistivity logs).

The analysis of such data has great importance in providing the information useful for engineering calculations and decision-making needed for civil, mining or petroleum engineering projects. The drilling machine is used in almost all mining engineering operations such as mine site investigations, exploration drilling, foundation and rock

bolt and blast hole drilling, etc. Also, the idea of using drilling parameters to characterize the rock either at the working face while drilling the blast hole or when drilling into the roof and walls for support installation has been around for a long time (Rostami. et al. 2015). Therefore, the MWD technique may be a potential indirect method to characterize the rocks either at the site or using the experimental drilling setup in laboratory. The recent developments in sensor technology could increase the reliability and accuracy of the drill monitoring system, as shown in Fig.1.1. The recorded drilling data, such as thrust, torque, penetration rate etc., enables the drilling technician to approximate the UCS and other properties of rocks in and around the proposed project site (He et al., 2020).



Fig.1.1 An overview of the drilling process monitoring apparatus (DPM)

#### 1.4 Concept of Specific Energy in Drilling

In rock drilling, specific energy (SE) is the minimum energy needed to excavate the unit volume of rock. The amount of energy needed depends greatly on the nature of the rock and its characteristics (Davaranpanah et al., 2016). Teale studied the specific energy for rotary drilling in 1965, and he deduced the relationship considering the required thrust and rotational energy at the bit-rock interface. Yasar et al. (2011)

represent specific energy as another idea for evaluating rock drillability. A single index cannot judge rock drillability as it is affected by various parameters (Yarali and Soyer. 2013). These parameters include mechanical properties, geological parameters, hardness, and energy properties. Therefore, understanding the relationship between drilling specific energy and rock properties may be useful for engineers and drilling technicians.

### **1.5 Problem Statement**

Physico-mechanical properties of rocks are essential parameters often required in the planning and design of various rock engineering projects. In general, rock strength properties are determined in the laboratory using the core specimen of a particular geometry. In most of the mining and construction sites, these properties are not readily available. The standard method for rock testing involves certain problems or constraints to get a proper and quality core samples needed for such a laboratory trial. Besides, coring is tedious, time-consuming, and expensive.

The proposed research aims to assess and predict some of the vital physico-mechanical properties of sedimentary rocks using an indirect method that uses an empirical relationship and no core samples. The proposed research work also includes determining the specific energy of drilling and its strength of the relationship with rock properties.

### **1.6 Research Objectives**

1. To develop the prediction mathematical model to find the relationship between selected mechanical parameters obtained during rotary drilling of sedimentary rocks and their physico-mechanical properties.
2. To evaluate the comparative performances of multiple regression analysis and artificial neural network (ANN).
3. To investigate the strength of the relationship between specific energy of drilling and rock properties.

## **1.7 Thesis Outline**

This research mainly examines the relationship between mechanical drilling responses obtained during the rotary type rock drilling and the physico-mechanical strength properties of rocks. This research is also extended to investigate the relationship between rock properties and the specific energy of drilling.

The seven chapters are presented in this thesis in a logical order to fulfill the aim of the research objectives as follows:

### **Chapter-1**

This chapter briefly describes the problem associated with measuring the rock properties using the direct method, the potential of "measurement while drilling technique" (MWD) to estimate the vital properties of rocks and the concept related to specific drilling energy.

### **Chapter-2**

In this chapter, an extensive literature survey concerned to research objectives are covered, including the different drill operating parameter and drilling responses obtained during the drilling process for rock characterization, prediction of the rock properties using regression model and artificial neural network, and the relationship between drilling specific energy and rock properties.

### **Chapter-3**

An experimental methodology, machine and measuring instruments used in current research work, an experimental setup arrangement and their working principles, and data acquisition methods are explained in this chapter. Besides, a detailed testing procedure of physico-mechanical properties at the laboratory is discussed.



## **Chapter-4**

This chapter discusses the individual influence of drill parameters and rock strengths, such as UCS and other properties, on drilling responses. Also, discussions on the individual influence of drill operating parameters and UCS on drilling responses are discussed.

## **Chapter-5**

In this chapter, the mathematical model development for each rock property using the statistical and a soft-computing technique, i.e., ANN, checking their prediction performance, correlations of drilling responses with rock strength property is discussed.

## **Chapter-6**

In this chapter, computation of drilling specific energy, the relationship between specific energy and rock properties, and the influence of weight on bit or drilling thrust on specific energy are discussed.

## **Chapter-7**

The conclusions are summarised, and also the scope and recommendations for future work are discussed briefly.

## **1.8 Closure**

This thesis concentrates on the indirect approach with an importance on the development of mathematical models. Using the secondary methods does not imply that the direct methods are not significant. In general, some kinds of laboratory or in-situ tests should always be included in a project. The secondary or indirect approaches can only be used to supplement the direct methods. Sabatini et al. (2002) state: “Correlations, in general, should never be used as a substitute for an adequate subsurface investigation program, but rather to complement and verify specific

project related information.” The above comment about correlations also refers to indirect methods included in this thesis.



# ***CHAPTER-2***

## **CHAPTER 2**

### **2. LITERATURE REVIEW**

This chapter deals with a comprehensive literature study, including the indirect measurement of rock properties using the index and MWD techniques, statistical modeling techniques, soft-computing techniques and the relationship between rock properties and drilling specific energy.

#### **2.1 General**

While designing construction projects or carrying out excavations, the knowledge of the physico-mechanical properties of rocks such as compressive strength, tensile strength, hardness, density, etc., in or around the geological site will help the design department a safe, effective, and economical design. The International Society of Rock Mechanics (ISRM) has developed a series of suggested methods for measuring rock properties both in the laboratory and in situ since 1974. The direct laboratory methods include measurement of density, porosity, water content, hardness, point load strength, uniaxial compressive strength, tensile strength, shear strength, and the entire stress-strain curve for intact rock uniaxial compression, etc. Ulusay and Hudson (2007) compiled and edited these tests, including site characterization and field tests. Due to some of the difficulties and limitations associated with laboratory or direct methods, as discussed in chapter 1, developing efficient indirect methods that use no core samples and comparatively faster than the direct method is in the scope of the study.

#### **2.2 Indirect Measurement of Uniaxial Compressive Strength (UCS)**

Schmidt (1951) developed a compact device known as Schmidt hammers, especially for non-destructive testing of concrete. It measures surface rebound hardness. The

Schmidt hammer is one of the extensively used portable measuring instruments to evaluate the rock strength indirectly. Aydin (2009) recommended a revised suggested approach, which replaces the earlier ISRM record to determine the hardness of rock surfaces both in laboratory and site and to use it as an index for UCS and Young's modulus of rock material.

The Schmidt hammer, developed by a company known as Proceq in Zurich, Switzerland (Proceq 1977a), measures the rebound length of a spring-loaded plunger released onto the surface of a rock surface as its hardness. Proceq has also developed a lighter and a tiny unit of equipment known as an Equotip hardness tester (Proceq 1977b) which measures the hardness of metallic material. Verwaal and Mulder (1993) examined the feasibility of predicting UCS from the L-values or hardness value of Equotip using samples of different rock types and showed the relationship of UCS and L-values by representing as a diagram.

Kawasaki et al. (2000) used the Equotip test to estimate the rock strength directly at the site. This investigation was centered on unweathered rocks. It ascertained the influences of the test conditions, including the size, shape, roughness, and impact direction. Similarly, Kawasaki et al. (2002) conducted tests such as Equotip hardness, unconfined compression, and elastic wave measurement using the various core samples of igneous and sedimentary rocks. It is recommended that UCS can be measured with acceptable errors from Equotip L-values or hardness value applying the equation  $UCS = aL + b$ , where  $L$  is Equotip hardness, 'a' and 'b' are coefficients based on rock types.

Szlavin (1974) examined whether there are statistically significant correlations among the mechanical properties of rocks, which would enable estimates to be made of one property from any other single property. Various tests such as UCS, BTS, shore hardness, indentation, specific energy, and abrasivity were carried out on many samples, and the mean value was computed and utilized in the analysis. A program was designed so that the test outcomes would feed into a computer. The correlation among the variables was collected in terms of regression coefficients and correlation coefficients. A comparison of the results revealed that most of the mechanical

properties, i.e., strength, and hardness, could be determined with fair accuracy from each other. However, greater errors are associated with the determination from abrasivity. It was also reported that the ratio of UCS and specific energy is approximately constant.

To determine the rock's hardness, and use it as an index for uniaxial compressive strength, Szwedzicki (1998) suggested a standard indentation test including the utilization of a standard indenter, the stipulation of a loading rate, standards for the termination of the test, etc. It was reported that a standardized indentation test would permit the determination of the mechanical properties of rock and ensure the strong relationship between indentation hardness index and the uniaxial compressive strength. It also suggested that the indentation hardness index could be used to distinguish the hardness of the rock and serve as an efficient approach for the determination of UCS.

The point load test (PLT) is a simple and economical measurement system used to calculate a rock strength index. Broch and Franklin (1972) have revealed this approach has potential in rock engineering and thus suggested the testing procedure to the International Society for Rock Mechanics (ISRM, 1973). The PLT device and method facilitate the efficient and cost-effective measurement of core or lump rock samples in either a field or laboratory environment. In this method, the rock sample is compressed between conical shape steel plates until the sample fails in a testing trial. The pressure applying to the rock sample is recording by a pressure gauge. Initially, the point load strength index (PLSI) is determined using the corresponding failure pressure and sample diameter. UCS was then determined by the developed relationship between the UCS and PLSI.

Sulukcu and Ulusay (2001) proposed the block punch index test as an index for the classification of rock materials based on their strength. This test was originally developed at Delft University, Netherland. Block Punch Index (BPI) test is an index test for UCS and tensile strength, in which a small section of a core is subjected to an accelerating load until the central piece of the specimen is punched out. The test apparatus is similar to a point load test machine with the conical steel plates replaced with lower and upper punching blocks. As per the ISRM suggested method, the

circular specimen should be split into three parts for the valid BPI test. Thus, the block punch index (BPI) is determined using the specimen's failure load and its geometric data.

Kamil Kayabali and Levent Selcuk (2010) developed a novel method known as nail penetration test (NPT) to evaluate the uniaxial compressive strength of intact rocks. A powerful gas nailer of 130 Joules and nails ranging from 25mm to 60mm in length were the tools used for experimenting. A total of 65 different rock blocks, including metamorphic, igneous, and sedimentary rock types, were used as the test samples. Five nail shots were performed on each rock block sample, and average values of nail penetration depth were noted down. Later, the average nail penetration depths were correlated with actual UCS. The result revealed that the NPT could correlate well with UCS better than PLIT and SRH and estimate the UCS of intact rocks up to 100MPa.

Lama and Vutukuri (1978) and Carmichael (1982) tabulated enormous lists of several mechanical properties of sedimentary rocks collected from the field study conducted throughout the world. Wong et al. (1997) reported the UCS, tensile strength, and physical properties of different sandstones around that Japan. The laboratory test results on North Sea sandstone and shale were summarized by Bradford et al. (1998) and Horsrud (2001).

### **2.3 Application of Measurement While Drilling Technique (MWD) in the Geotechnical Field**

Measurement while drilling (MWD) is a technique that enables measuring and collect different types of real-time data on the rock mass during the drilling process. The concept of monitoring a drill's performance by detecting variations in drilling conditions during borehole drilling has been widely explored since the introduction of the practice by Schlumberger in 1912 (Cooper et al.2004). The first attempts to apply and adopt MWD technology to the mining industry were initiated around the 1970s. MWD systems record physical forces and pressures during the drilling. These include 'actions' such as down-thrust, rotary speed and 'reactions' including torque, penetration rate, or acoustic parameters such as vibrations (Cooper et al.2004). The United States Bureau of Mines (USBM) has been examining the empirical relationship between



rotary drilling parameters and the mechanical properties of rock for the past thirty years (Clark. 1982). Drill operating and corresponding drilling responses data collected during a rock drilling process can be used to infer rock mass characteristics (Khorzoughi and Hall. 2016). The recorded MWD parameters can provide the essential information on rock strength properties that could generally only be discovered by recovering samples or in-situ testing (Lucifora et al., 2013; Li et al., 2014).

Many studies revealed a close relationship between drill operating parameters and rock mass properties (Paone and Madson. 1966; Paone et al.1969; Howarth et al. 1986; Karpuz et al. 1990; Kharaman. 2002; Erosy and Waller.1995; Basarir et al.2014; Basarir and Karpuz.2016). Leighton et al. (1982, 1983) and Hagan and Reid (1983) examined the use of recorded drilling parameters to determine zones of strong and weak rock in open pit blast hole drilling. In eastern European lignite mining operations, monitored drilling was utilized to define the extent of very hard argillaceous iron ore bands. Variations in rock hardness were determined based on changes in drill energy consumption (Hojdar. 1986).

Basarir et al. (2016) attempted to develop mathematical models for uniaxial compressive strength (UCS) using the drilling parameters. The drill parameters, such as bit load (BL), bit rotation (BR), and penetration rate (PR) collected from many exploration drilling activities carried out by a research institute in Turkey. PR was recorded by varying any one of the parameters and keeping another parameter constant. With these data, the model was developed using multiple regression techniques. The selected variables explain the variation in the dependent variable up to 78%. PR is the most significant parameter with the coefficient of determination of 59.5%. Bit load has a strong effect on rock mass strength with a coefficient of determination of 24.8%. The validity of the developed model was checked using performance indices. Results showed that this approach could be adopted for preliminary evaluation of rock mass strength often required for mining design projects.

Kalantari et al. (2018) attempted to develop an analytical model using the core parameters of rocks, such as internal friction angle and cohesion values. As a part of

determining these parameters, drilling parameters such as the penetration rate, thrust, and torque collected during conventional type drilling. During the drilling of rocks such as travertine, onyx, and rhyolite having the UCS of 48 MPa, 100 MPa, and 152 MPa, the thrust and torque were changed significantly for different penetration rates at various bit speeds. Using this approach, the analytical model could estimate the UCS for travertine, onyx, and rhyolite with an error of 20%, 21%, and 6%, respectively.

Vijay et al. (2019) studied the wear rate of the tungsten-carbide drill bit during the rotary rock drilling. In this, the thrust induced between bit and rock was recorded for various sandstone rock samples varying UCS from 13.7 MPa to 51.67 MPa using different combinations of drill operating parameters. Among the drilling of different rock-strength, the maximum thrust was appeared for high strength rock with UCS 51.67 MPa.

Huang and Wang (1997) conducted a set of rock drilling experiments at the laboratory to understand the mechanics of diamond core drilling. The various drill operating parameters are taken into account to investigate the drillability of diamond impregnated bits. They were; a weight on bit, applied torque, penetration rate (PR), spindle speed, and rock strength. The experimental results showed that the PR and drilling torque increased exponentially as the weight-on-bit increased. The following equations relating the torque, weight-on-bit, and UCS are suggested with good correlation coefficients.

$$\text{Torque} = 6.426 e^{0.0003} \times \text{Weight on bit}$$

$$\text{Torque} = 103.26 \text{ UCS}^{-0.468}$$

Karpuz et al. (1990) studied the drillability of rotary blast hole drillings at open-cast lignite mines in Turkey. It was conducted at 96 different locations of 16 lignite mines to evaluate the relationship between formation properties and drill data such as penetration rate, thrust, RPM. The collected drill response data examined the association between rock properties such as uniaxial compressive strength, cohesion, tensile strength, density, and penetration rate. The results showed that the uniaxial compressive strength correlates with the drilling parameter with the highest correlation coefficient. Also, an assessment was carried out on the required amount of

drilling thrust, drilling speed to have a different penetration rate for various rock strengths (UCS) and represented as a chart.

Bhatnagar et al. (2011) carried out the drilling experiment using polyethylene-oxide (PEO) added with water as a flushing media. From the drilling data, it was observed that at 285 revolutions per minute (r.p.m), the maximum ROP was 7cm/min at 800N, but the ROP increased to 8.1 cm/min and 16.2 cm/min with 471 r.p.m and 1122 rpm, respectively at the same load. It is concluded that the speed is significantly influencing the ROP independently. It was also observed at all speeds that as the thrust was increasing, the ROP was also increasing.

Bhatnagar et al. (2011) carried out the drilling experiment using the polyethylene-oxide (PEO) added with water as a flushing media. From the drilling data, it was observed that at 285 r.p.m, to reach an ROP of 7cm/min, the required thrust was 800N, but for the same ROP, the thrust was around 630N at 470 r.p.m. Similarly, the thrust required was 800N at 687 r.p.m. to reach 12cm/min, but for the same ROP, the required thrust was around 650N at 1122 r.p.m. It is concluded that the thrust level is decreasing as the speed is increasing for a particular ROP.

Bhatnagar et al. (2011) carried out the drilling experiment using the polyethylene-oxide (PEO) added with water as a flushing media during marble drilling. From the drilling data, it was observed that the torque developed was 4.2 N-m at 285 r.p.m and 800 N. Similarly, the torque was 4.1 N-m at 471 r.p.m and 800 N. The torque was 3.5 N-m at both 687 r.p.m. and 1122 r.p.m. under the thrust of 800 N. It is concluded that the speed is influencing the torque independently. It was also observed that there was a linear relationship between the thrust and torque at all speeds.

Rao and Misra (1998) investigated the effect of drill operating parameters such as bit thrust, bit speed, and bit diameter on torque. The experiment was conducted using a conventional drilling setup with minor modifications to apply different loads on a drill bit. The torque was measured with a developed wheel-spoke dynamometer. During the sandstone drilling, at 300 r.p.m, under the bit thrust of 195 N, the torque developed was up to 0.5 N-m, but the torque increased to 2.5 N-m at 500 N bit thrust using the same speed. Similarly, during limestone drilling, using 300 r.p.m, the torque

increased to 0.6 N-m at 195 N. It was then increased to 3.2 N-m at 500 N. Therefore, it is concluded that the torque increases as the thrust on the bit increase at a particular bit speed.

Rao and Misra (1998) conducted a drilling experiment using a conventional drilling setup with minor modifications to apply different loads on a drill bit. The torque developed at the bit-rock interface is measured with a developed wheel-spoke dynamometer. During the sandstone drilling running at a particular speed and load, with a drill bit diameter of 15mm, the torque developed was 3.1 N-m. But it was 5 N-m when the 35mm drill bit for the same running conditions. Similarly, during the limestone drilling with the same working conditions, the torque developed was 5 N-m using the 15mm drill diameter. It was then developed to 6.2 N-m when the drill bit diameter of 35mm was used. It was concluded that the torque is increasing with drill bit diameter for a particular load and speed conditions.

Rao et al. (2002) conducted laboratory diamond drilling trials on a medium-size vertical drilling machine. A specially intended dynamometer was used to measure the thrust and the torque forces during the rock drilling. During the drilling of a limestone block at 1180 r.p.m, the minimum torque level developed to 1.5 N-m, 2 N-m, 2.3 N-m, 3.5 N-m, and 5 N-m with different bit thrust of 195 N, 272 N, 342 N, 424 N, 550 N, respectively with a 12mm bit diameter. Similarly, as the bit diameter increased from 12mm to 45mm, the torque increased from 1.5 N-m to 2.2 N-m under the bit thrust of 195 N. But, at higher thrust, i.e., 550 N, the torque could increase from 5 to 8.9 N-m. These results concluded that the drilling torque increased with increasing bit thrust and bit diameter.

Basarir et al. (2014) carried out a study on the diamond drill bit's penetration rate during rotary drilling. The data was collected from various boreholes having different UCS of rocks ranging from 36MPa to 82MPa. Among the various rock strength ranges, the machine could utilize a bit load of 486 to 2268 kgs and speed ranging from 200 to 500 r.p.m. to reach the penetration rate of 0.2 cm/min to 11.4 cm/min. The increase in bit load was 366.67% in terms of percentage, and the increase in bit speed was 150%.

Kivade et al. (2015) conducted a drilling experiment using a jackhammer for sedimentary rocks. The UCS of the rock was 112.3MPa. The experimental result observed that the bit could reach a penetration from 0.2mm/sec to 2.99mm/sec as the inlet air pressure increased from 392 KPa to 588 KPa (50%).

Hagan and Reid (1983) discussed the use of MWD to improve blasting efficiency. It was reported that drill response parameters such as penetration rate and torque could identify the harder layers, coal seams, fractured rock, and cavities. Based on these findings, blast design may be altered. It was also said that the penetration rate is relatively low for the rock of high strength.

Paone et al. (1969) carried out drilling experiments with impregnated diamond drill bits on different rocks. In this experiment, the penetration rate was recorded for the drill parameters such as weight on bit (WOB) and bit rotation speed (RPM) and later related to some of the important rock properties. From the experimental results, it was concluded that there is an interaction between WOB, RPM, uniaxial compressive strength, hardness, and penetration rate.

Erosy and Waller (1995) carried out the drilling operations on various rock types in the laboratory with polycrystalline diamond compact (PDC) and impregnated diamond core bits using a fully instrumented drilling rig at various rotational speeds and drill thrust. The regression analysis was then employed to generate predictive models of penetration rates from the machine operating parameters and rock properties. Results show a close correlation between drill thrust, rotational speed, penetration rate, and hardness.

Yasar et al. (2011) conducted a study using rock drilling set up to examine the interaction among the multiple drill parameters and the physico-mechanical attributes of cement mortar, used as a substitute for natural rock. Since mortars were produced with different aging times, their UCS was also varied and determined in the laboratory. At various drilling speeds, the thrust, torque, and penetration rate (PR) were measured for different mortar samples. It could be observed from the data analysis that thrust and torque had a linear relationship with the PR. Also, the PR was increasing with the increase of both applied thrust force and torque.

Roy and Adhikari (2007) conducted a measurement of noise produced during the drilling of blast holes. From the in situ data, it was concluded that a noise level generated during the rock drilling was a potential tool to identify the rock as a soft, medium, or hard, which might help to select the appropriate explosives.

Yari (2018 a, b) have attempted to approximate both igneous and sedimentary rocks' geo-mechanical properties during rotary drilling. The drilling was carried out for various rocks using the drill operating parameters of bit speed 830 r.p.m, overall thrust force of 400N, and bit diameter of 18mm. During the drilling of each rock type, the sound level signal was captured for a particular time with the DAQ system. The frequency component from the time domain acoustic signal was then extracted and used for analysis. The results revealed that a particular rock's dominant frequency could correlate with properties such as UCS, BTS, and SRN. Using this approach, the model would predict the UCS, BTS and SRN with errors of 8.76%, 5.76%, and 8.87%, respectively.

Khoshouei and Bagherpour (2020) conducted the drilling experiment using a self-developed drilling machine with a loading arrangement of 1000N. During the drilling with a 12mm bit, the sound level, vibration level, and frequency of sound were collected for igneous rock. The sound level, vibration level, and acoustic frequency could vary up to 13.09%, 31.21%, and 2.48%, respectively, during the drilling of different characteristic rocks. It was seen from the multiple regression analysis that all the collected response parameters could influence the UCS, BTS, and Schmidt rebound number (SRN) with  $R^2$  values of 0.92, 0.83 and 0.81, respectively.

Kumar et al. (2011) conducted drilling operations on various rocks with the main interest of assessing the strength and hardness of the drilling rocks. The different combinations of drill operating variables such as bit diameter, bit speed, and penetration rate were used for drilling the rocks. During the drilling of each rock type using a particular combination of drill variables, the sound level was recorded. It was then concluded from the experimental results that both drill operating variables and rock properties were liable to the sound level produced during the drilling.

Kumar et al. (2012) carried out laboratory work to examine the relations between sound level produced during drilling and physico-mechanical properties such as UCS, BTS, and porosity of sedimentary rocks. This study developed empirical relations between drill parameters, sound level, and rock properties. The relationship was good for UCS with an  $R^2$  value of 89.93%, and it was 88.91% and 88.12% for BTS and porosity, respectively.

Kumar et al. (2019 a, b, c) conducted the drilling experiment to estimate rock strength properties. The CNC milling machine was used to drill on various sedimentary rocks with different combinations of drill operating variables such as penetration rate, drill diameter, and speed. For each combination of drill operating variables, an acoustic parameter such as frequency of drilling sound was acquired with a data acquisition system (DAQ). The experimental results concluded that the difference in acoustic parameters was due to different drill operating parameters and rocks with different strengths.

Itakura et al. (2001; 2008) discussed that if “balling up” occurs in deeper holes, torque and thrust data appeared higher than usual drilling. Therefore, it is important to implement efficient borehole flushing to prevent this phenomenon. Thus, it was concluded that it was necessary to maintain a sufficient quantity of flushing water/air during drilling, especially for fine-grained rocks.

Automated drill monitoring is a relatively new technique that involves instrumentation and software to record the drilling parameters developed, i.e., penetration rate, thrust, torque, etc., as drilling proceeds. Several functional areas of application of instrumented drilling techniques were outlined by Brown et al. (1978, 1984) as:(1) the ability to provide a measure of the physical properties of the rocks being drilled based upon the correlation between specific energies and rock compressive strength and the known area geology, and (2) the ability to indicate the presence of major discontinuities such as open or clay-filled joints or faults.

West Virginia University conducted a study to develop a real-time roof geology detection system and an information system to understand the geological structure of mine roof using the rock bolting drill operating parameters (Peng et al.2003; Peng et

al.2005a; Peng et al.2005b; Tang et al. 2004; Tang 2006). In this system, the penetration rate and drill bit speed was controlled with a closed-loop control system with efficient feedback system. The newly devised system could register the drilling parameters, such as thrust, torque, rotational speed, and penetration for every millisecond on a separate chip placed at the operator cabin.

Scoble et al. (1987) discussed ground characterization during the drilling process in surface mines. It was the ongoing mining automation research at McGill University, Canada. The parameters, such as dill thrust, penetration rate, torque, etc., were collected using the automated drill monitoring system. Field studies showed that the analysis of recorded drilling parameters could permit the determination of UCS and associated properties.

King et al. (1993) described an unsupervised learning approach and the expert system coupled with an instrumented roof bolter. It was primarily devised to investigate the geological characteristics of the underground coal mine roof. In this system, drilling parameters could be measured and calculated specific drilling energy. By the application of a microcomputer, critical drilling parameters are immediately read and interpreted. This facility made the operator notify unsafe roof conditions.

Itakura et al. (2001) exhibited the laboratory and in situ experimental results of a rock bolt drilling inbuilt with a data acquisition system that collects the mechanical drilling data such as thrust, torque, rotational speed, and stroke. The system could predict the '3D' geo-structure of strata and the design of rock bolting pattern. Field experiments in coal mines using the instrumented roof bolter showed that the software incorporated could examine the mechanical data log and showed discontinuities points with the neural network analysis.

Finfinger (2003) carried out a set of tests to determine the correlation between drill operating parameters and geo-mechanical roof rock properties such as voids, fractures, location of layers boundary, and rock strength. The trials were carried out in the laboratory employing a specially created rock structure that simulated the same conditions as mine roof strata. It was observed that when the bit was moving through



different layers of rocks having various features like strength, porosity, etc., there were considerable changes in thrust, torque, and drill bit speed and the piercing rate.

Luo et al. (2002) attempted to estimate the uniaxial compressive and shear strength of different manufactured blocks simulating the typical coal mine roof strata. During the drilling operation, the thrust and torque could be recorded at various penetrations per revolution. The experimental data showed that the drilling thrust increased significantly as the uniaxial compressive strength and penetration per revolution increased. Similarly, the drilling torque was increasing as the shear strength and penetration per revolution was increasing.

Tang (2006) developed a methodology for tracking the roof geology using the drilling response parameters obtained during the roof bolting operations. During the drilling process assisted by pneumatic power, it was observed that the feed pressure tends to drop when the voids were encountered. It was analyzed from experimental results that the prediction error is less for the voids above 3.2 mm. Also, the magnitude of feed pressure was comparable to the penetration rate and bit rotation. Therefore it was concluded that variations in penetration rate and bit rotation could be utilized to estimate rock strength.

Rostami et al. (2015) attempted to detect the void during the drilling of two concrete blocks. In this arrangement, a hard concrete block is kept over the soft concrete block. There was a tiny recess between the two concrete blocks that presented to simulate a “void.” A sound and vibration sensor (accelerometer) was attached to the drill head unit. During the drilling process, it was noticed that the amplitude of the vibration signal tends to reduce as soon as the drill bit reached the void location. It is concluded that a decline in the vibration signal is due to the bit running through the void.

Brown and Barr (1978) conducted early research on the dependency between drilling parameters and various geo-mechanical characteristics. It was concluded from the experimental results that only continuous recording of operating parameters like thrust, torque, penetration rate, flushing pressure, etc. could provide information on the mechanical properties of the rocks.

Brown et al. (1984) practically confirmed the applicability of MWD technology in the mining industry and concluded that the system could estimate the physical and mechanical properties of the rocks based on mechanical specific energy (MSE).

Schunnesson (1990) conducted primary research on the responding of drilling parameters in rotary percussive drilling. It was inferred from the drilling data that a single parameter like penetration rate could be a potential parameter to evaluate the quality of rock if properties varied considerably among geologic zones. Similarly, if variations in properties between geologic zones were insignificant, the rock quality evaluation using a single parameter might not hold good. In such cases, it might require several drill parameters and output to examine the quality of rocks.

Schunnesson (1996) conducted the experimental investigation on the preliminary evaluation of rock quality based on measurement while drilling parameters. It was investigated that how drilling parameters, such as torque, penetration rate (PR), and revolutions per minute (RPM) reacted to structural flaws in the rock mass. The outcomes of this study showed that many times variations of PR and RPM were directly proportionate to the intensity of rock fracturing. However, it was also shown that excessive fracturing could reduce PR and RPM with a rise in torque simultaneously.

#### **2.4 Application of Multiple Regression Models in Geotechnical Field**

Multiple regressions (MR) are a statistical technique that was practiced in 1908 by Pearson (Benesty.2009). It is employed to forecast the event dependent on one or more factors. The value to be predicted from the number of variables is called a dependent variable or criterion, or response. The variables accountable for predicting the response are called the independent variable or predictors. Multiple regressions can be used to develop the mathematical model for an engineering system and investigate the influence of various elements or factors on the system's response. Recently, there has been a steady increase in regression modeling in engineering geology due to its potential to yield reliable and accurate results.

Kahraman et al. (2003) investigated the effect of rock properties on penetration rate during the percussive blast hole drills. The data was collected at an open-pit mine on various rock types. Later, the determination of rock properties such as UCS, BTS, SRN, natural density, and modulus of elasticity was carried out. Each property was then correlated with PR separately using a simple linear regression method. The results showed that, except for the density and p-wave velocity, the other mechanical properties are related to the penetration rate with the high determination of coefficients.

Kahraman et al. (2003) studied the effect of ratio of young's modulus and uniaxial compressive strength on penetration rate in both percussive and rotary drilling. The data was obtained from various experimental work conducted by different researchers. The correlation between these parameters was examined using a simple linear regression method.

Ince et al. (2019) experimented with predicting the UCS of pyroclastic rocks collected from different Central Anatolia places. The rock properties such as dry density, saturated density, porosity, and point load index were measured in the laboratory and used for predicting the UCS. The rock properties were regressed against the actual UCS of rocks using the multiple regression method, and thus the prediction model was developed. In the developed model, all the independent variables could include and explain the dependent variable up to 82%.

Minaeian and Ahangari (2013) experimented with estimating the UCS of rocks using different rock samples. In this study, a total of 140 standard core specimens for UCS, p-wave velocity, and Schmidt hammer tests were prepared. With the regression method, the UCS was correlated with p-wave and SRH separately. The data analysis found that the  $R^2$  value for correlation of p-wave velocity with UCS was highest equal to 0.92.

Vijay et al. (2019) conducted an investigation on predicting the physico-mechanical properties of rocks during rock drilling. In this experiment, the dominant frequency of the sound signal was collected separately for each rock-type drilling. By employing

multiple regression techniques, the drill operating parameters and their corresponding acoustic frequency were correlated with rock properties.

Kumar et al. (2011) carried out a rock drilling experiment to investigate the relationship between sound level produced during the drilling and rock properties. During the drilling of different rocks, the sound level for a different combination of drill parameters was measured. It was then correlated with rock properties using the second-order multiple regression method. The result shows that the models could predict rock properties with acceptable errors.

Basarir and Karpuz (2016) attempted to predict rock mass strength using diamond drilling parameters. In this study, the drilling data such as bit rotation, bit weight, and penetration rate are gathered from the various explorations drilling process. Later, a multivariate regression method was employed to establish the relationship between drilling data and rock strength.

Khandelwal and Singh (2009) attempted to correlate the physico-mechanical properties of coal measures rocks with P-wave velocity. The sedimentary rocks such as shale, sandstone, coal samples were used as rock samples. The physico-mechanical properties such as UCS, tensile strength, density, Poisson's ratio, modulus of elasticity, and p-wave velocity were determined at the laboratory. The p-wave velocity was then correlated with each rock property using the simple linear regression method. It was seen that the UCS and density were well correlated with the p-wave velocity with a high coefficient of determination value.

Khoshouei and Bagherpour (2020) conducted the drilling experiment on different igneous rocks to examine the relationship between the rock properties and acoustic and vibration parameters obtained during drilling. The prediction model for various rock properties such as UCS, tensile strength, and Schmidt rebound number was built with a multiple regression method using acoustic and vibration parameters as the independent variables.

Basarir and Dincer (2017) developed multiple regression with linear and non-linear modeling techniques to predict p-wave velocity from the field drilling data such as thrust(T) and penetration rate(PR). The statistical analysis observed that both could

include in the models to have a high significance  $R^2$  value.

Kahraman and Gunaydin (2008) attempted to predict the performance of larger diameter circular saw during the sawing of five travertines, two limestones, and one dolomitic rock. The performance of the saw was based on the capability of the machine to cut the different rocks. The performance was then correlated with different rock properties using both simple linear and multiple regression methods. It was concluded from the statistical results that performance can be measured accurately with the multiple regression method rather than the simple regression method.

Kivade et al. (2015) carried out a study on the prediction of penetration rate (PR) during rotary rock drilling. In this experimental study, ten rocks having different rock properties were drilled using various drill operating parameters. Multiple regression models were used to establish the relationship between PR and drill operative parameters and rock properties. The results showed that the developed model could predict the response with less error.

## **2.5 Applications of Artificial Neural Networking (ANN) Techniques**

Due to its compatibility for various fields, including science and engineering research and its effectiveness, ANN is becoming popular among researchers, designers and planners. Therefore ANN has been successfully used in industrial applications also. In recent years the application of ANN is increasing in geotechnical and geological applications (Romeo et al. 1995; Singh et al. 2001; Sonmez et al. 2006; Rafiq et al. 2001; Singh et al. 2004; Kahraman et al. 2006; Tiryaki 2008; Yilmaz and Yuksek 2008; Yilmaz and Yuksek 2009; Yagiz et al. 2009; Sarkar et al. 2010; Ceryan et al. 2012; Rabbani et al. 2012; Yagiz et al. 2012; Rezaei et al. 2012; Tonnizam et al. 2014; Momeni et al. 2014).

Tiryaki B (2008) attempted to estimate the UCS and Young's modulus (E) of rocks from other rock properties such as cone indenter hardness, dry density, and shore hardness. The multiple non-linear and ANN models were developed to predict UCS and E. Compared to the regression model, ANN models could increase the  $R^2$  value by 14.54% and 6% for UCS and E, respectively. Similarly, the error is decreased for UCS and E by 15.9% and 37.62% than the regression models.

Kahraman et al. (2006) investigated the feasibility of predicting the saw ability in terms of production hour ( $\text{m}^2/\text{hour}$ ) of a circular saw fitted with impregnated diamond bits during the cutting process of carbonate rocks. Shear strength parameters of rocks were used as predictors for saw ability, and both multivariate regression and ANN were used to develop the model. Using the ANN model, the prediction of production/hour was increased with an increase of the  $R^2$  value from 0.749 to 0.945. Similarly, the prediction error is greatly decreased up to 18.52%

Kivade et al. (2015) examined the possibility of predicting some of the vital properties of rock such as UCS, tensile strength, and SRN using the penetration rate and sound parameters obtained during the drilling process. ANN models were developed using different training algorithms such as `traingda`, `trainrp`, `trainscg`, and `trainlm` algorithms. From the results, it was observed that the prediction error is less for `trainlm` algorithms, and it was concluded that the `trainlm` is the best algorithm for geological problems.

Zorlu et al. (2008) investigated the relation between UCS and petrographic parameters of sandstone. The input parameters represented the petrographic parameters, including packing density, quartz content, and grain contact type. The model was developed using multivariable regression and ANN approaches. The results showed that the ANN model could gain the VAF by 52%, and RMSE was decreased by 17.13% than the regression model.

Yilmaz and Yuksek (2008) investigated the estimation of UCS and Young's modulus (E) from other properties of gypsum. The properties, including slake durability, SRN, porosity, and PLI, were used to estimate the responses with multiple regression methods. In the regression technique, the input parameters could explain the variance in UCS and E by 85% and 88%, with RMSE of 2.05 and 2.53, respectively. Similarly, the ANN model could explain the variance in UCS and E as 91% and 95% with RMSE values of 1.65 and 2.28, respectively. From the results, it is concluded that the ANN model is predicting UCS and E more accurately than the regression model.

Moulenkamp and Grima (1999) examined the usage of hardness value of rocks and some of their physical properties to estimate the UCS. The model was developed by

both regression and ANN models. In the ANN model, the network was trained with the Levenberg-Marquardt algorithm. The prediction capacity of both models was checked using the performance indices. It was concluded from the results that the ANN model is most precise in the prediction of response than the regression models.

Singh et al. (2001) attempted to predict the strength properties, including UCS and tensile strength of schistose stones from the petrographic properties. The prediction model is developed using both regression analysis and ANN. It was reported from the analysis that the ANN model could predict the strength properties more accurately than the regression model.

Ceryan et al. (2012) examined the usage of some of the rock properties to predict UCS. The input parameters were porosity and P-wave velocity and were collected from many carbonate rock samples. Levenberg–Marquardt algorithm (LM-ANN) was used to build ANN models and compare their performance factors such as adjusted determination coefficient, error, and VAF with statistical regression model performance indicators. It was seen that the LM-ANN could predict the dependent variables precisely than the regression method.

Kumar et al. (2013a) investigated the capability of predicting some of the vital rock properties employing ANN models. A data set including the drill operating variables such as bit diameter, speed, the penetration rate, and the equivalent sound level was used as a predictor. The responses were UCS, tensile strength, density, p-wave velocity, porosity, and elasticity modulus. The measure of goodness of the fit showed that the ANN model was predicting the result almost as same as the experimental results and concluded that ANN models are precise for estimation of rock properties during the drilling process.

Kumar et al. (2013b) carried out an empirical study to assess the correlation between acoustic parameters obtained during rock drilling and physico-mechanical properties of sedimentary rocks. An acoustic parameter such as sound level produced while drilling the different rocks considering bit speed, bit diameter, and the penetration rate was recorded. Later the model is developed with multivariate regression (MR) and artificial neural network (ANN) method. After analyzing the results, it was observed

that the value of RMSE and MAPE was more for MR than the ANN model. Hence, it was concluding that ANN is the best predictive tool than MR.

Kahraman (2015) attempted to predict the diamond drill bit's penetration rate (PR) using the drilling parameters and the rock characteristics such as the UCS, the BTS, and the abrasiveness. In this study, the PR is predicted by multivariable regression and the ANN analysis. The results showed that the prediction of penetration rate was more accurate than the ANN model, and the performance was better than the regression model.

Gurocak et al. (2012) conducted an empirical study on developing a predictive model for the tensile strength of rocks using umpteen samples. The input parameters were IS (50), SRN, and density. In this study, a separate regression model for tensile strength was developed using simple linear and multiple regression models. Similarly, two soft computing ANN models, such as radial basis function network (RBFN) and multi-layer perceptron network (MLPN) were developed. Later, the model performance would examine by comparing the coefficient of multiple correlations ( $R^2$ ). Results showed that the ANN model developed with MLPN would predict the response more accurately.

Majdi and Rezaei (2013) studied a comparative evaluation of ANN and multiple regression (MR) models to estimate the UCS of rocks. For this, a lab test database consisting of 93 data sets including rock type, hardness, density, and porosity was used as predictors and UCS as a response. The performance indices were used to analyze the effectiveness of derived models. This assessment inferred that the ANN model's performance is significantly better than the MR model.

Ferentinou and Fakir (2017) used artificial intelligence to establish the relationship between UCS and some other rock properties. An ANN model using the back-propagation method was developed to predict UCS. The input parameters were density, point load index, tensile strength ( $\sigma_t$ ), and lithology. The lithology was introduced in the model as the qualitative input. The results showed an R-value of 99% for the training set and  $R = 92\%$  for the test set. It was then concluded that the ANN technique is efficient and useful for evaluating the UCS of rocks.



## **2.6 Relationship between Drilling Specific Energy and Rock Properties**

The word specific energy was coined by Teale (1965) with referring to the rock drilling process. He derived a relationship between drill operating parameters and a specific energy for rotary rock drilling considering various drilling data collected from several rotary-type rock drilling sources. The experimental results showed that the specific energy in many rock drilling processes could compare with the compressive strength of the drilling rocks. It was then assumed that a relationship of some kind should exist between them.

Kolapo (2020) investigated the rock drilling process to determine the impacts of rock properties on the specific energy. The drilling parameters such as penetration rate thrust, torque, drill hole area, and bit rotational speed were collected during the drilling of laterite, sandy clay, sandstone, granite, and quartzite situated at different depths from 3-60 meter collected at four different locations. The specific energy was then calculated using Teale's equation and correlated with the UCS and tensile strength of the drilled rocks. The experimental results and analysis showed that UCS and tensile strength were well correlated with specific energy with an  $R^2$  value above 80%.

Tiryaki and Dikmen (2006) examined the relationship between specific energy (SE) obtained from rock cutting experiments on different sandstone and their engineering properties. Specific energy of cutting for each sandstone was computed using the derived equation. Its strength was then correlated with rock properties using the Pearson correlation (R). The experimental results showed that UCS, tensile strength, density, and Schmidt rebound number have a good correlation coefficient with the cutting-specific energy, with  $R = 0.942, 0.823, 0.862,$  and  $0.890,$  respectively.

Yasar et al. (2011) conducted a study on rock drilling using a laboratory drilling set-up to examine the interaction between the specific energy of drilling and the compressive strength of cement mortar, a substitute for natural rock. Since the different mortar had been prepared using various aging times, their UCS was also varied. At various drilling speeds, the thrust, torque, and penetration rate were measured for various mortars having different physico-mechanical properties. The

need for specific energy during the drilling of various mortars was then calculated using the collected data. The results showed that drilling-specific energy was linearly varying with the UCS of mortars.

Mohammadi et al. (2017) investigated the influence of different geo-mechanical properties of rocks on drilling specific energy (DSE). The geo-mechanical parameters such as UCS, modulus of elasticity, and internal friction angle were collected at different depths from two vertical wells in SW-Iran oil fields. The data collected was categorized into training and testing data, and two separate regression models were developed using both data. From statistical analysis, it was observed that the UCS has a good correlation coefficient with drilling specific energy in both models with  $R = 0.63$  and  $R = 0.84$ , respectively.

Huang and Wang (1997) studied the utilization of specific energy during the diamond core drilling of sedimentary and igneous rocks. For that, a series of 36 laboratory drilling tests were conducted. The drillability of the drill bit was investigated using the penetration rate, applied torque, bit thrust, drill speed, and specific energy of drilling. The experimental results showed that the specific energy varied from  $2 \text{ GJ/m}^3$  to  $12 \text{ GJ/m}^3$  for the various rocks having UCS ranging from  $73.12 \text{ MPa}$  to  $163.41 \text{ MPa}$ . Similarly, as the drilling thrust increased from  $900 \text{ N}$  to  $2700 \text{ N}$ , the specific energy decreased from  $15 \text{ GJ/m}^3$  to  $4 \text{ GJ/m}^3$ .

Reddish and Ergul (1996) studied the drilling specific energy during the drilling of sedimentary type rocks. A modified portable rotary type drilling setup operated by  $12\text{V}$  NiCd batteries was used for experimental purposes. A digital ammeter was used to measure the current supply to the drill unit during the drilling process. The current and voltage was a direct measure of energy input into a particular drilling test. During the drilling of different rocks, it was observed that the drilling energy decreased as the PR increased. Similarly, the drilling energy had a linear relationship with rock strength (UCS).

Balci et al. (2004) conducted a study on the relationship between specific energy required during rock cutting and the mechanical properties of rock. A total of 23 rocks were collected from various mines in Turkey. For rock cutting, a full-scale linear

rock cutting machine installed with a dynamometer was used. During the cutting of each rock type, the specific energy (SE) was computed with thrust force data collected from a dynamometer. The relationship between the SE and the rock properties was examined employing statistical methods. The outcomes showed a good correlation between the SE and mechanical properties, such as UCS and tensile strength.

Kalantari et al. (2018) carried out the drilling experiment on three rock types, having different rock strengths using the sharp and blunt drill tool with different diameters and cutting angles. The required thrust and torque were collected from the data loggers for different indentation rates and drill bit speed. The analytical models for normal and tangential force were developed considering thrust, torque, internal frictional angle of rocks, and bit cutting parameters. The analytical model for drilling specific energy and rock strength (UCS) was also developed for both drilling tools with these basic models. The analytical model results showed a strong relation between drilling specific energy and UCS with  $R^2=0.99$  for both sharp and blunt tools with a diameter of 8 mm and a cutting angle of 15 degrees. Similarly, the  $R^2$  value was 0.98 and 0.99 for a blunt and sharp tool with a diameter of 8 mm and a cutting angle of 20 degrees.

Ersoy and Atici (2004) studied the performance characteristics of circular diamond saws during the cutting process of various rock types. In this experiment, 16 type rocks with five clustered groups were used and were cut with a diamond saw at various feed rates, depth of cut, and speed. The analytical model was developed for cutting forces using the basic horizontal, vertical and axial forces measured during the cutting action. The specific energy was calculated with cutting forces and rock cutting parameters. It was then correlated with rock properties and operating parameters. The results showed that the specific energy was decreasing as the feed rate and depth of cut increased. Similarly, it was also observed that that the specific energy of cutting was linearly varying with UCS.

Li and Itakura (2012) proposed an in situ method for evaluating the UCS of rocks using specific energy, based on an analytical model of drilling processes. The drilling data were obtained from a field experiment using an intelligent drilling machine and

used for the computation of specific energy. The results showed that the UCS of the rocks could predict reliably from the specific energy of drilling.

Finfinger (2003) applied Teale's (1965) specific energy model for the specific set of drilling conditions used in roof bolting operations in underground coal mines to determine the mine roof rocks' strength. The average specific energy obtained for different machine conditions was then correlated with the average UCS of rocks. The results showed that there is an almost linear relationship between UCS and the specific energy of drilling.

Bakar et al. (2018) studied the possibility of predicting the specific energy of a button bit used in rotary-percussion rock drilling based on geo-mechanical properties of rocks. Specific energy was computed using the mechanical drilling data collected at different site locations. The rock properties are determined from rock cores collected at the same sites. The specific energy of different rocks was then correlated with their respective rock properties using a simple linear regression technique. The results indicated that the UCS, BTS, and Schmidt rebound numbers were well correlated with drilling specific energy with the  $R^2$  value of 0.88, 0.73, and 0.72, respectively.

## **2.7 Summary**

In this chapter, a comprehensive literature survey on different techniques used to estimate the rock properties are presented. The literature review shows that the measurement while drilling technique using drill parameters such as thrust, torque, bit speed etc., or vibration parameters was widely used to assess physical properties of rocks such as cracks, voids, discontinuity directly at the site. But the correlation of drill operating parameters such as thrust, torque, bit speed or bit diameter, along with vibration data with vital rock properties like UCS, BTS, SRN and density for their estimation purposes, is very limited. Therefore, to address these constraints, this thesis intended to understand the drilling process under different operating conditions and observe the behavior of drilling responses that have a good relationship with the rock properties during the rotary drilling process.

However, since drilling is an important operation used often in many rock engineering projects, the direct measurement of such data may be useful for instant estimation of

strength properties and others for further advancement of projects. Also, the same method may also be useful at laboratory capacity if the core samples of rocks are not readily available. Also, the analysis of drilling specific energy in most previous research work is limited to UCS. The extension of an analysis of specific energy concerning other properties of rocks may help understand it better.



# ***CHAPTER-3***

## **CHAPTER 3**

### **3. METHODOLOGY, EXPERIMENTAL SETUP AND ROCK PROPERTIES**

#### **3.1 Introduction**

This chapter describes the detailed experimental setup, methodology, equipment/instruments, and experimental procedures followed in the current research work. The properties such as UCS, BTS, SRN, and density of each rock type carried out at the rock mechanics laboratory are also discussed.

#### **3.2 Methodology**

The methodology of the research work is presented through a flow chart, as shown in Fig. 3.1. The methodology of the research work is presented through a flow chart, as shown in Fig. 3.1. Well-prepared six types of sedimentary rock samples of the cubical shape having 16cm, including shale, three types of fine-grained sandstones and two types of limestones representing the different strengths were collected from Andhra Pradesh and Rajasthan mine sites through a Decorative Stone Agency located at Bangalore. Each type of rock consisted of 3 blocks collected from the same rock mass. Two blocks are utilized to remove the core samples required to test uniaxial compressive strength (UCS), Brazilian tensile strength (BTS) at the rock mechanics laboratory and determined as per the ISRM guidelines. The Schmidt Rebound Number (SRN) and density are determined using the same blocks before removing the cores. One block from each rock type is exclusively used for conducting the drilling experiment.

Rotary-type rock drilling operations were carried out using the BMV45 T20 CNC vertical milling center (VMC). Three diamond-impregnated core drill bits with a



different diameter, three penetration rates, and three drill bit speeds are used to drill each rock type. Drilling experiments were carried out on different rocks, i.e., one type of shale (SH), three types of fine-grained sandstone such as pink (SS-1), red (SS-2) and banded (SS-3) sandstones and two types of limestone (LS-1 and LS-2) using diamond impregnated core drill bits (12, 16, and 20 mm) on VMC by changing bit speed (400, 500, and 600 r.p.m.) and penetration rate (3, 4, and 5 mm/min). The thrust induced and torque developed at the bit-rock interface is measured for all bit-rock combinations considered, using a piezo-electric type drill tool dynamometer as shown in Fig.3.3 A and Fig.3.3 B.

Similarly, the vibration signal emanated from the drill head is captured for the same bit-rock combinations using a piezo-electric type accelerometer with a mounting magnetic base attached to the drill head, as shown in an enlarged Fig.3.3 B. The signal is then transmitted to DAQ and LabVIEW application software for further processing, such as the frequency component extraction. Later, the collected data are utilized to build predictive models to estimate physico-mechanical rock properties and also drilling specific energy is analyzed using statistical tools.

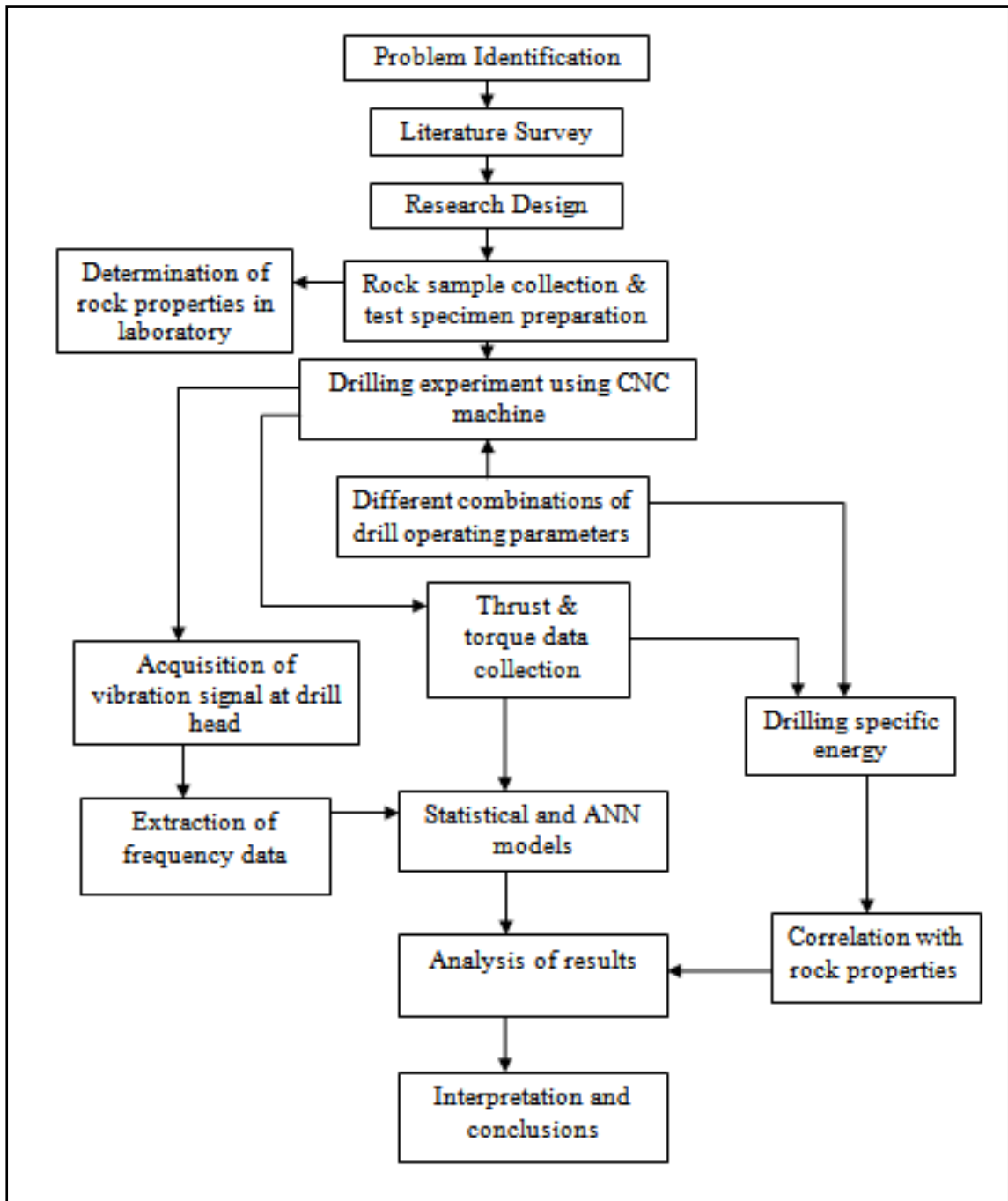


Fig.3.1 Flow chart of research methodology

### 3.2.1 Details of parametric variations

Table 3.1 Details of parametric variations

Parameters	Variables
<b>Laboratory investigations</b> (A) Drilling operations	
<b>(a) Bit parameters</b> 1. Bit type 2. Bit geometry 3. Bit diameter	Diamond core drill bit Diamond impregnated bit 12,16 and 20 mm
<b>(b) Operational parameters</b> 1. Penetration rate (mm/min) 2. Drilling speed (r.p.m) 3. Bit diameter (mm)	3,4,5 mm/min 400, 500, and 600 rpm 12,16 and 20mm
<b>(c) Rock parameters</b> 1. Type 2. Rock properties considered	Shale (1), Sandstone (3) and Limestone (2) <b>UCS, BTS, SRN and density</b>
<b>(d) Drilling responses</b>	Thrust, torque and vibration frequency
<b>(e) Drilling conditions</b>	Dry condition

Table 3.1 shows the details of the variables to be studied for the experimental purpose.

### 3.3 Experimental Setup

A detailed view of the rock drilling experimental set-up is shown in Fig. 3.2 and 3.3. The experimental set-up consists of the following machines/equipment, rock samples and measuring devices.

1. CNC–Vertical Milling Center (VMC)

2. Drill tool dynamometer with digital indicator
3. NI-9234 - acoustic/vibration data acquisition system (DAQS)
4. Cubical sedimentary type rock samples of size 16cm.

Rock drilling operations were carried out using a CNC type heavy-duty vertical milling center (VMC). It consists of a rigid base on which the machine table is fixed, and the table could travel in 3-dimensions operated by pneumatic power. Like the spindle speed and penetration rate, the table movement can be controlled using a numerical control program (NC program). Once the numerical value of drill bit speed and the penetration rate is assigned in the NC program, both would operate and maintain the assigned values till the end of the particular operation.

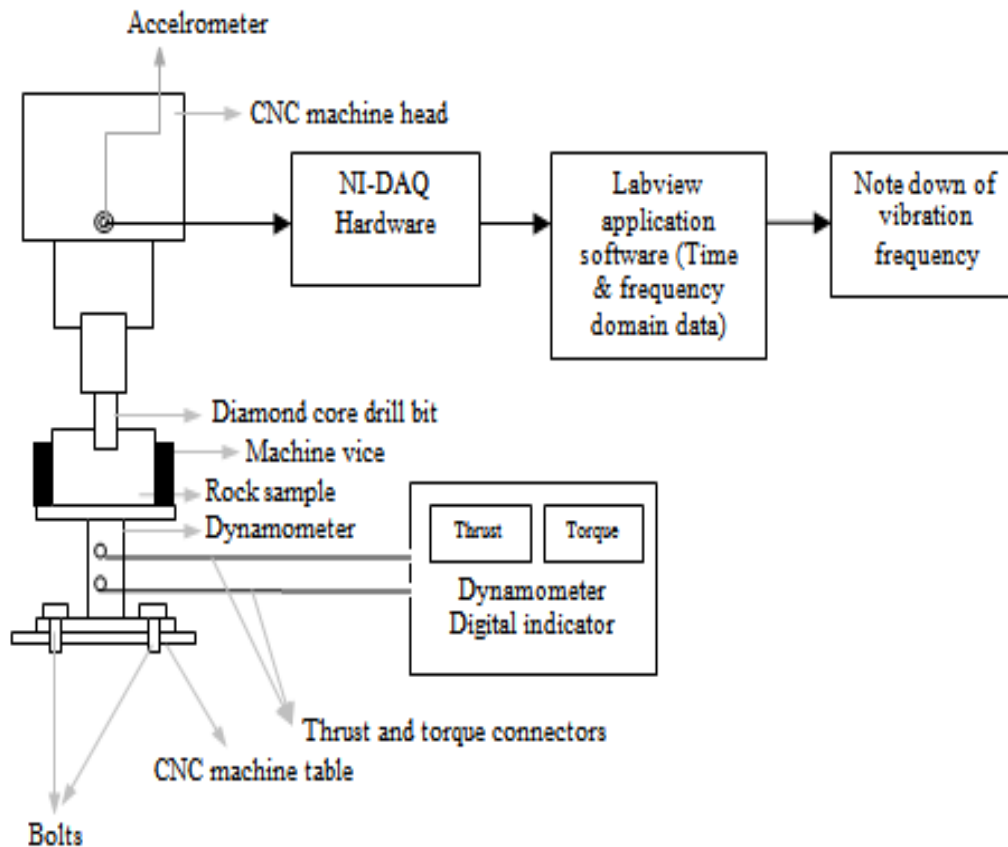
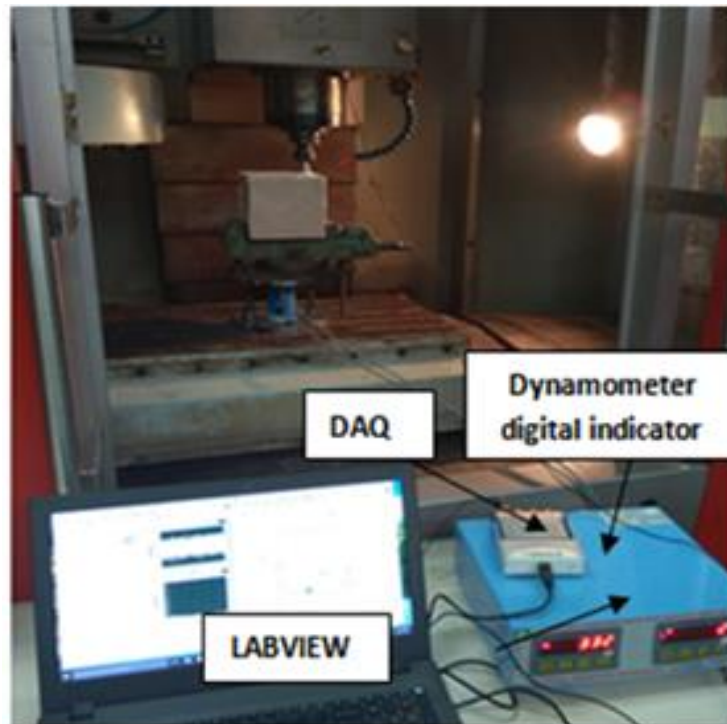


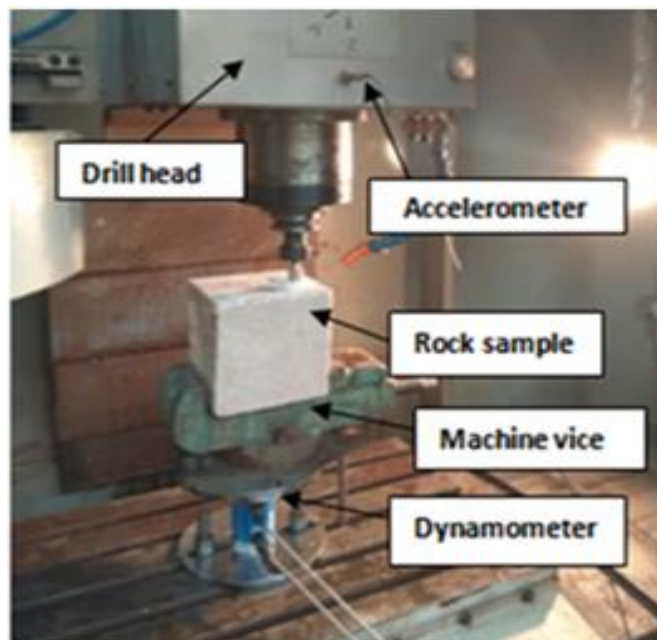
Fig.3.2 Schematic diagram of the experimental setup

The bit-thrust inducing and torque developed at the bit-rock interface during the drilling of different rock types is measured using an IEICOS made digital type drill tool Dynamometer. The vibration signal at the drill head is captured with NI-9234, 4-channel sound/vibrations data acquisition system working at the sampling rate of

1.562 to 51.3 Kilo samples/s. The entire drilling process was performed at room temperature (27° C).



A: Detailed view of experimental setup



B: Enlarged view of drilling experiment

Fig.3.3 Experimental setup

### 3.3.1 CNC–vertical milling center (VMC)

In this experimental study, the rock drilling operations were performed on the BMV45 T20 computer numerical control (CNC) vertical milling center, as shown in Fig.3.4.

Important specification of this CNC machine is as follows:

Dimensions of the machine table: 450 mm × 900 mm

Maximum traverse of machine table: X = 600mm, Y = 450mm, Z = 500mm

Range of spindle speed: 1-10000 r.p.m.

Range of penetration rate: 1-10000 mm/min

Maximum loading capacity of table: 500 kg

Power: 11.9 KW, 415 V, 3 Phases, 50 Hz

Air pressure – 6 bar

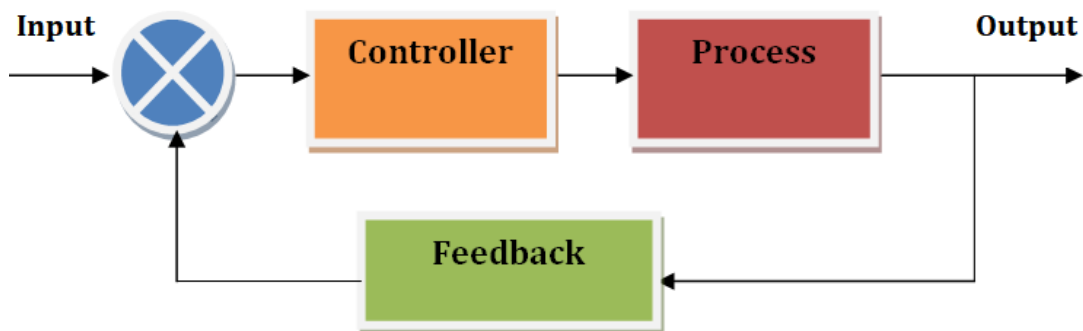


Fig.3.4 BMV 45 T20 CNC vertical milling center

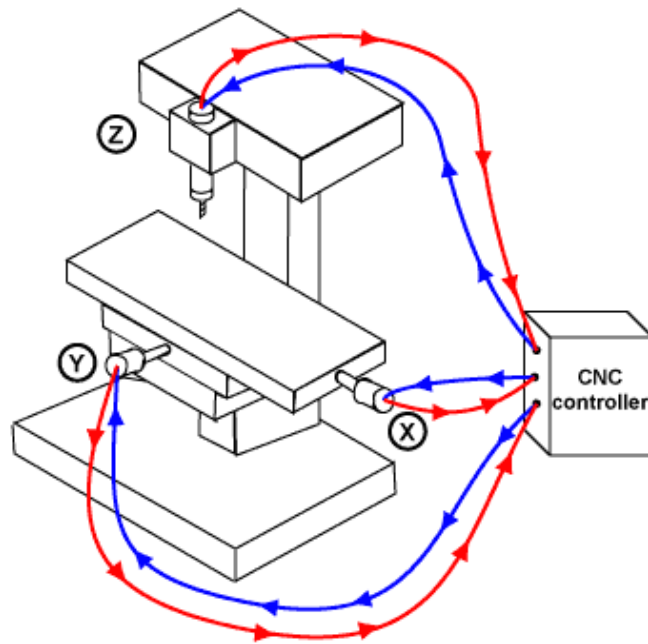
VMC is a machine used for drilling, boring and milling operations on different materials, and it is controlled by a closed-loop control system, as shown in Fig.3.5. In

this system, a subsystem is designed called feedback, which would continuously monitor the difference of input and output data. For example, during the drilling of a particular material, if the penetration rate of the bit in the numerical control program (input) is assigned as 2mm/min, then the bit has to penetrate the material at the same penetration rate irrespective of strength or other properties of the material being drilled. The feedback control system would continuously monitor the bit's performance using a measuring system to ensure whether the bit is moving at the same rate or not at any point in time. At any time, if the measured data is not matched with the input data, then the feedback system would send the equivalent signal continuously to the servo-motor control system to achieve the given penetration rate by adjusting and applying the appropriate thrust and torque to the bit. This process will continue until the particular operation is completed. There are two types of feedback systems, analog or digital type. The analog systems map the variation of mechanical variables such as position and velocity in voltage levels. In digital type, the electrical pulses are used for controlling the output errors. Closed-loop control systems are very effective and reliable since they can observe running conditions in real-time by feedback subsystems and automatically compensate continuously for any differences. The closed-loop CNC systems can work with an accuracy of 0.0001 of an inch.

It is assumed that the drilling method may affect the inducing of thrust, torque at the bit-rock interface, and also the acoustic signal emanating from the drill head. Therefore, the testing procedure is standardized throughout the entire drilling operation of various rock types.



A: Block diagram of closed loop control system



B: Schematic diagram of closed loop control system in actual CNC machine

Fig.3.5 Closed loop control system

### 3.3.2 Diamond impregnated core drill bits

A typical diamond-impregnated core drill bits of diameters 12, 16 and 20 mm are used for drilling operations. An impregnated diamond drill bit has a cylindrical, hollow crown structure with a lower portion containing diamond particles and a steel shank attached to the crown structure at its upper end. The diamond particles are dispersed within a metal matrix at the lower portion of the crown, as shown in Fig.3.6



Fig.3.6 Diamond impregnated core drill bits



### 3.3.3 Digital type drill tool Dynamometer

The IEICOS drill tool dynamometer comprises two major parts, as shown in Fig.3.7. The first one is the drill tool dynamometer (sensor body), and the second is the digital indicator used for noting down the thrust and torque. The sensor body consists of a cylinder with both ends welded with approximately 10mm thick steel plates. There are four long circular cuts on both plates to fix them to the machine table and machine vice. With the T-bolt and nut, the lower plate is securely fastened to the T-slots provided in the machine table, and on the top plate, the machine vice is directly fixed with suitable fasteners. The machine vice is used to hold the different rock samples firmly during the drilling process. Primarily, the sensor body has an individual full bridge strain gauge network to measure two forces, i.e., thrust and torque. The output of these strain gauge bridges is available via the 5-pin DIN connector sockets on the body. The measuring range of thrust and torque is 5000N and 200N-m, with a sensitivity of 1N and 1N-m, respectively. The thrust and torque inputs are provided at the sensor body connected to the output of the display unit using two separate cables of length approximately two meters.



Fig.3.7 Drill tool dynamometer

During the drilling of rock samples, the bit-force and torque are exerted on the sensor body. As the sensor is subjected to axial and shear force, the equivalent analog signal is triggered in the sensor body and it passes to the signal conditioner coupled with the sensor body. In the signal conditioner, the analog signal is converted to a digital signal for showing the value of thrust and torque at digital indicators provided in the signal conditioner box.

### 3.3.4 NI-9234 Data Acquisition System (DAQ)

Data acquisition (DAQ) is the process of measuring an electrical or physical phenomenon such as voltage, current, temperature, acceleration, or acoustic parameters with a computer. A DAQ system consists of sensors, DAQ measurement hardware, and a computer with programmable software. In the present research work, an accelerometer sensor, NI-DAQ hardware, and LabVIEW application software constitute the data acquisition system used to acquire acoustic data at the machine's drill head.

#### a) Accelerometer

As shown in Fig.3.8, accelerometer measures acceleration, which is the rate of change of the velocity of an object measured in meters per second squared ( $m/s^2$ ) or in G-forces (g). A single unit of G is equivalent to  $9.8 m/s^2$ . Accelerometers are useful for sensing vibrations of mechanical systems. In the present work, the drill head's vibration was measured with the accelerometer model No. YMC121A10 IEPE (Integrated electronics Piezo-electric) with measuring range and sensitivity  $\pm 500g$  and  $9.81 MV/g$ , respectively.



Fig.3.8 Accelerometer sensor (with magnetic base)

### b) NI-9234 DAQ Hardware

DAQ hardware, as shown in Fig.3.9, acts as the interface between a computer and the sensor. It primarily digitizes analog signals coming out from the sensor so that a computer can interpret them. The three key components of a DAQ device used for measuring a signal are the signal conditioning circuitry, analog-to-digital converter (ADC), and computer bus. In the present work, model no. NI-9234 DAQ hardware specifically designed to acquire sound and vibration signal with the sampling range of 1.652-51.2 KS/s, a maximum frequency of 13.1072 MHz was used.



Fig.3.9 NI-DAQ hardware

### 3.4 Determination of Vibration Frequency at Drill Head

When a system is subjected to vibration, the peak amplitude of vibration appears at specific frequencies within the frequency spectrum and is known as the dominant frequency. It carries the maximum energy among all frequencies found in the spectrum (Telgarsky.2013).

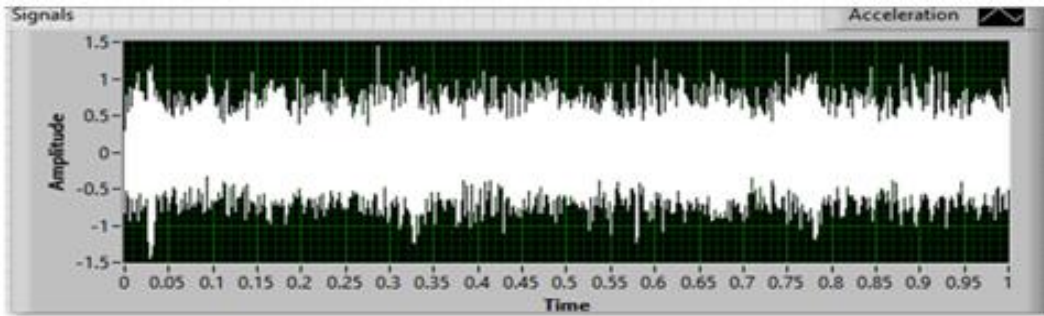


Fig.3.10 Time-domain vibration signal

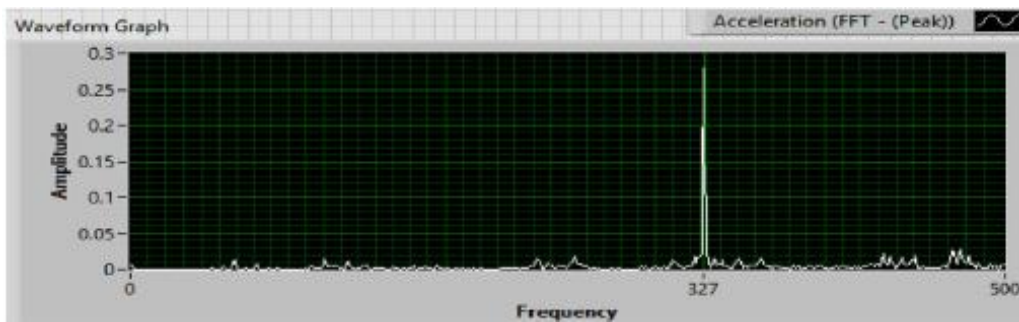


Fig.3.11 Frequency-domain vibration data (sandstone-2, Z = 337 Hz)

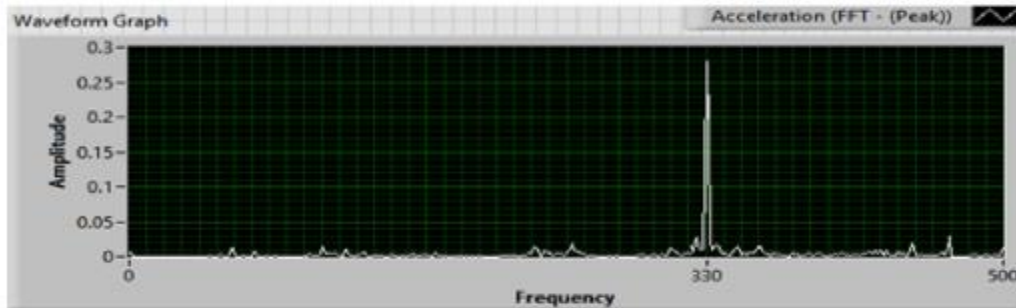


Fig.3.12 Frequency-domain vibration data (sandstone-3, Z = 340 Hz)

In the current study, the vibration signal emanating from the drill head during drilling of various rocks is captured with a four-channel sound/vibrations DAQ system working at the sampling rate of 1.652 to 51.2 Kilo Samples/sec. The accelerometer is mounted on the drill head using a magnetic bracket, as shown in Fig.3.3B. In this system, vibration of the drill head is picked up by an accelerometer in the form of an analog signal, and it is imparting to the DAQ hardware or signal conditioning device. In the signal conditioning device, the analog signal is transformed into a digital signal.

The digitized signal is then sent to LabVIEW application software to extract the time-series vibration signal, as shown in Fig. 3.10. Fig. 3.11 indicates that the dominant vibration frequency of the drill head during the drilling of sandstone-2 at a particular set of machine operating parameters was 337 Hz with the highest amplitude of 0.26 g. Similarly, the dominant vibration frequency was 340 Hz during the drilling of sandstone-3, as shown in Fig. 3.12. The frequency component of the time-domain signal is extracted using the appropriate Fast Fourier Transformation (FFT) algorithm, as shown in Fig. 3.13.

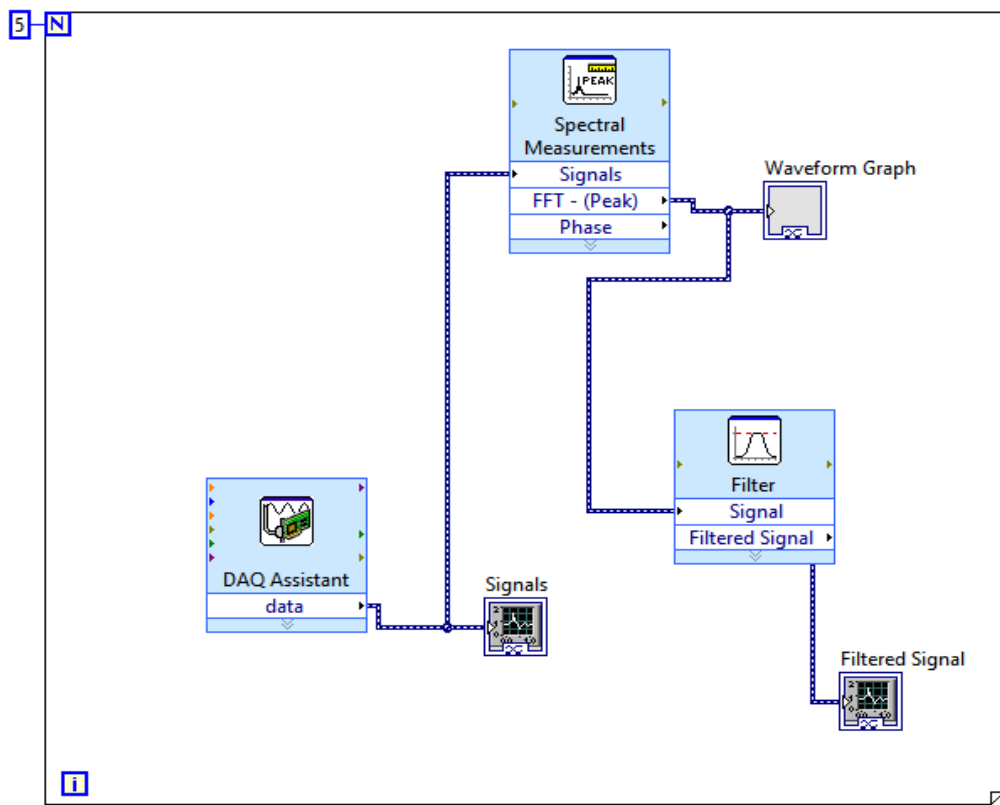


Fig.3.13 FFT algorithm

### 3.5 Experimental Procedure

In this experiment, a total of six types of sedimentary rocks, including one type shale, three type fine-grained sandstones, and two type limestones representing different physico-mechanical properties, were used for drilling operations. It is assumed that the drilling method might affect the inducing of thrust, torque at the bit-rock interface, and also the vibration signal emanating from the drill head. Therefore, the testing

procedure is standardized throughout the entire drilling operation of various rock types. The rock properties such as uniaxial compressive strength (UCS), Brazilian tensile strength (BTS), Schmidt rebound number (SRN), and density are determined at the laboratory as per the ISRM standards. Sophisticated measurement systems were used to record both thrust induced and torque developed at bit-rock interaction during the drilling of various rocks using different combinations of drill operating parameters. Similarly, the vibration signal emanated from the machine head was also captured along with thrust and torque.

Initially, the dynamometer with the sensor body is mounted on the machine table securely with suitable fasteners. Machine vice was then fixed on the sensor body with bolt and nut and ensured the proper electrical connectivity between sensor body and display unit. Similarly, the vibration sensor, i.e., accelerometer, is fixed on the drill head using a magnetic bracket and ensured the proper electrical connectivity between DAQ hardware and sensor. Later, the rock sample having the cubical shape with dimensions of 16 cm is tightly fixed in the machine vice.

The major obstructions for precise measurement of thrust and torque while drilling a hole are usually influenced by two disturbing phenomena. The first one is the compaction effect caused by the accumulation of rock dust along the drill bit at the hole's bottom surface. The second reason for the imprecise measurement is drill bit wears, especially when high silica content or abrasive rocks such as sandstones are being drilled. Both effects cause an artificial increment of thrust and torque. Unless taking some precaution measures, the measurement of both parameters would be wrong. Therefore, these effects need to be corrected to get the real values that would correspond to the absence of such disturbing phenomena.

For each rock type, 27 holes with a depth of 30 mm are drilled with 27 combinations of drill operating parameters (drill bit diameter of 12, 16, and 20mm  $\times$  drill bit speed of 400, 500, and 600 rpm  $\times$  penetration rate of 3, 4, and 5mm/min = 27 drill operating conditions). The following methods were used to measure the drilling responses, such as thrust, torque, and vibration parameters during the drilling of 27 holes on each rock type.

1. During the drilling of each hole with a particular drill operating condition, a hose pipe fitted with an appropriate size nozzle carrying the compressed air was often

directed towards the drill bit and the drilling hole. This arrangement intends to flush out the dust generated inside the drilled hole and aiding quick cooling of heat generated at the bit surface due to friction between bit and rock material. Thus, melting of the impregnated diamond matrix and consequently wear rate is avoided up to some extent. Also, as drilling of a particular hole was completed, the bit surface was wiped with the water-wet cotton and cooled further using a hair-dryer for a few seconds. In addition, during the entire drilling process, the drill bits were often visually inspected to ensure wear. If it was found worn out or damaged, immediately the drilling was carried out with a new drill bit.

2. During the drilling of each hole, when the drill bit was advanced through 5, 10, 15, 20, 25, and 30mm depth, the thrust induced and torque developed at the bit-rock interface were noted down using a digital indicator of the dynamometer. Later, the arithmetic average of six-thrusts and six-torques was calculated for a particular hole and used for analysis purpose. Similarly, for each hole, at least three times, the vibration signal of 1 sec with five iterations emanated from the drill head along with its frequency domain data extracted, as explained in section 3.4., was noted down at different depths randomly. It was observed that the vibration frequency data taken for a particular hole with particular machine conditions were consistent. However, the same procedure was followed to measure thrust, torque and vibration frequency for remaining drilling holes on the particular rock type.

3. Similarly, the same procedure was followed for the remaining five types of rocks. Thus a total of 162 (= 6 rocks  $\times$  27 test conditions) data set comprising each drilling response such as thrust, torque and vibration frequency are gathered. Later, they were used to develop multiple regression, ANN models, and computation of drilling-specific energy.

### **3.6 Determination of Actual Properties of Rocks at Laboratory**

Core specimens required to determine rock properties such as uniaxial compressive strength and Brazilian tensile strength in the laboratory are prepared as per the ISRM guidelines. Similarly, Schmidt rebound number and densities are determined using the rock block and core following the ISRM guidelines.

### 3.6.1 Uniaxial compressive strength (UCS)

UCS is an essential strength property of rocks used in many rock engineering applications. Fig.3.14 showing the AIM-317E-Mu compression testing equipment used to measure UCS in the present work. It has a loading unit with a maximum loading limit of 2000kN. To determine the UCS, NX-size core specimens, having a length and diameter of 54 mm and 135 mm, respectively, were prepared as per ISRM standards (Ulusay and Hudson 2007). At least five core specimens should be used to determine the UCS of each rock type. Before using the cores for testing, it was made dry using the electric oven. The specimen was subjected to a constant load rate of 1kN/sec in the testing machine until the cracks initiated (failure) in it. The UCS was calculated with the failure load and specimen dimensions using Eq.3.1. The essential statistical description of UCS is summarized in Table 3.2.

$$UCS(MPa) = \frac{F}{A} \quad (3.1)$$

Where, F = Failure load in Newton, and A = Area of specimen cross section in mm<sup>2</sup>



Fig. 3.14 UCS testing machine



Table 3.2 Laboratory test results of UCS

Rock types	Statistical description of UCS (MPa)			
	Min	Max	SD	Mean
Shale	19.3	19.8	0.27	19.6
Sandstone-1	37.2	37.9	0.35	37.5
Sandstone-2	64.1	65.3	0.61	65.1
Sandstone-3	72.1	72.9	0.40	72.4
Limestone-1	95.3	95.9	0.32	95.3
Limestone-2	118.6	119.6	0.46	119.2

### 3.6.2 Brazilian tensile Strength (BTS)

Tensile failure in rock will occur when the effective stress becomes tensile and equals or exceeds rock tensile strength. Usually, the rock materials exhibit low tensile strength due to the micro-crack presence in the rock materials. In this test, a Brazilian tensile strength (BTS) machine with a 100 kN loading capacity is used to determine the BTS, as shown in Fig.3.15. The large dial indicator calibrated in terms of kN is mounted on the machine, and each division represents 0.5 kN.

The core specimen was prepared as per the guideline of ISRM. A core specimen, having a 54mm diameter and a thickness of 27mm, was prepared. Any irregularities around the peripheral surface were removed using the polishing machine. Similarly, end faces were made flat and parallel to each other within the tolerance limit of 0.25 mm and 0.25 degrees, respectively. The load was continuously applied around the specimen's periphery until it failed within 15-30 seconds. The failure load was recorded in the dial indicator and was used to calculate the tensile strength of the rock using Eq.3.2. Five trials were conducted using five specimens, and the arithmetic average of all five test results was used for analysis purposes. The same procedure was conducted for other types of rocks. The essential statistical description of BTS is summarized in Table 3.3.

$$BTS(MPa) = \frac{2 \times F}{\pi \times D \times T} \quad (3.2)$$

Where

F = Failure load in Newton

D = Diameter of specimen in mm

T = Thickness of specimen in mm



Fig.3.15 Brazilian indirect tensile strength testing

Table 3.3 Laboratory test results of BTS

Rock types	Statistical description of BTS (MPa)			
	Min	Max	SD	Mean
Shale	1.465	1.621	0.125	1.613
Sandstone-1	3.514	3.648	0.051	3.452
Sandstone-2	4.054	4.350	0.154	4.219
Sandstone-3	7.406	7.692	0.128	7.504
Limestone-1	7.842	8.310	0.169	8.106
Limestone-2	7.918	8.241	0.216	8.721

### 3.6.3 Schmidt rebound number (SRN)

Schmidt rebound hammer tester as shown in Fig.3.16 was developed to measure the UCS of concrete indirectly by measuring its surface hardness. But later, it was extended to measure the hardness of rocks. It consists of a spring-loaded hammer that can be pressed against the material to be tested. Initially, ten points on the rock surface were marked at a regular interval using a chalk piece.



Fig. 3.16 Schmidt hardness tester

Table 3.4 Laboratory test results of SRN

Rock types	Statistical description of SRN			
	Min	Max	SD	Mean
Shale	21	25	1.41	23
Sandstone-1	40	44	1.35	42
Sandstone-2	46	51	1.85	49
Sandstone-3	48	53	1.85	51
Limestone-1	54	56	0.74	56
Limestone-2	58	62	1.31	59

At each point, the hammer was pressed against the rock by positioning the hammer vertically downward and same time holding the button located near the hammer. The scale measuring the rebounding displacement of the hammer is directly calibrated in

terms of a hardness number. Thus, the hardness of rocks can be measured at any point on the rock surface. The same procedure was repeated at all marked points and noted down the readings. The arithmetic mean value is calculated from ten values. The number close to the mean value is then selected as the final reading. The essential statistical description of SRN is summarized in Table 3.4.

### 3.6.4 Dry density of rock ( $\rho$ )

Density is a measure of mass per unit volume. The density of each rock type sample is determined after the removal of moisture from it. The moisture was removed by placing the samples in an electric oven at approximately 80°C at least for one hour and was allowed to dry at room temperature (Ulusay and Hudson 2007). After drying the sample, its weight was measured using a digital weighing machine. The volume of the core sample is measured by its dimensions. The density of the sample is measured using Eq.3.3.

$$\rho(\text{gm/cc}) = \frac{\text{Mass}}{\text{Volume}} \quad \text{gm/cc} \quad (3.3)$$

Table 3.5 Laboratory test results of density

Rock types	Statistical description of Density (g/cc)			
	Min	Max	SD	Mean
Shale	2.0389	2.0623	0.0078	2.0521
Sandstone-1	2.2058	2.2587	0.0199	2.2587
Sandstone-2	2.5489	2.5941	0.0155	2.5848
Sandstone-3	2.5801	2.5989	0.0087	2.5930
Limestone-1	2.6125	2.6521	0.0142	2.6589
Limestone-2	2.9210	2.9539	0.0115	2.9442

Three rock samples are used to measure the density of each rock. Later, the average value was calculated for each rock type and used for further data analysis. The primary statistical descriptions of the dry density of different sedimentary rocks are given in Table 3.5.

### **3.7 Summary**

This chapter mainly describes experimental methodology, experimental procedure, the machine and instruments used for drilling and the measurement of drilling responses. The determination of actual rock properties in the laboratory is also discussed.

# ***CHAPTER-4***

## **CHAPTER 4**

### **4. RESULTS OF EXPERIMENTAL INVESTIGATION**

#### **4.1 Importance of Drilling Responses Produced during the Rock Drilling Process**

During the rock drilling process, the strength of rock has a significant influence on the axial and rotational drilling force required. Therefore, to cause a rock to break during drilling is a matter of applying sufficient axial (thrust) and rotational force (torque) with a tool to exceed the strength of the rock (Hartman and Mutmansky 2002). During the drilling of particular rock strength, the thrust and torque are also depend on drill operating parameters such as drill bit diameter, spindle speed, and penetration rate. However, in this study, the relationship of acoustic drilling response (Kumar et al.2012; Khoshouei and Bagherpour, 2020), such as vibration frequency induced at the drill head during the drilling of different rock, is also investigated along with the thrust and torque.

#### **4.2 Influence of Drill Operating Parameters and UCS on Drilling Responses**

In this section, the trend of drilling responses is analyzed following the drill operating parameters such as penetration rate (PR), spindle speed (SS), and drill diameter (DD), and UCS of rocks since the UCS of the rock is used as the main strength property to analyze the feasibility of many rock engineering problems. Fig.4.1, 4.3, and 4.5 represent the trend of drilling responses such as thrust, torque, and vibration frequency, respectively, produced during the drilling of various compressive strength rocks at different drill operating parameters. As shown in Fig. 4.2 and 4.4, drill operating parameters and UCS of rocks could explain most of the variance in drilling thrust and torque, and they have a specific trend. The definite trend of vibration frequency is not explained by penetration rate and drill diameter as shown in Fig.4.5. However, it is observed that the spindle speed could explain most of the variance in

inducing vibration frequency at the drill head than the UCS, as shown in Fig.4.6. The entire drilling data, including drill responses, is shown in ANNEXURE-I.

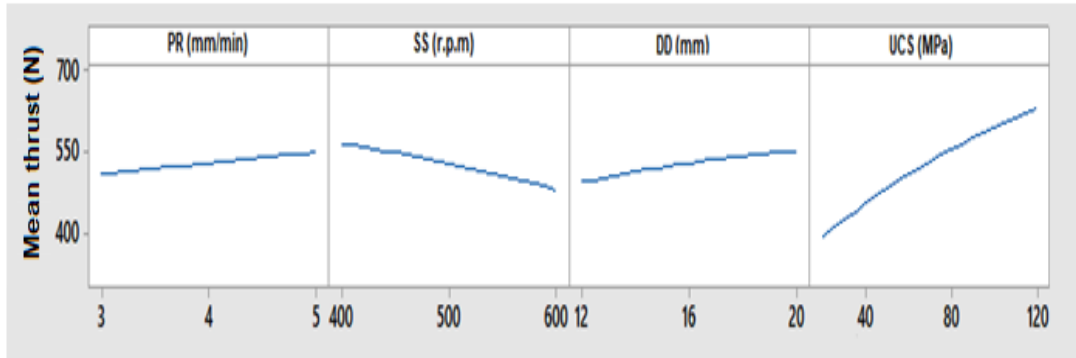


Fig 4.1 Main effect plots (Thrust)

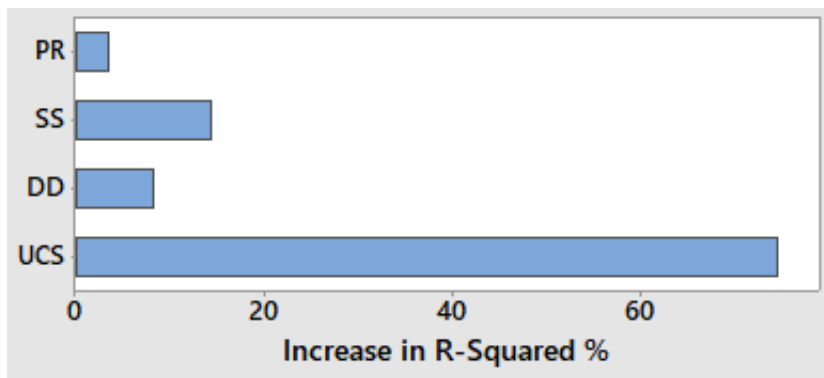


Fig 4.2 Incremental impact of variables on thrust

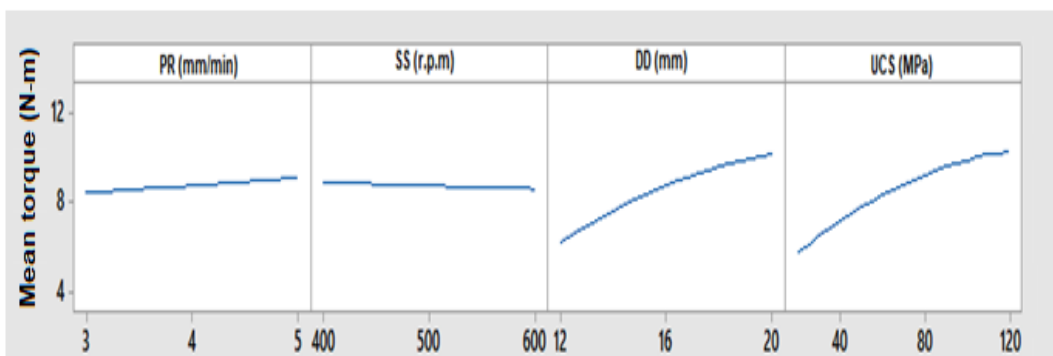


Fig 4.3 Main effect plots (Torque)





Fig 4.4 Incremental impact of variables on torque

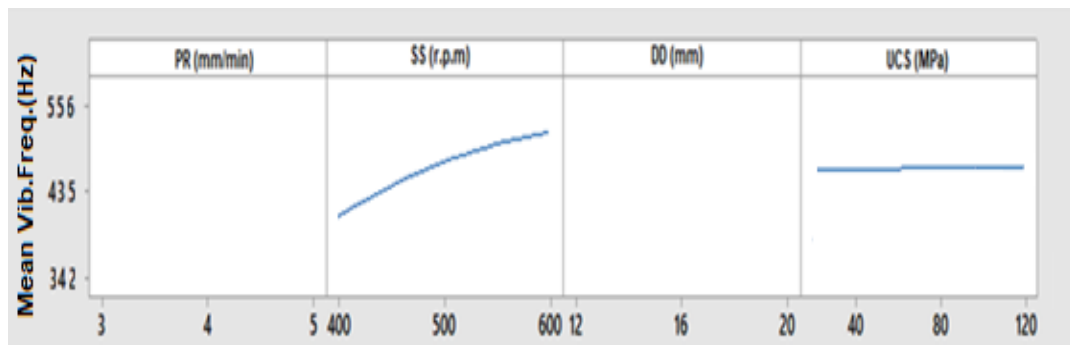


Fig 4.5 Main effect plots (Vibration frequency)

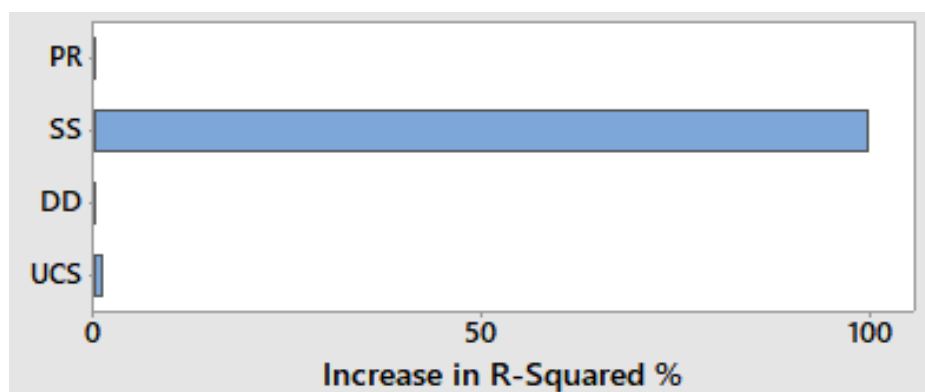


Fig 4.6 Incremental impact of variables on vibration frequency at drill head

### 4.3 Influence of penetration rate on drill thrust and torque at bit-rock interface during the drilling of different rocks

Fig.4.7 shows the variations of mean thrust and its level during the drilling of various rocks using different penetration rates (PR) with an average spindle speed and drill diameter of 500 r.p.m. and 16mm, respectively. During the drilling of any rock type, it was observed that as the PR increases from 3 to 4 mm/min and 4 to 5mm/min, the mean thrust level was increased (Abbas et al.2020) as shown in Table 4.1. The reason may be that as the penetration rate increases during the drilling of a particular rock type, the resistance offered by the rock may also increase. It is also observed with a particular PR that the mean thrust increases as the UCS and other properties of rock increase. It may be because as the strength and other properties of rocks are increasing, they may offer more resistance against drill bit PR. Since the CNC-vertical milling center used for drilling the rocks is equipped with the closed-loop control system, the machine could adjust the required higher thrust according to the increased PR and rock properties.

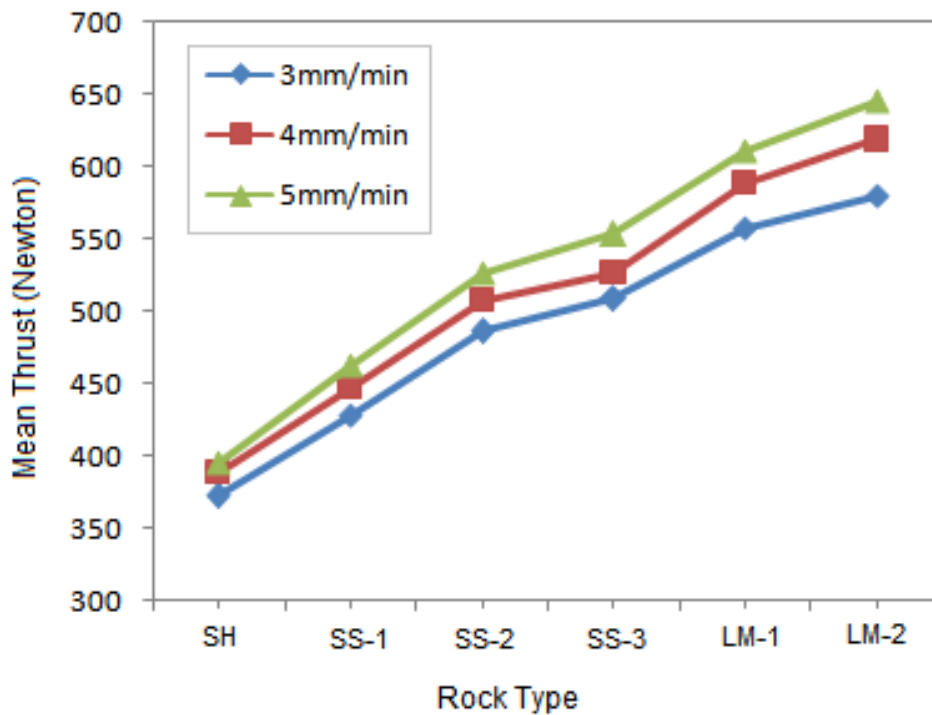


Fig. 4.7 Influence of penetration rate and rock properties on drill thrust

Table 4.1 Mean thrust at different penetration rate of drilling

Rock type (UCS in MPa)	Penetration Rate (mm/min)			
	3 mm/min	4 mm/min	5 mm/min	Change in %
Shale (SH)- 19.6 MPa	372	388	395	6.18 %
Sandstone-1(SS-1)- 37.5 MPa	427	447	462	8.19 %
Sandstone-2 (SS-2)-65.1 MPa	486	507	526	8.23 %
Sandstone-3 (SS-3)-72.4 MPa	508	526	553	8.85 %
Limestone-1 (LM-1)-95.3 MPa	558	588	610	9.31 %
Limestone-2 (LM-2)-119.2 MPa	580	618	645	11.20 %
Change in percentage (%)	55.91 %	59.27 %	63.29 %	-

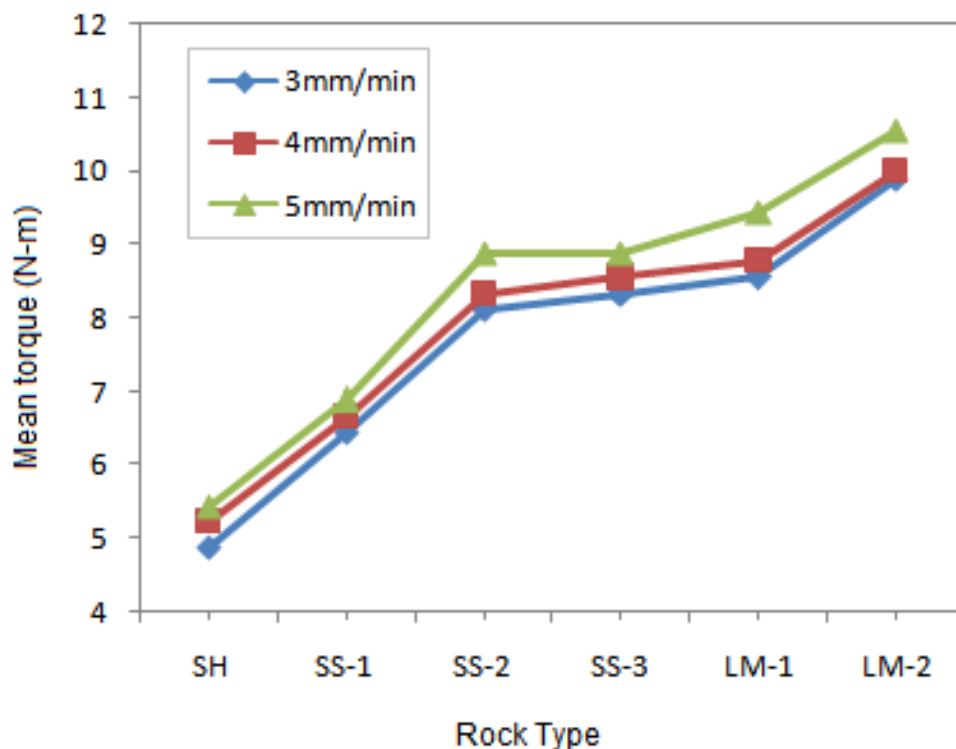


Fig. 4.8 Influence of penetration rate and rock properties on torque

Fig.4.8 shows the variations of mean torque and its level during the drilling of various rocks using different penetration rates (PR) with an average spindle speed and drill diameter of 500 r.p.m. and 16mm, respectively. During the drilling of any rock type, it was observed that as the PR increases from 3 to 4 mm/min and 4 to 5mm/min, torque

development at the bit-rock interface almost follows the same trend as that of thrust. Therefore, it can imply a linear relationship between thrust and torque (Bhatnagar.2011). It is also seen that the mean torque is almost increasing at a particular penetration rate as the UCS and other properties of rock increase. Table 4.2 shows the mean torque induced at the bit-rock interface during the drilling of various rocks with different PR.

Table 4.2 Mean torque at different penetration rate of drilling

Rock type (UCS in MPa)	Penetration Rate (mm/min)			
	3 mm/min	4 mm/min	5 mm/min	Change in %
Shale (SH)- 19.6 MPa	4.88	5.22	5.44	11.47 %
Sandstone-1(SS-1)- 37.5 MPa	6.44	6.66	6.88	6.83 %
Sandstone-2 (SS-2)-65.1 MPa	8.11	8.33	8.88	9.49 %
Sandstone-3 (SS-3)-72.4 MPa	8.33	8.55	8.91	6.96 %
Limestone-1 (LM-1)-95.3 MPa	8.55	8.77	9.44	10.40 %
Limestone-2 (LM-2)-119.2 MPa	9.88	10.11	10.55	6.78 %
Change in percentage (%)	102.45 %	93.67 %	93.93 %	-

#### 4.4 Influence of spindle speed on drill thrust and torque at bit-rock interface during the drilling of different rocks

Fig.4.9 shows the variations of mean thrust and its level during the drilling of various rocks using different spindle speeds with an average PR of 4mm/min and drill diameter of 16mm. During the drilling of any rock type, it was observed that the mean thrust level is decreasing as the spindle speed (SS) changes from 400 to 500 r.p.m. and 500 to 600 r.p.m.as shown in Table 4.3. Its reason may be that the drilling energy is the combination of thrust and rotational energy, as shown in Eq. 5.21 and, both would act during the drilling of a hole. However, when the spindle speed increases, the incremental change in speed may cause the increase of rotational energy, and that energy may assist in achieving the particular penetration rate rather than be assisted by the thrust energy. Due to this, the thrust energy may reduce at high spindle speed

(An et al. 2015; Abbas. et al. 2020). It is also seen that the mean thrust is increased at a particular speed as the UCS and other properties of rock increase. It may be because as the strength and other properties of rocks are increasing, they may offer more resistance against drill bit penetration at a particular speed.

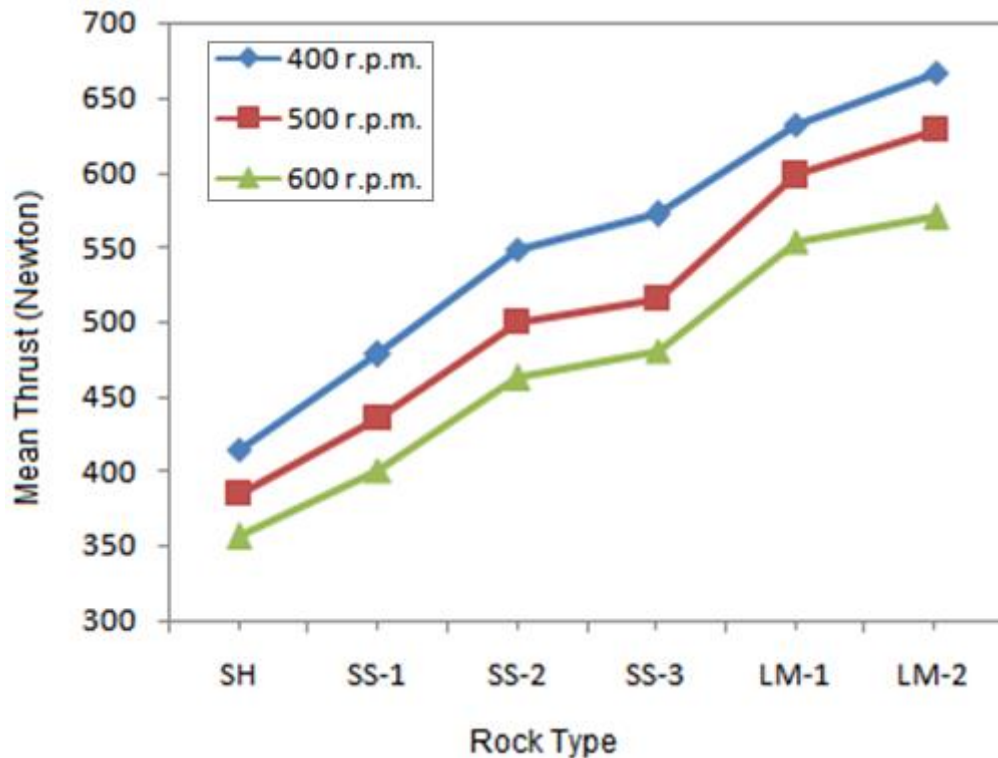


Fig. 4.9 Influence of spindle speed and rock properties on drill thrust

Fig.4.10 shows the variations of mean torque and its level during the drilling of various rocks using different spindle speeds with an average penetration rate and drill diameter of 4mm/min and 16mm, respectively. During the drilling of any rock type, it was observed that the torque level is decreasing as the spindle speed changes from 400 to 500 r.p.m. and 500 to 600 r.p.m.as shown in Table.4.4. However, the torque level developed at the bit-rock interface is not proportionately varying at different spindle speed for different rocks (Rao 2002; Bhatnagar et al. 2011). It is also seen that the torque is almost increasing at a particular spindle speed as the UCS and other properties of rock increase.

Table 4.3 Mean thrust at different spindle speed of drilling

Rock type (UCS in MPa)	Spindle speed (r.p.m.)			
	400 r.p.m.	500 r.p.m.	600 r.p.m.	Change in %
Shale (SH)- 19.6 MPa	414	385	356	16.29 %
Sandstone-1(SS-1)- 37.5 MPa	478	435	400	19.50 %
Sandstone-2 (SS-2)-65.1 MPa	548	501	462	18.61 %
Sandstone-3 (SS-3)-72.4 MPa	572	515	480	19.16 %
Limestone-1 (LM-1)-95.3 MPa	632	598	554	14.07 %
Limestone-2 (LM-2)-119.2 MPa	667	628	570	17.01 %
Change in percentage (%)	61.12 %	63.18 %	60.45 %	-

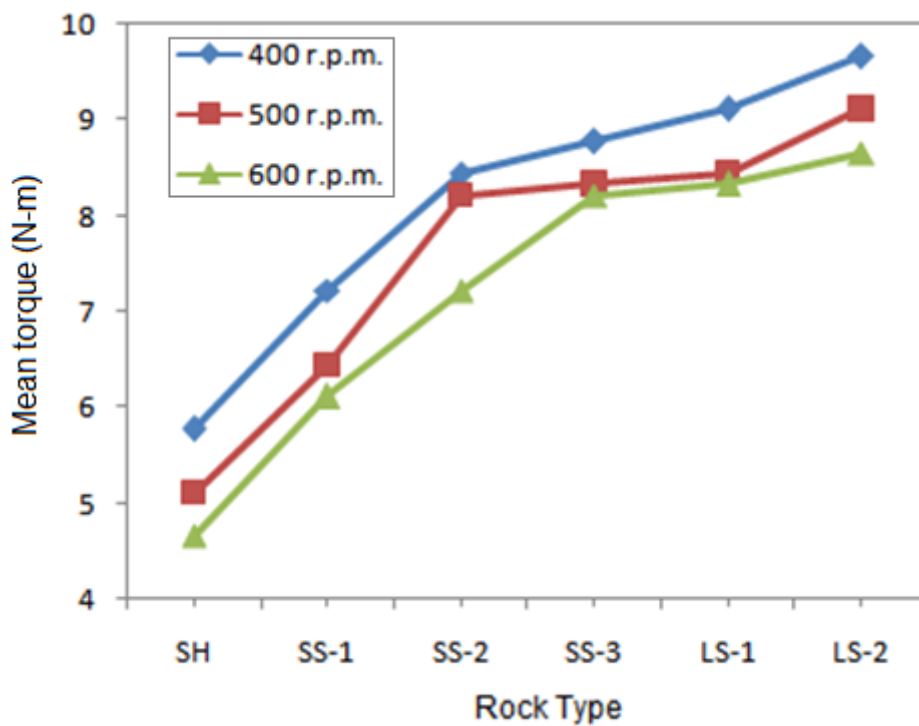


Fig. 4.10 Influence of spindle speed and rock properties on torque.

Table 4.4 Mean torque at different spindle speed of drilling

Rock type (UCS in MPa)	Spindle speed (r.p.m.)			
	400 r.p.m.	500 r.p.m.	600 r.p.m.	Change in %
Shale (SH)- 19.6 MPa	5.77	5.11	4.66	23.81 %
Sandstone-1(SS-1)- 37.5 MPa	7.22	6.44	6.11	18.16 %
Sandstone-2 (SS-2)-65.1 MPa	8.44	8.22	7.22	16.89 %
Sandstone-3 (SS-3)-72.4 MPa	8.77	8.33	8.22	6.69 %
Limestone-1 (LM-1)-95.3 MPa	9.11	8.44	8.33	9.36 %
Limestone-2 (LM-2)-119.2 MPa	9.66	9.11	8.66	11.54 %
Change in percentage (%)	67.41 %	78.27 %	85.83 %	-

#### 4.5 Influence of drill diameter on drill thrust and torque at bit-rock interface during the drilling of different rocks

Fig.4.11 shows the variations of mean thrust and its level during the drilling of various rocks using different drill diameters with an average penetration rate and spindle speed of 4mm/min and 500 r.p.m., respectively. During the drilling of any rock type, it was observed that the thrust level is increasing as the drill diameter (DD) changes from 12 to 16mm and 16 to 20mm. The reason may be that when the drilling hole area is increasing, the volume of the material to be removed also increases. For removing the higher volume, the machine may utilize the higher thrust. It is also seen that the mean thrust is increasing at a particular drill diameter as the UCS and other properties of rock increase. Table 4.5 shows the mean thrust induced at the bit-rock interface during the drilling of various rocks with different diameter bits.

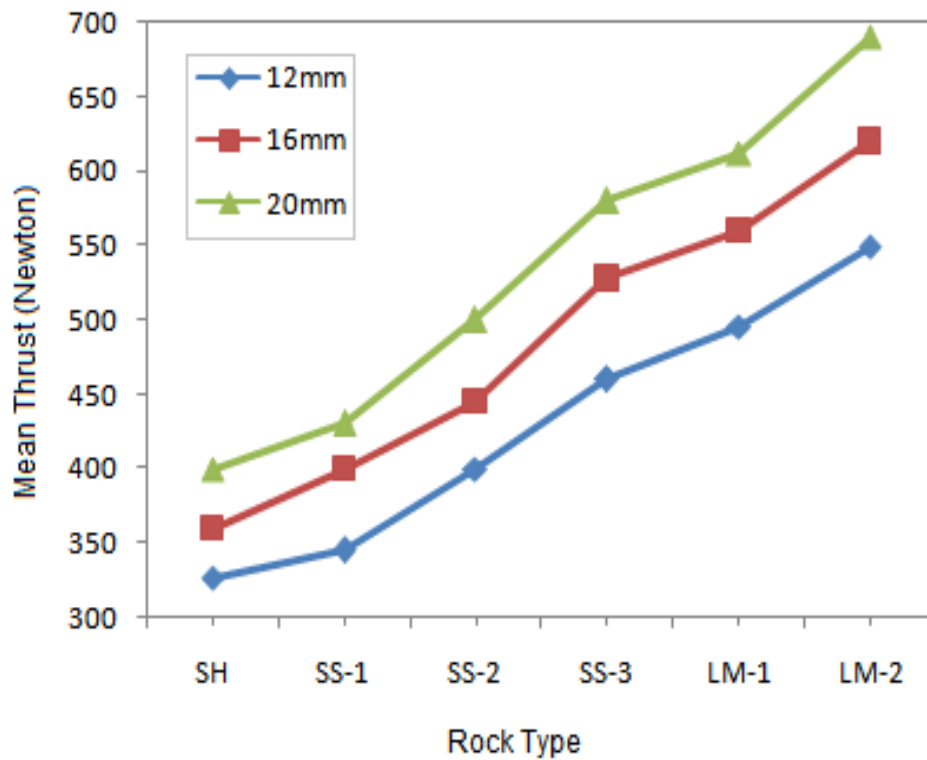


Fig. 4.11 Influence of drill diameter and rock properties on drill thrust

Table 4.5 Mean thrust at different drill diameters of drilling

Rock type (UCS in MPa)	Drill Diameter (mm)			
	12 mm	16 mm	20 mm	Change in %
Shale (SH)- 19.6 MPa	327	360	400	22.32 %
Sandstone-1(SS-1)- 37.5 MPa	345	401	430	24.63 %
Sandstone-2 (SS-2)-65.1 MPa	400	445	502	25.50 %
Sandstone-3 (SS-3)-72.4 MPa	460	527	580	26.08 %
Limestone-1 (LM-1)-95.3 MPa	495	560	612	23.63 %
Limestone-2 (LM-2)-119.2 MPa	550	620	690	25.45 %
Change in percentage (%)	68.19 %	72.22 %	72.51 %	-



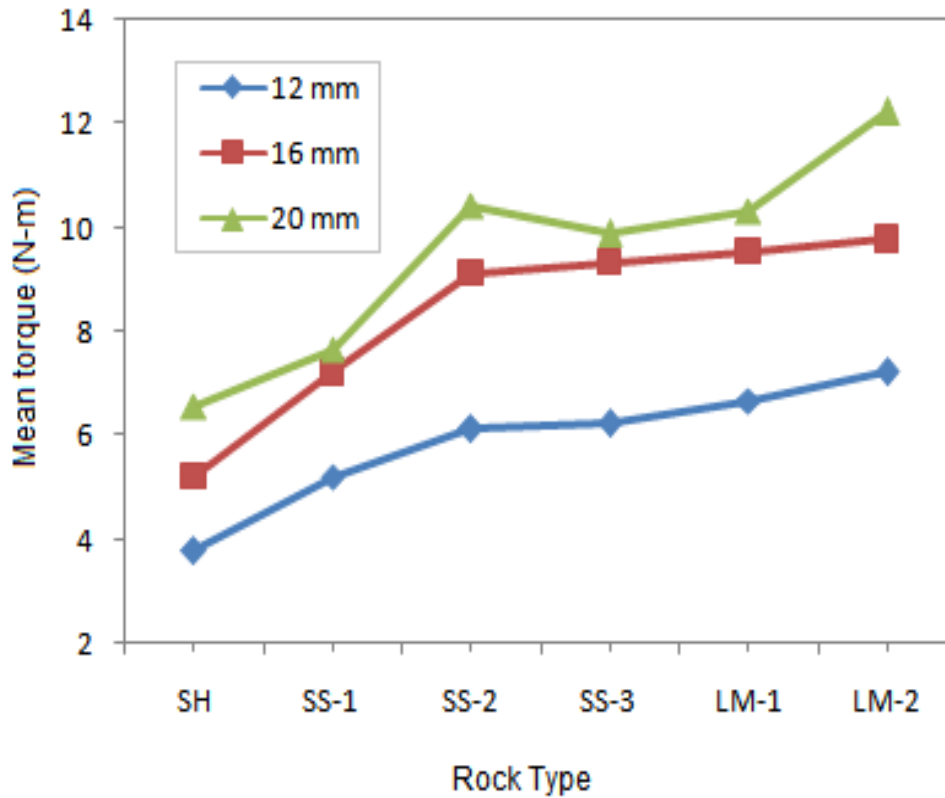


Fig. 4.12 Influence of drill diameter and rock properties on torque

Table 4.6 Mean torque at different drill diameter of drilling

Rock type (UCS in MPa)	Drill Diameter (mm)			
	12 mm	16 mm	20 mm	Change in %
Shale (SH)- 19.6 MPa	3.77	5.22	6.55	73.74 %
Sandstone-1(SS-1)- 37.5 MPa	5.22	7.22	7.66	46.74 %
Sandstone-2 (SS-2)-65.1 MPa	6.11	9.11	10.44	70.86 %
Sandstone-3 (SS-3)-72.4 MPa	6.22	9.33	9.88	58.84 %
Limestone-1 (LM-1)-95.3 MPa	6.66	9.55	10.33	55.10 %
Limestone-2 (LM-2)-119.2 MPa	7.22	9.77	12.22	69.25 %
Change in percentage (%)	91.15 %	87.16 %	86.56 %	-

Fig. 4.12 shows variations of mean torque and its level during the drilling of various rocks using different drill diameters with an average penetration rate and spindle speed of 4mm/min and 500 r.p.m., respectively. During the drilling of any rock type,

it was observed that the mean torque level is increasing as the drill diameter (DD) changes from 12 to 16mm and 16 to 20mm. The reason may be that the torque increases with the increase of thrust and drilling hole area (Chugh. 1992; Rao et al.2002). It is also seen that the torque is almost increasing at a particular drill diameter as the UCS and other properties of rock increase. Table 4.6 shows the mean torque developed at the bit-rock interface during the drilling of various rocks with different diameter drill bits.

#### 4.6 Influence of drill diameter on bit-pressure during the drilling of different rocks

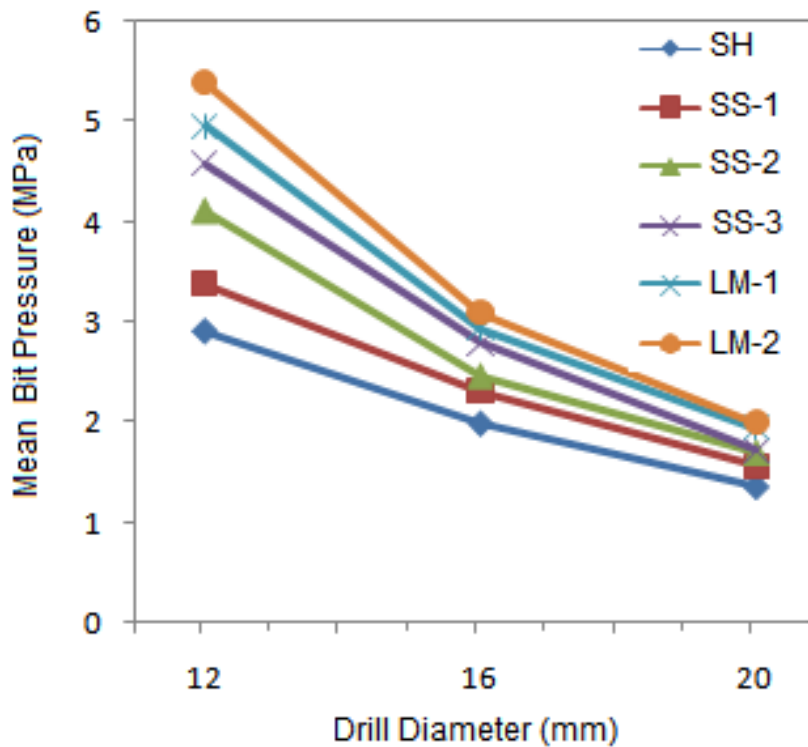


Fig. 4.13 Influence of drill diameter and rock properties on bit-pressure

Fig.4.13 shows the variation of mean bit-pressure and its level during the drilling of various rocks using different drill diameters with an average penetration rate and spindle speed of 4mm/min and 500 r.p.m., respectively. During the drilling of any rock type, it was observed that the mean bit-pressure is decreasing as the drill diameter (DD) changes from 12 to 16mm and 16 to 20mm. It may be due to that

although the thrust and bit contact area increases with the increase of drill diameter during the drilling of any rocks, it was observed that the increase in overall thrust is comparatively lower than the increase in overall bit area during the drilling of each rock type. Since the bit-pressure is the directly proportional thrust and inversely proportional to bit area, the bit pressure may reduce with an increase of drill bit diameter. It is also seen that the mean bit-pressure is increasing at a particular drill diameter as the UCS and other properties of rock increase. Table 4.7 shows the variation of mean bit-pressure and level for different bit diameters during the drilling of various rocks.

Table 4.7 Mean bit-pressure at different drill diameters of drilling

Rock type (UCS in MPa)	Bit-Pressure (MPa)			Change in %
	12 mm	16 mm	20 mm	
Shale (SH)- 19.6 MPa	2.89	1.98	1.36	112.5 %
Sandstone-1(SS-1)- 37.5 MPa	3.36	2.30	1.56	115.38 %
Sandstone-2 (SS-2)-65.1 MPa	4.12	2.45	1.69	143.78 %
Sandstone-3 (SS-3)-72.4 MPa	4.57	2.79	1.73	164.16 %
Limestone-1 (LM-1)-95.3 MPa	4.95	2.94	1.94	155.15 %
Limestone-2 (LM-2)-119.2 MPa	5.38	3.09	1.99	170.35 %
Change in percentage (%)	86.15 %	56.06 %	46.32 %	

#### 4.7 Influence of spindle speed on vibration frequency during the drilling of different rocks

Fig. 4.14 shows the variations of mean vibration frequency and its level during the drilling of various rocks using different drill bit speed with an average penetration rate and drill diameter of 4mm/min and 16 mm, respectively. It was observed that the mean vibration frequency is slightly increasing with the increase of rock properties. But, it is significantly increasing as the spindle speed is increasing. Table 4.8 shows the mean vibration frequency induced at the drill head during the drilling of various rocks with different spindle speeds.

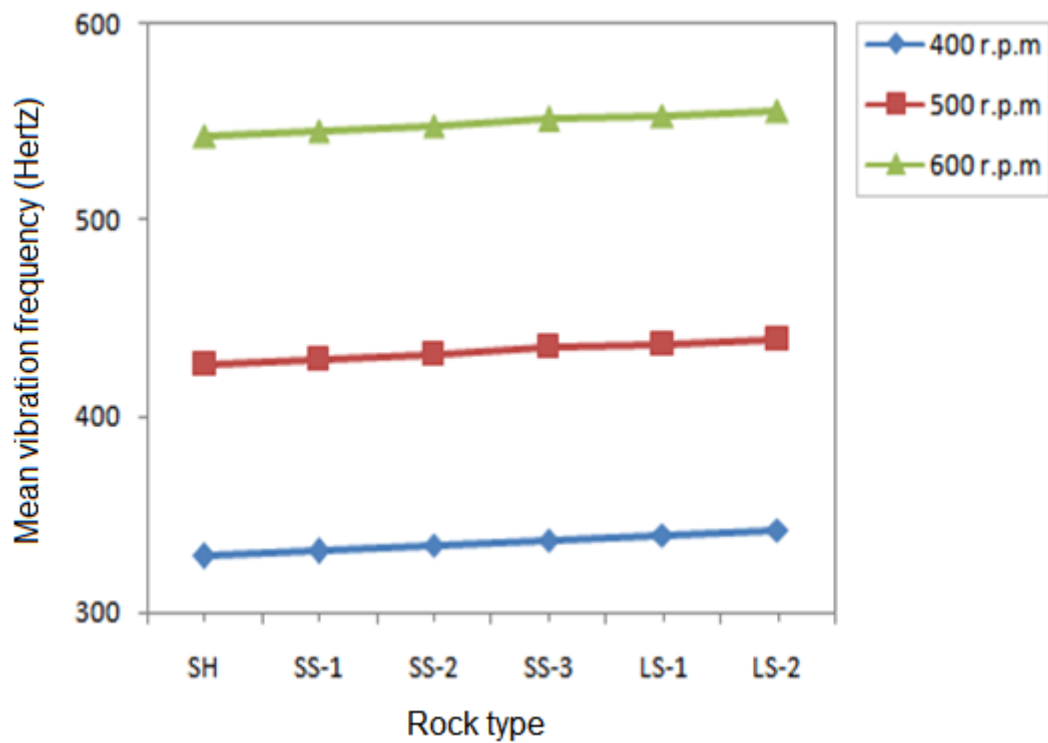


Fig. 4.14 Influence of spindle speed and rock properties on vibration frequency

Table 4.8 Mean vibration frequency at different spindle speeds of drilling

Rock type (UCS in MPa)	Vibration frequency(Hz)			
	400 r.p.m.	500 r.p.m.	600 r.p.m.	Change in %
Shale (SH)- 19.6 MPa	328	426	543	65.54 %
Sandstone-1(SS-1)- 37.5 MPa	331	429	546	64.95 %
Sandstone-2 (SS-2)-65.1 MPa	334	432	548	64.07 %
Sandstone-3 (SS-3)-72.4 MPa	337	435	551	63.50 %
Limestone-1 (LM-1)-95.3 MPa	339	436	552	62.83 %
Limestone-2 (LM-2)-119.2 MPa	340	439	553	62.64 %
Change in percentage (%)	3.65 %	3.05 %	1.84 %	-

#### **4.8 Summary**

During the drilling of different rocks considering various drill operating parameters, the variation of thrust produced and torque developed at bit-rock interface was significant. However, the vibration frequency at the drill head was less responsive compared to thrust and torque.



# ***CHAPTER-5***

## **CHAPTER 5**

### **5. STATISTICAL AND ANN MODELING**

#### **5.1 Introduction**

Statistics is the analytical science concerning with gather, analyzing, and interpreting scientific data. The statistical model is a powerful statistical tool used to develop a mathematical model from the continuous experimental data. For the development of a statistical model, the continuous variation of variables in a process is a prerequisite. The model also estimates the uncertainty interval of the scientific hypotheses and gives the average results of experiments to improve the accuracy of the results. The amount of error generated using a prediction model would give information regarding the performance of the model.

In the present study, the significance of drill operating parameters and drilling responses reflecting the physico-mechanical properties of sedimentary rocks are investigated using statistical analysis. A statistical model such as single and second-order multiple regression models is developed to predict each rock property. Along with regression analysis, "Analysis of variance" (ANOVA) is also generated to analyze the contribution of each drilling response to define the particular rock property. Besides, a soft computing technique known as the artificial neural network was also used to develop the model and analyzed statistical and soft computing techniques' comparative performance.

#### **5.2 Multiple Linear Regression Analysis**

The multiple linear regression method is one of the statistical techniques used to investigate and establish the relationship between a dependent and several predictor variables using mathematical relations. The mathematical modeling for Physico-mechanical properties such as UCS, BTS, SRN, and density are developed using the



drill operating variables and drilling responses. Minitab 18, statistical application software was used to perform statistical operations.

In this rock drilling process, the variations of drilling responses (thrust, torque, and vibration frequency) are assumed to be the function of drill operating parameters and physico-mechanical properties of rocks. The mathematical model for establishing the relationship between rock properties, drill operating parameters and drilling responses can be written as:

$$y = f(x_1, x_2, x_3, x_4, x_5, x_6) + \psi \tag{5.1}$$

In Eq. 5.1,  $x_1, x_2,$  and  $x_3$  are the drill operating variables such as penetration rate, spindle speed, drill bit diameter. Similarly,  $x_4, x_5,$  and  $x_6$  are the drilling responses, namely thrust, torque, and vibration frequency, and  $\psi$  is fitting error. The drill operating parameters are identified as penetration rate (PR) in mm/min, drill bit diameter (DD) in mm, and spindle speed (SS) in r.p.m. The drilling responses are thrust (T) in Newton, torque (TQ) in N-m, and vibration frequency (Z) in Hertz. Similarly, the rock properties such as uniaxial compressive strength, Brazilian tensile strength, Schmidt rebound number, and density are designated as UCS, BTS, SRN, and density, respectively. In general, if the model involves 'n' independent variables and a dependent variable, then correlation between them with a single order could be expressed as shown in Eq.5.2.

$$y = \beta_0 + \beta_1 x_1 + \beta_2 x_2 + \dots + \beta_n x_n + \psi \tag{5.2}$$

Where

$y$  = Dependent variable

$x_1, x_2, x_3 \dots x_n$  = Independent variables

$\beta_0, \beta_1, \beta_2, \dots, \beta_n$  = Regression coefficients

$\psi$  = Fitting error

Similarly, a second order multiple regression model may be expressed as shown in Eq.5.3.

$$y = a_o + \sum_{i=1}^n a_i x_i + \sum_{i=1}^n a_{ij} x_i^2 + \sum_{i < j}^n a_{ij} x_i x_j + \psi \tag{5.3}$$

In Eq. 2,  $a_o$  indicates the arbitrary constant,  $a_i$  signifies the linear source of  $x_i$ ,  $a_{ij}$  outlines the rectilinear source of  $x_i$ , and  $a_{ij}$  presented in the fourth term is generated

due to the multiplied results of  $x_i$  and  $x_j$ . The last term denoted by  $\psi$  represents the error.

### **5.3 Analysis of Variance (ANOVA)**

Analysis of variance or ANOVA is a statistical technique applied to check the significant variation between the mean of two or more groups. ANOVA is widely used to examine the quantitative influence of the independent variables over the dependent variable. In most of the statistical software, the ANOVA table would come up with a regression model. This analysis is also used to find the quality characteristic of the significant parameters. Similarly, F-test is a kind of statistical test that is quite flexible. F-tests can simultaneously assess many model terms, allowing them to analyze the fits of several linear models. In contrast, t-tests can evaluate just one term at a time. F value can be evaluated using the following equation (Kothari 1985).

$$F = \frac{\text{Estimate of population variance between sample variance}}{\text{Estimate of population variance within sample variance}} \quad (5.4)$$

### **5.4 Development of Multiple Regression Model for Physico-Mechanical Properties of Rocks including vibration parameter (Type-I)**

The Type-I multiple regression models are developed for physico-mechanical properties of rocks such as UCS, BTS, SRN, and density using the drilling responses, including thrust, torque and vibration frequency. For developing the prediction model for each rock property, 162 (= 6 rock types 27 test conditions) sets of experimental data including drill operating parameters, drill responses, and actual rock properties are used.

During the development of multiple regression models, the backward elimination method was used as a screening technique. For example, during the simulation of the regression model, the independent variables are removed from the variable list if the absolute  $t$  value of any independent variable is not greater than the tabulated  $t$  value at a 95% confidence level in the ANOVA table. In that case, that variable is removed from the variable list. The multiple regression procedure was then continued using the remaining independent variables until the remaining independent variables cannot be removed from the model, and thus the model is generated.

### 5.4.1 Development of regression model for prediction of UCS

The best-fit regression model for prediction of UCS is developed and is given in Eq.5.5.

$$UCS = -42.3 - 7.569 \times PR - 0.463 \times SS - 3.622 \times DD + 0.3225 \times T + 2.301 \times TQ + 0.560 \times Z \quad (5.5)$$

Table 5.1. Statistical results of UCS model

<b>A: Model summary (UCS)</b>				
R <sup>2</sup>	Adjusted R <sup>2</sup>	Predicted R <sup>2</sup>	Error	
94.49	94.28	93.98	7.99	
<b>B: Importance of model</b>				
Factor	Coefficient	t-value	p-value	
Constant	-42.3	-2.21	0.029	
PR	-7.569	-9.61	0.000	
SS	-0.463	-3.05	0.003	
DD	-3.622	-14.42	0.000	
T	0.3225	27.39	0.000	
TQ	2.301	5.66	0.000	
Z	0.560	4.03	0.000	
<b>C:ANOVA</b>				
Source	DF	Adj SS	F value	p-value
Regression	6	170100	443.34	0.000
PR	1	5902	92.30	0.000
SS	1	593	9.28	0.003
DD	1	13294	207.90	0.000
T	1	47990	750.47	0.000
TQ	1	2050	32.06	0.000
Z	1	1040	16.27	0.000
Error	155	9912	-	-
Total	161	180012	-	-

Table 5.1A shows that the developed model explains total variation in the observed UCS up to 94.49%. The importance of regression coefficients is shown in Table 5.1B. It was observed that the value of p for each variable is statistically significant as  $p < 0.05$  with a 95% confidence level. In addition, the determined  $\pm t$  values are also significantly greater than the tabulated t values (For 6 degrees of freedom, Total DF = generated DF - 1,  $t = 2.015$  at 95% confidence level). Therefore, the null hypothesis is rejected and concluded that there is statistical significance between predictors and

UCS. Among the drilling responses, the thrust (with an adjusted sum of the square = 47990 and F-Value = 750.47), as shown in the ANOVA Table.5.1C, is highly responsive for the variation of UCS. Besides, the computed F value is also very high indicating that the model's adequacy is good enough for prediction purposes.

Table 5.2 Actual and predicted values of Type-I UCS model

Rock type	Actual UCS (MPa)	Predicted UCS (MPa)	Error (%)
Shale (SH)	19.6	17.2	12.24
Sandstone-1(SS-1)	37.5	41.0	8.94
Sandstone-2 (SS-2)	65.1	66.9	2.82
Sandstone-3 (SS-3)	72.4	75.4	4.30
Limestone-1 (LM-1)	95.3	96.3	1.07
Limestone-2 (LM-2)	119.2	110.4	7.58

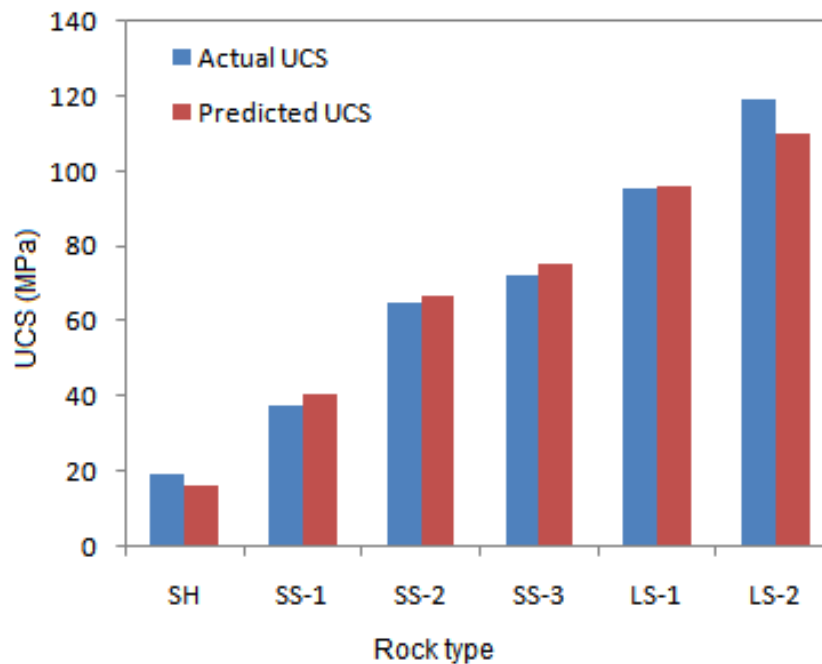


Fig: 5.1 Comparison of actual and predicted values of Type-I UCS model

In Table 5.2, the actual and predicted UCS of each rock type is summarized along with prediction error in percentage. Fig.5.1 shows the comparisons of actual and predicted UCS.

### 5.4.2 Development of regression model for prediction of BTS

The best-fit regression model for prediction of UCS is developed and is given in Eq.5.6

$$BTS = -0.91 - 0.5728 \times PR - 0.0582 \times SS - 0.2482 \times DD + 0.02508 \times T + 0.0989 \times TQ + 0.0642 \times Z \quad (5.6)$$

The BTS model could explain the complete variation in the actual BTS up to 88.12 %, as shown in Table 5.3A. The regression coefficients and their significance are shown in Table 5.3B. It was observed that the value of p for each variable is statistically significant as  $p < 0.05$  with a 95% confidence level.

Table 5.3 Statistical results of BTS model

<b>A: Model summary (BTS)</b>				
R <sup>2</sup>	Adjusted R <sup>2</sup>	Predicted R <sup>2</sup>	Error	
88.12	87.65	87.17	0.9355	
<b>B: Importance of model</b>				
Factor	Coefficient	t-value	p-value	
Constant	-0.91	-2.45	0.000	
PR	-0.5728	-6.21	0.000	
SS	-0.0582	-3.28	0.001	
DD	-0.2482	-8.45	0.000	
T	0.02508	18.21	0.000	
TQ	0.0989	3.95	0.000	
Z	0.0642	2.19	0.039	
<b>C:ANOVA</b>				
Source	DF	Adj SS	F value	p-value
Regression	6	1005.57	191.47	0.000
PR	1	33.80	38.62	0.000
SS	1	9.39	10.73	0.001
DD	1	62.45	71.34	0.000
T	1	290.25	331.60	0.000
TQ	1	13.65	4.32	0.000
Z	1	3.25	15.60	0.039
Error	155	135.68	-	-
Total	161	1141.25	-	-

Furthermore, the determined  $\pm t$  values exceeded the tabulated t values (For 6 degrees of freedom, Total DF = generated DF - 1,  $t = 2.015$  at 95% confidence level).

Therefore, the null hypothesis is rejected, and the alternate hypothesis, i.e., there is a statistical significance between predictors and BTS, is accepted. As shown in Table 5.3 C, the adjusted SS and F-value concluded that thrust is highly responsive to BTS variations among the drilling responses. Since the F-value of regression is high, it suggests that the overall fitting of the data to the model or its adequacy is good. The actual and predicted BTS of each rock type along with prediction error in percentage is summarized in Table 5.4. Fig.5.2 shows the comparisons of actual and predicted BTS.

Table 5.4 Actual and predicted values of Type-I BTS model

Rock type	Actual BTS (MPa)	Predicted BTS (MPa)	Error (%)
Shale (SH)	1.6	1.67	4.37
Sandstone-1(SS-1)	3.4	3.48	2.35
Sandstone-2 (SS-2)	4.2	4.02	4.28
Sandstone-3 (SS-3)	7.5	6.8	9.33
Limestone-1 (LM-1)	8.1	7.87	2.83
Limestone-2 (LM-2)	8.7	8.4	3.44

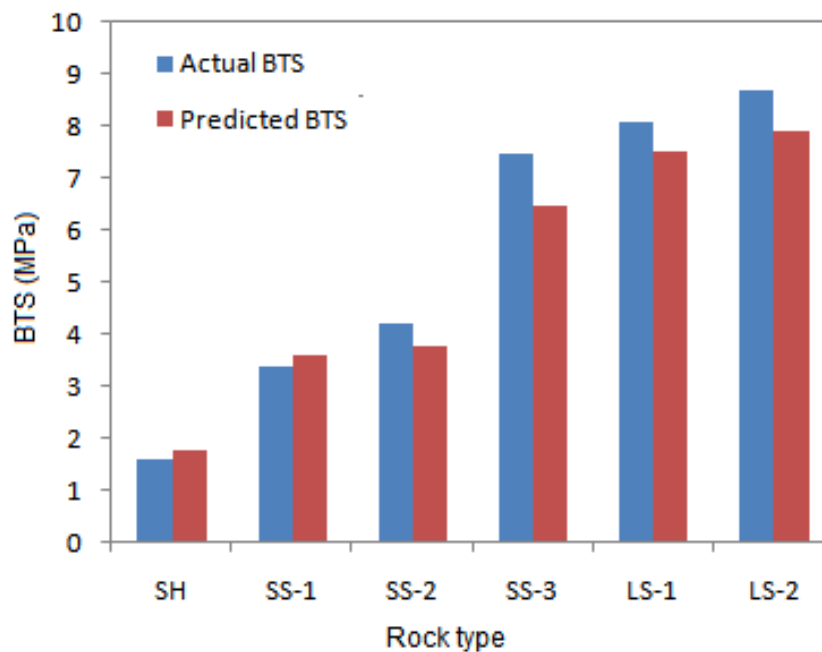


Fig.5.2 Comparison of actual and predicted values of Type-II BTS model

### 5.4.3 Development of regression model for prediction of SRN

The best-fit regression model for prediction of SRN is developed and is given in Eq.5.7

$$SRN = -12.06 - 2.678 \times PR + 0.04910 \times SS - 1.409 \times DD + 0.11276 \times T + 1.210 \times TQ \quad (5.7)$$

Table 5.5 Statistical results of SRN model

<b>A: Model summary (SRN)</b>				
R <sup>2</sup>	Adjusted R <sup>2</sup>	Predicted R <sup>2</sup>	Error	
87.76	87.37	86.69	4.23	
<b>B: Importance of model</b>				
Factors	Coefficients	t-value	p-value	
Constant	-12.06	-2.83	0.000	
PR	-2.678	-6.45	0.000	
SS	0.04910	10.72	0.000	
DD	-1.409	-10.74	0.000	
T	0.11276	20.76	0.000	
TQ	1.210	5.73	0.000	
<b>C: ANOVA</b>				
Source	DF	Adj SS	F value	p-value
Regression	5	20031	223.76	0.000
PR	1	744.7	41.59	0.000
SS	1	2026.6	114.87	0.000
DD	1	2064.9	115.33	0.000
T	1	7715.9	430.96	0.000
TQ	1	587.3	32.80	0.000
Error	156	2793.0	-	-
Total	161	22824.0	-	-

During the initial regression simulation for SRN, it was noted that the p-value for spindle speed was greater than 0.05. Also, the p-value for vibration frequency at the drill head was very close to the value of 0.05 (p=0.048). Since the thrust and torque are collected for different spindle speed with other drill operating parameters, it could not be omitted. Instead, the least influencing drilling response, i.e., vibration frequency, was omitted, and the regression process was simulated once again with the remaining variables. The results showed that the SRN model could explain the variations up to 87.76% in the actual SRN, as shown in Table 5.5A. The regression

coefficients and their significance are shown in Table 5.5B. Since the p-value of each independent variable is less than 0.05 at 95% confidence level, and similarly computed absolute t values (For 5 degrees of freedom, Total DF = Generated DF - 1,  $t = 2.132$  at 95% confidence level) are greater than the tabulated values, there is a significant statistical relationship between independent or predictors and dependent or SRN. As shown in Table 5.5 C, the adjusted SS and F-value concluded that thrust is highly responsive to SRN variations among the drilling responses. However, the adequacy of the model is also good as the overall F-value value of regression is high. . The actual and predicted SRN of each rock type along with prediction error in percentage is summarized in Table 5.6. Fig. 5.3 shows the comparison of the SRN of rocks measured in the laboratory and the SRN predicted using the regression model

Table 5.6 Actual and predicted values of Type-I SRN model

Rock type	Actual BTS (MPa)	Predicted BTS (MPa)	Error (%)
Shale (SH)	23	25.12	8.69
Sandstone-1(SS-1)	42	47.24	11.90
Sandstone-2 (SS-2)	49	43.79	12.24
Sandstone-3 (SS-3)	51	46.30	9.80
Limestone-1 (LM-1)	56	50.02	10.71
Limestone-2 (LM-2)	59	52.09	13.55

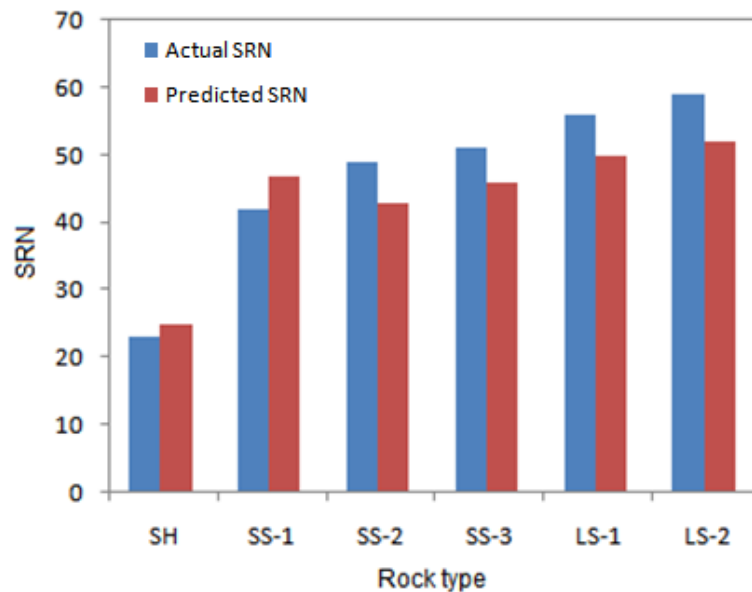


Fig.5.3 Comparison of actual and predicted values of Type-II SRN model



#### 5.4.4 Development of regression model for prediction of density

The best-fit regression model for prediction of density is developed and is given in Eq.5.8

$$\text{Density} = 1.584 - 0.06468 \times PR - 0.00320 \times SS - 0.03485 \times DD + 0.002598 \times T + 0.03038 \times TQ + 0.00404 \times Z \quad (5.8)$$

Table 5.7 Statistical results of Density model

<b>A: Model summary (Density)</b>				
R <sup>2</sup>	Adjusted R <sup>2</sup>	Predicted R <sup>2</sup>	Error	
92.06	91.75	91.35	0.084	
<b>B: Importance of model</b>				
Factor	Coefficient	t-value	p-value	
Constant	1.584	7.91	0.000	
PR	-0.06468	-7.86	0.000	
SS	-0.00320	-2.02	0.045	
DD	-0.03485	-13.28	0.000	
T	0.002598	21.13	0.000	
TQ	0.03038	7.15	0.000	
Z	0.00404	2.79	0.006	
<b>C:ANOVA</b>				
Source	DF	Adj SS	F value	p-value
Regression	6	12.5396	299.40	0.000
PR	1	0.4310	61.74	0.000
SS	1	0.0285	4.08	0.045
DD	1	1.2312	176.38	0.000
T	1	3.1152	446.28	0.000
TQ	1	0.3572	51.17	0.000
Z	1	0.0542	7.76	0.006
Error	155	1.0820	-	-
Total	161	13.6216	-	-

Table 5.8 Actual and predicted values of Type-I density model

Rock type	Actual density gm/cc	Predicted density gm/cc	Error (%)
Shale (SH)	2.0521	2.0741	1.07
Sandstone-1(SS-1)	2.2587	2.2882	1.30
Sandstone-2 (SS-2)	2.5848	2.5190	2.54
Sandstone-3 (SS-3)	2.593	2.5838	9.80
Limestone-1 (LM-1)	2.6589	2.7556	3.63
Limestone-2 (LM-2)	2.9542	2.8838	2.38

Table 5.7A shows that the generated model explains the total variation in the actual density up to 92.06%. The value of regression coefficients and their importance is shown in Table 5.7B. The value of p for all variables is statistically significant as their  $p < 0.05$  with a 95% confidence level. Besides, the computed  $\pm t$  values are more than tabulated t values (For 6 degrees of freedom, Total DF = generated DF - 1,  $t = 2.015$  at 95% confidence level). Therefore, the model could be selected as a valid one for the estimation of density. The influence of drilling response on defining the density is shown in Table 5.7C. From the higher adjusted SS and F-value, it is concluded that thrust is a major drilling response followed by torque. Since the overall F-value of regression is high, it implies that the overall fitting of the data to the model or its adequacy for prediction purposes is good. Table 5.8 shows the actual and predicted density of each rock type along with prediction error in percentage. Fig. 5.4 compares the density of rocks measured in the laboratory, and the density predicted using the regression model.

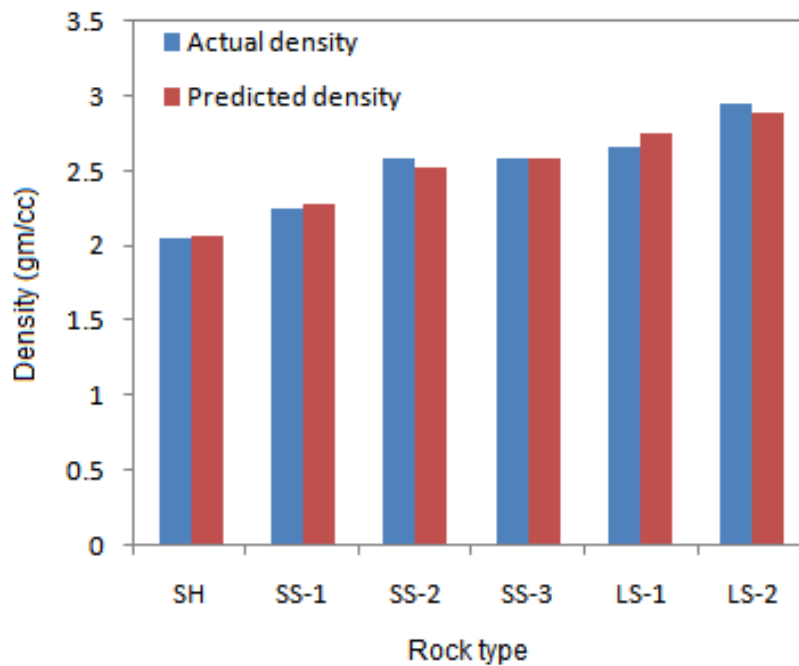


Fig.5.4 Comparison of actual and predicted values of Type-II density model

## 5.5 Evaluation of Prediction Performance of Type-I Models

The efficiency or performance of any developed model needs to be checked to ensure its applicability. In the present study, the prediction performances of the developed models are investigated using the three indices known as variance account for (VAF), root mean square error (RMSE) and mean absolute percentage error (MAPE), as shown in Eq.5.9 – 5.11, respectively.

$$VAF = \left[ 1 - \frac{\text{var}(m - p)}{\text{var}(m)} \right] \times 100 \quad (5.9)$$

$$RMSE = \sqrt{\frac{1}{N} \sum_{i=1}^N (m - p)^2} \quad (5.10)$$

Where ‘ $m$ ’ and ‘ $p$ ’ are measured and predicted values of a response, respectively, and  $N$  is the data size. The model would predict the response with 100% perfection with zero errors if VAF and RMSE values are 100 and 0, respectively. The mean absolute percentage error (MAPE) is a statistical measure of how accurate a prediction model would perform, and measures the accuracy as a percentage and can be calculated as follows:

$$MAPE = \frac{1}{N} \sum_{i=1}^N \left| \frac{(m - p)}{m} \right| \times 100 \quad (5.11)$$

Table 5.9 Performance indices of Type-I models

Response	Indices of Model Performance			
	VAF (%)	RMSE (DV unit)	NRMSE (%)	MAPE (%)
UCS (MPa)	94.49	7.84	7.87	9.51
BTS (MPa)	88.12	0.91	12.81	9.58
SRN (MPa)	<b>87.76</b>	4.15	11.49	7.35
Density(gm/cc)	92.06	0.10	11.03	2.70

Normalizing the RMSE, identified as NRSME, may be useful to make RMSE scale-free by converting it into a percentage using the Eq.5.12.

$$NRSME = \frac{RMSE}{(Max(DV) - Min(DV))} \quad (5.12)$$

Where

DV = Dependent variable

The value of performance indices for each rock property is shown in Table 5.9. It is observed that the independent variables explain more than 85% variance in the dependent variable in all cases. Similarly, the normalized root mean square error (NRMSE) and MAPE values for all rock properties are within the acceptable limit (less than 15%). Therefore, the type-I models developed with single-order multiple regression methods can predict the physico-mechanical properties with an acceptable error.

## 5.6 Correlations Strength between UCS and Drilling Responses

For most engineering structures like underground mines, foundations for reservoirs, civil constructions, and many rock engineering projects, it could observe that the supporting rocks would be subjected to compression loading. Uniaxial compressive strength is a strength parameter that measures the bearing capacity of the compression loading. Therefore the UCS is a quite interesting strength parameter to study. In this investigation, the drilling responses are collected during the drilling of various rocks having different UCS and other rock properties. The significance of the correlation between drilling responses and UCS is checked using the Pearson correlation coefficient, as shown in Table 5.10. The Pearson correlation coefficient is used to investigate the strength of the relationship between two variables and is designated by the letter 'R'. Mathematically, and it can be written as shown in Eq.5.13.

$$R = \frac{\sum_{i=1}^n (x_i - \bar{x})(y_i - \bar{y})}{\sqrt{\sum_{i=1}^n (x_i - \bar{x})^2} \sqrt{\sum_{i=1}^n (y_i - \bar{y})^2}} \quad (5.13)$$

Table 5.10 Cross correlation matrix.

Source	Thrust (T)	Torque (TQ)	Vibration Frequency (Z)	UCS
Thrust (T)	1	0.648	-0.285	0.844
Torque (TQ)	0.648	1	-0.005	0.580
Vibration Frequency (Z)	-0.285	-0.005	1	0.051
UCS	0.844	0.580	0.051	1

Table 5.11 Standard statistical table for strength of correlation

Strength of correlation	Range of absolute correlation coefficient (r)
Very strong	0.91-1.0
Strong	0.71-0.9
Moderate	0.51-0.7
Weak	0.31-0.5
Very weak	0.01-0.3

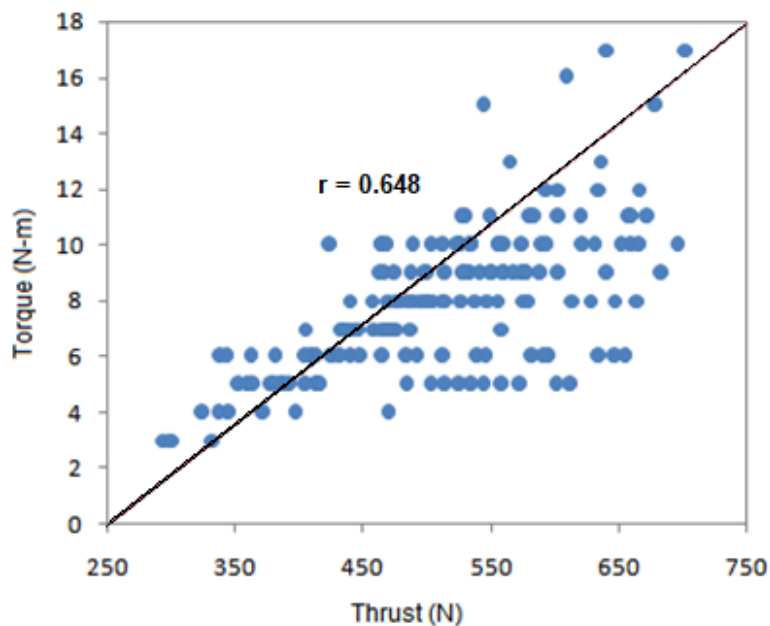


Fig.5.5 Variations of thrust and torque

In Eq.5.13,  $x_i$  and  $y_i$  are the individual data points, and  $\bar{x}$  and  $\bar{y}$  are the average value of  $x$  and  $y$  data set respectively. As per the standard statistical table for the strength of the correlations, as shown in Table 5.11, it was concluded that the thrust has strong correlation strength with UCS, with  $R = 0.844$ . Similarly, the torque has a moderate correlation strength with UCS, with  $R = 0.580$ . The vibration frequency induced at the drill head has very weak correlation strength with UCS, with  $R = 0.051$ . However, the

strength of the relationship between thrust and torque is moderate with  $R = 0.648$  and has an almost positive linear relationship, as shown in Fig.5.5.

### 5.7 Development of Multiple Regression Model for Physico-Mechanical Properties of Rocks Excluding Vibration Parameter (Type-II)

The performance indices and validation of Type-I models, as shown in Tables 5.9 and 5.17A, respectively, indicated that the Type-I predictive models could predict the rock properties with acceptable errors, i.e., below 15%. However, the main problem associated with this method is capturing the vibration frequency at the drill head. Since the vibration frequency is less responsive to UCS as shown in Table 4.8 and Fig.4.14 and also capturing the vibration frequency at the drill head is a tedious, time-consuming and expensive process, the extended investigation on the prediction of rock properties using only thrust and torque data may have a wide scope.

Therefore, alternative prediction models identified by Type-II are developed by excluding the vibration data due to its high cost and lack of statistical significance. The Type-II models are developed for each rock property using thrust and torque data, as shown in Eq.5.14 – 5.17.

#### 5.7.1 Type-II UCS model

$$\begin{aligned}
 UCS = & 316.6 + 12.90 \times PR - 0.758 \times SS - 5.646 \times DD - 0.6702 \times T + 5.34 \times TQ \\
 & + 0.000498 \times S^2 + 0.000873 \times T^2 - 0.04175 \times PR \times T + 0.000838 \times SS \times T \\
 & + 0.2989 \times DD \times TQ - 0.01433 \times T \times TQ
 \end{aligned} \tag{5.14}$$

Table 5.12 Actual and predicted values of Type-II UCS model

Rock type	Actual UCS (MPa)	Predicted UCS (MPa)	Error (%)
Shale (SH)	19.6	17.2	12.56
Sandstone-1(SS-1)	37.5	41.0	4.63
Sandstone-2 (SS-2)	65.1	66.9	2.16
Sandstone-3 (SS-3)	72.4	75.4	1.93
Limestone-1 (LM-1)	95.3	96.3	2.10
Limestone-2 (LM-2)	119.2	110.4	3.06

In Table 5.12, the actual and predicted values of Type-II UCS model for each rock type is summarized along with prediction error in percentage. Fig.5.6 shows the comparisons of actual and predicted UCS.

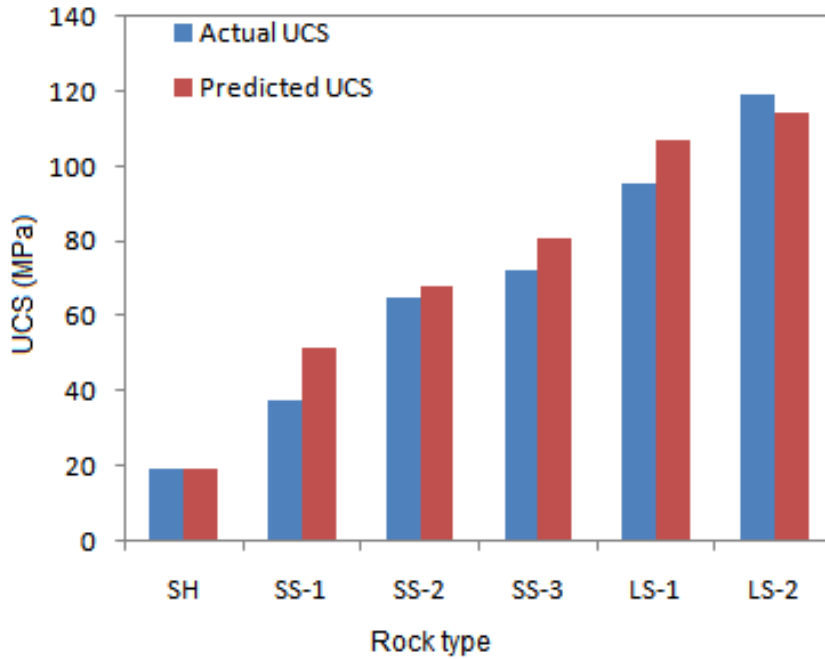


Fig.5.6 Comparison of actual and predicted values of Type-II UCS model

### 5.7.2 Type-II BTS model

$$\begin{aligned}
 BTS = & 12.51 + 0.503 \times PR - 0.0445 \times SS - 0.4124 \times DD - 0.0066 \times T - 0.035 \times TQ \\
 & + 0.000036 \times S^2 + 0.000026 \times T^2 - 0.00221 \times PR \times T + 0.000042 \times S \times T \\
 & + 0.0217 \times DD \times TQ - 0.000394 \times T \times TQ
 \end{aligned} \tag{5.15}$$

Table 5.13 Actual and predicted values of Type-II BTS model

Rock type	Actual UCS (MPa)	Predicted UCS (MPa)	Error (%)
Shale (SH)	1.6	1.67	4.37
Sandstone-1(SS-1)	3.4	3.48	2.35
Sandstone-2 (SS-2)	4.2	4.02	4.28
Sandstone-3 (SS-3)	7.5	6.8	9.33
Limestone-1 (LM-1)	8.1	7.87	2.83
Limestone-2 (LM-2)	8.7	8.4	3.44

In Table 5.13, the actual and predicted values of Type-II BTS model for each rock type is summarized along with prediction error in percentage. Fig.5.7 shows the comparisons of actual and predicted BTS.

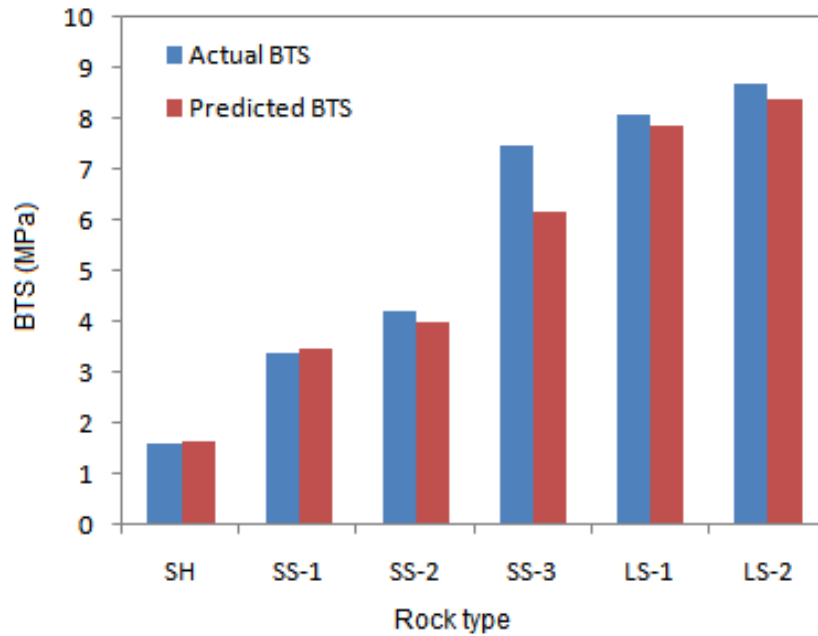


Fig.5.7 Comparison of actual and predicted values of Type-II BTS model

### 5.7.3 Type-II SRN model

$$\begin{aligned}
 SRN = & 46 - 3.40 \times PR - 0.0041 \times SS - 13.36 \times DD + 0.2105 \times T + 8.84 \times TQ \\
 & + 0.0615 \times D^2 - 0.000178 \times T^2 + 0.00725 \times PR \times SS - 0.3569 \times PR \times DD \\
 & + 0.401 \times PR \times TQ + 0.00717 \times SS \times DD - 0.000115 \times SS \times T - 0.00450 \times SS \times TQ \\
 & + 0.01510 \times DD \times T - 0.01324 \times T \times TQ
 \end{aligned} \tag{5.16}$$

Table 5.14 Actual and predicted values of Type-II SRN model

Rock type	Actual SRN	Predicted SRN	Error (%)
Shale (SH)	23	24.93	8.40
Sandstone-1(SS-1)	42	39.13	6.82
Sandstone-2 (SS-2)	49	49.53	1.09
Sandstone-3 (SS-3)	51	49.58	2.77
Limestone-1 (LM-1)	56	56.71	1.28
Limestone-2 (LM-2)	59	58.12	1.47



Table 5.14 shows the actual and predicted values of the Type-II SRN model for each rock type is summarized along with prediction error in percentage. Fig.5.8 shows the comparisons of actual and predicted SRN.

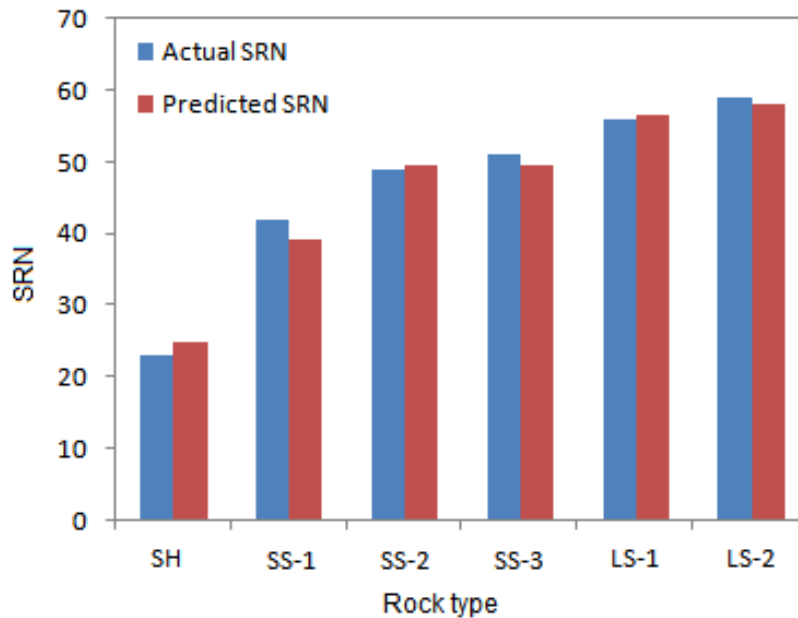


Fig.5.8 Comparison of actual and predicted values of Type-II SRN model

#### 5.7.4 Type-II density model

$$\begin{aligned}
 \text{Density} = & 1.647 + 0.0237 \times PR + 0.000560 \times SS - 0.0881 \times DD + 0.003386 \times T \\
 & - 0.0623 \times TQ - 0.003544 \times TQ^2 - 0.000166 \times PR \times T + 0.000086 \times SS \times TQ \\
 & + 0.00690 \times DD \times TQ
 \end{aligned} \tag{5.17}$$

Table 5.15 shows the actual and predicted values of the Type-II density model for each rock type is summarized along with prediction error in percentage. Fig.5.9 shows the comparisons of actual and predicted density.

Table 5.15 Actual and predicted values of Type-II density model

Rock type	Actual density gm/cc	Predicted density gm/cc	Error (%)
Shale (SH)	2.0521	2.0724	0.96
Sandstone-1(SS-1)	2.2587	2.2713	0.55
Sandstone-2 (SS-2)	2.5848	2.5689	0.61
Sandstone-3 (SS-3)	2.5932	2.5899	0.12
Limestone-1 (LM-1)	2.6589	2.7052	1.74
Limestone-2 (LM-2)	2.9542	2.9125	1.42

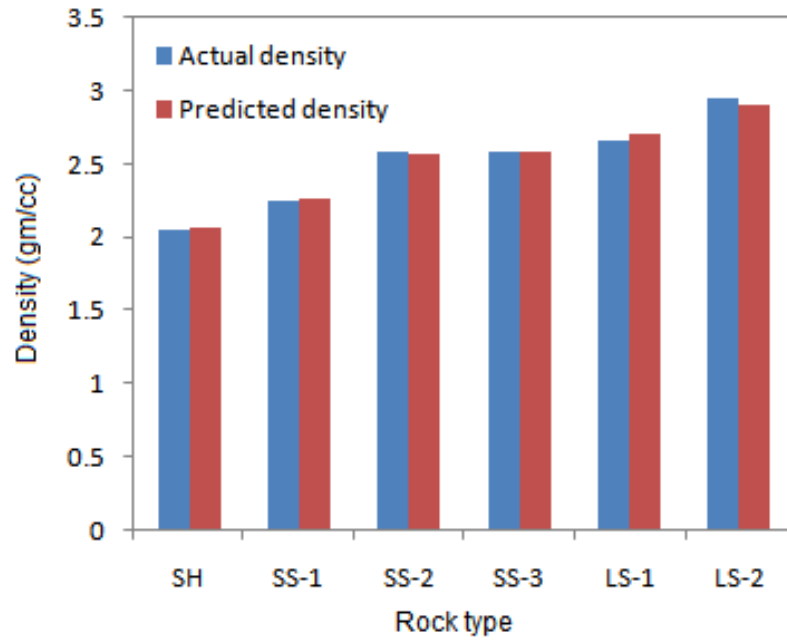


Fig.5.9 Comparison of actual and predicted values of Type-II density model

Table 5.2, 5.4, 5.6 and 5.8 shows the actual and predicted values of UCS, BTS, SRN and density, respectively using the Type-I models. Similarly, Table 5.12, 5.13, 5.14 and 5.15 shows the actual and predicted values of UCS, BTS, SRN and density, respectively using the Type-II models. From the comparative results of both Type-I and Type-II, it was observed that the Type-II models could predict the responses, i.e., UCS, BTS, SRN and density for each rock type, far better than the Type-I models with less prediction percentage error.

Table 5.16 Performance indices of the Type-II models

Response	Indices of Model Performance			
	VAF (%)	RMSE (DV unit)	NRMSE (%)	MAPE (%)
UCS (MPa)	97.52	5.27	5.29	7.74
BTS (MPa)	89.92	0.87	12.25	8.18
SRN (MPa)	96.04	2.59	7.19	4.63
Density(gm/cc)	93.71	0.079	7.86	2.46

It was also found that the second-order Type-II regression models could predict the rock properties comparatively better than the Type-I model, with a high  $R^2$  value and less NRMSE and MAPE, as shown in Table 5.16.

### 5.8 Validation of Type-I and Type-II UCS models.

The validation of the UCS models developed with both Type-I and Type-II approaches is checked using separate rocks such as shale, sandstone, and limestone blocks with the UCS, 14.21 MPa, 35.89 MPa, and 46.78 MPa, respectively. Each block was drilled using a set of drill operating parameters, and corresponding drilling responses were collected. The collected drilling responses were then assigned to the UCS model developed with Type-I and Type-II method, and thus the UCS was computed. The validation results are showing in Table.5.17. As shown in Table 5.17A and 5.17B, the Type-II UCS model can better predict the response, i.e., UCS, than the Type-I UCS model with less prediction error.

Table 5.17 Validation of UCS model

<b>A: Type-I model</b>				
Rock type	Actual UCS(MPa)	Predicted UCS(MPa)	Error	Percentage error
Shale	14.21	12.86	-1.35	9.5%
Sandstone	35.89	32.13	-3.76	10.4%
Limestone	46.78	43.29	-3.49	7.46%
<b>B: Type-II mode</b>				
Rock type	Actual UCS(MPa)	Predicted UCS(MPa)	Error	Percentage error
Shale	14.21	13.24	-0.97	6.82%
Sandstone	35.89	33.45	-2.44	6.79%
Limestone	46.78	44.59	-2.19	4.68%

### 5.9 ANN Modeling

Though relations developed among the variables using the statistical regression model are good enough to predict the response, they are confined by the degree of nonlinearity they could represent. This problem could be solved using the new soft computing technique known as the artificial neural network (ANN) model. In reality, an ANN tries to get a nonlinear association between independent and dependent variables. A simulation procedure of this sort is beneficial when there is a complicated nonlinear connection between input and output parameters (Dehghan et al.2010).ANN models are most suitable for cases where no definite mathematical relationship between the predictors and response or the relationship to be resolved is complex and

consumes much time (Zarin Pour, 2014). Its compatibility for multi-disciplines and performance would make the ANN so popular in engineering research.

ANN mirrors a biological brain, as shown in Fig.5.10. In the brain, there is a stream of coded information from the synapses towards the axon. The axon of each neuron sends information to several other neurons. The neuron receives the information at the synapses from a large number of other neurons. Groups of neurons are formed into subsystems, and integration of these subsystems form the brain. Fig.5.11 shows the simplified model of an artificial neuron that may simulate some important aspects of a real biological neuron. An ANN is a group of interconnected artificial neurons, interacting with one another in a concerted manner. In such a system, excitation is applied to the input of the network. Following some suitable operation, it results in the desired response. At synapses, there is an accumulation of some potential, which in the case of artificial neurons is modelled as connection weights. These weights are continuously modified based on suitable learning rules.

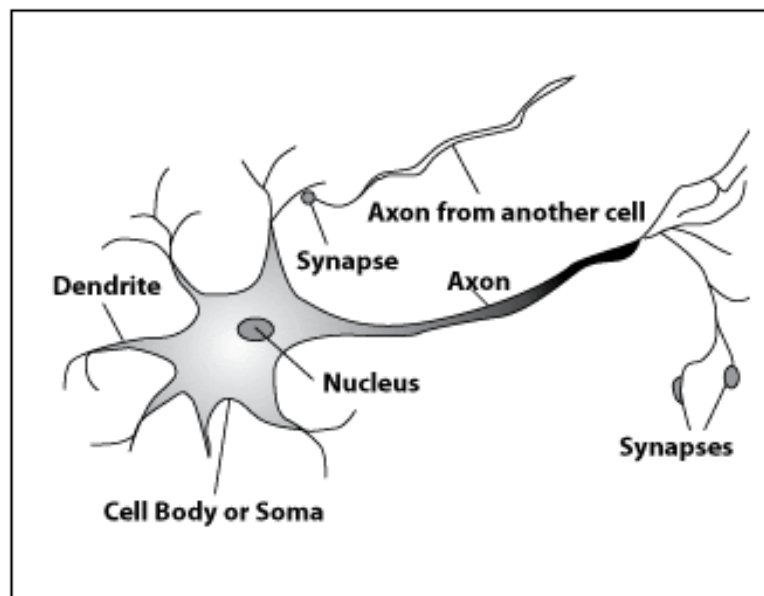


Fig.5.10 A biological neuron

**Dendrites:** Receives inputs, **Soma:** Process the inputs, **Axon:** Turn the processed inputs to outputs, **Synapses:** The electro mechanical contact between the neurons.

ANN is made of many neurons and a huge number of interactions between them. According to the structure of the connections, they have been identified as feed forward and recurrent networks. Feed forward networks have one way connections from input to output layer. They are most commonly used for prediction and nonlinear function fitting. Here the neurons are arranged in the form of layers. Neuron in one layer get inputs from previous layer and feed their outputs to the next layer. The last layer is called the output layer. Layers between the input and output layers are called as hidden layers and are termed as multilayered networks.

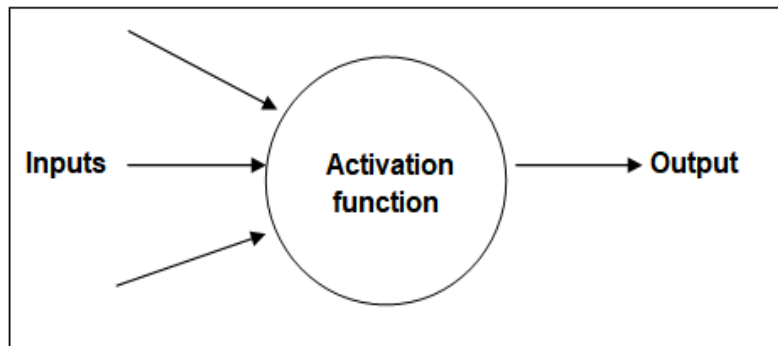


Fig.5.11 ANN neuron connection

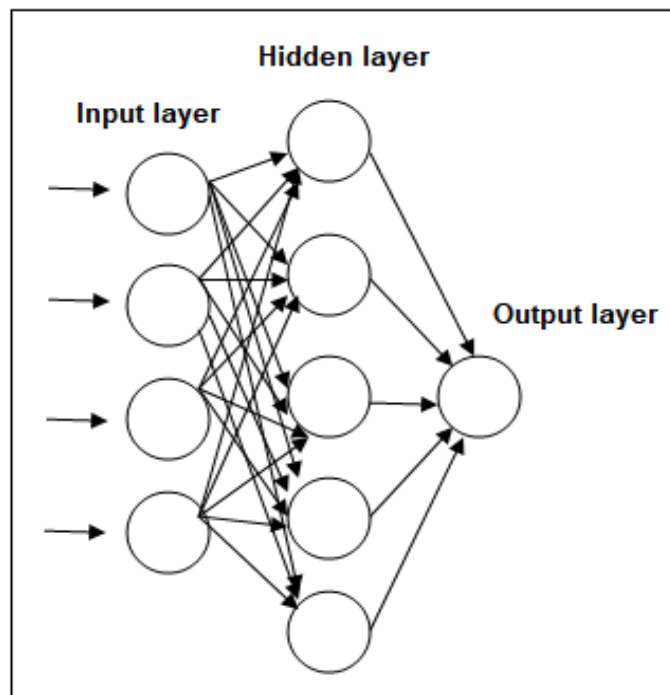


Fig.5.12 Multilayered ANN structure

Fig.5.12 shows schematic diagram of multilayered feed forward network. The number of nodes within the input and output layers are managed by the nature of problem to be solved and the number of input and output variables needed to define the problem. The number of hidden layers and neurons in the hidden layer is usually defined by trial and error method.

ANN studies the input-output relationships by suitably adjusting the synaptic weights in a process known as training. The weights of the given interconnection are adjusted using some learning algorithms. A learning cycle in an ANN model is as shown in Fig.5.13 (Meireles et al. 2003).

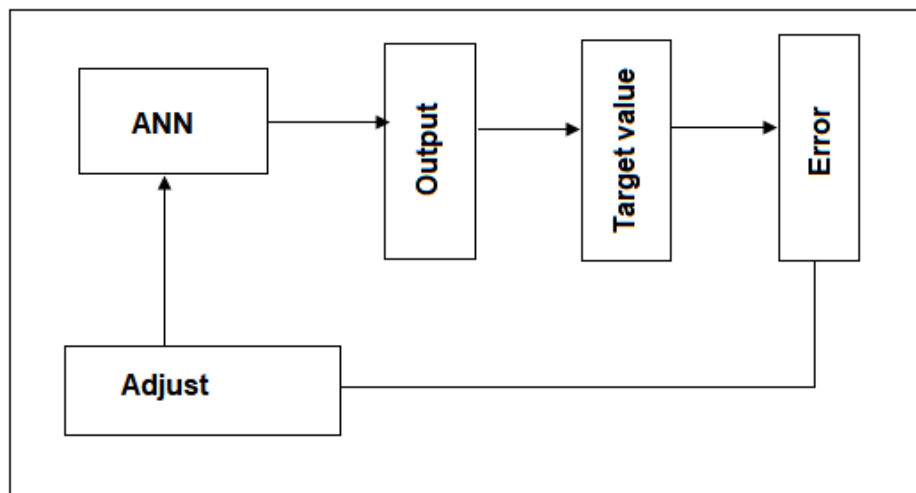


Fig.5.13 A Learning cycle in an ANN model

Learning methods in neural networks can be broadly classified into two types, namely, supervised and unsupervised learning. In supervised learning, target values or desired responses are known and given to ANN during training so that ANN can adjust its weights to match its output to the target values. Before the learning algorithms are applied to update the weights, all the weights are initialized randomly (Haykin 1999). The network using this set of inputs produces its own outputs. These are compared with the target outputs, and the difference between them called the error is used to modifying the weights.

In unsupervised learning, the network develops its classification rules by extracting information from the inputs presented to the network. In other words, using the correlation of input vectors, the learning rule changes the network weights to group

the input vectors into clusters. By doing so, similar input vectors will produce similar network outputs since they belong to the same cluster. In the present study, the feed-forward network known as Multilayer Perceptron (MLP) is used to develop the prediction model of rock properties.

### 5.9.1 Multilayer perceptron neural network (MLPNN)

In this study, multilayer perceptron (MLP) is utilized to develop the models for rock properties. MLP is a widely employed network architecture that comprises three layers, namely input, hidden, and output layers, as shown in Fig.5.8. In multilayer perceptron, a transfer function is used to get the output by sending the weighted sum of the inputs and bias parts to the activation level, and units are provided in a layered topology known as a feed-forward neural network. To predict the output efficiently, the number of hidden layers and neurons is also an important point in the execution of ANN. The input parameters are entering the feed-forward neural networks during the training stage, as shown in Fig.5.14.

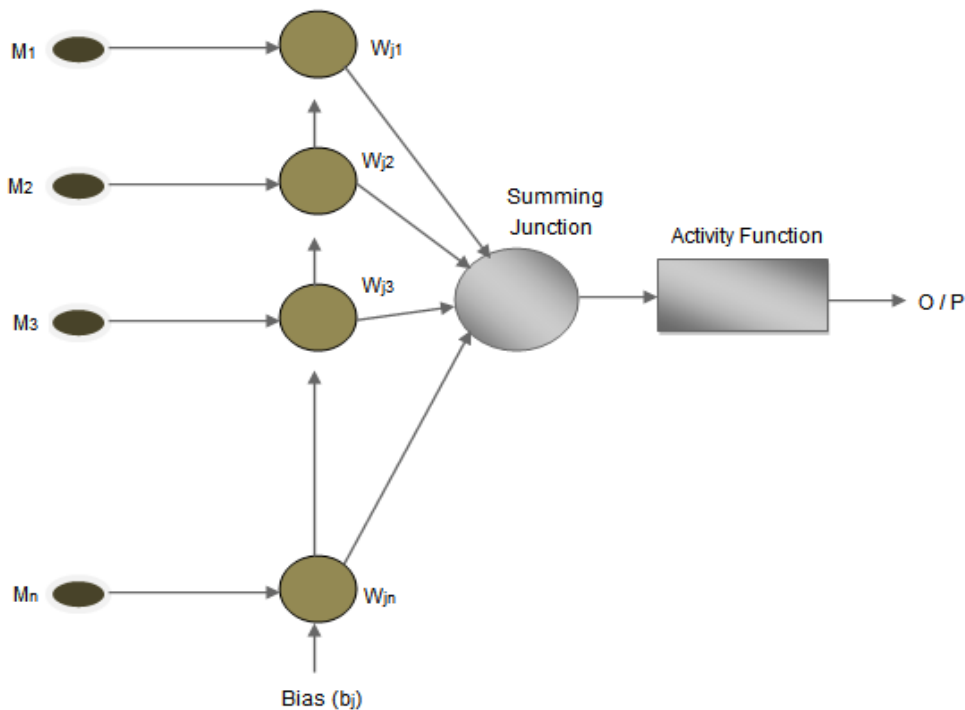


Fig.5.14 Information processing through a neuron

Each product of input parameters ( $M_i$ ) and a weight function ( $W_{ij}$ ) are summed into junction with a bias ( $b_j$ ) of the neurons is given in Eq.5.18 (Ghritlahre and Prasad.2018). In the present study, the input parameters such as drill operating parameters and drilling responses were applied, and the output parameters are the rock properties.

$$X = \left( \sum_{i=1}^n (W_{ij} M_i) \right) + b_j \quad (5.18)$$

The use of the single hidden layer in an ANN model is enough to approximate the given function with desired accuracy (Hornik et al.1989). The output obtained from the network through each input would be matched with the fixed target output, and thus the error is computing. Different functions are available to train the networks to have the target output from a particular input. There are two usually employed transfer functions in the hidden layer such as Tansig and Logsig (Ghritlahre and Prasad.2018). The extensively accepted activity function is the sigmoid function, and it is representing as shown in Eq.5.19.

$$F(X) = \frac{1}{1 + e^{-X}} \quad (5.19)$$

Several trials were carried out to set the optimum number of neurons in the hidden layer. The optimum number of neurons in the hidden layer is selecting so that the RMSE and MAPE is minimum for those numbers. The ANN output would analyze with the actual value at each performance using the particular number of neurons, and thus errors can be calculated.

In this investigation, the ANN model, shown in Fig.5.15 with MLPNN architecture, is used to predict rock properties. ANN algorithms such as Levenberg–Marquardt (trainlm), resilient back-propagation (trainrp), and scaled conjugate gradient back-propagation (trainscg) are used for training the network using Matlab software.



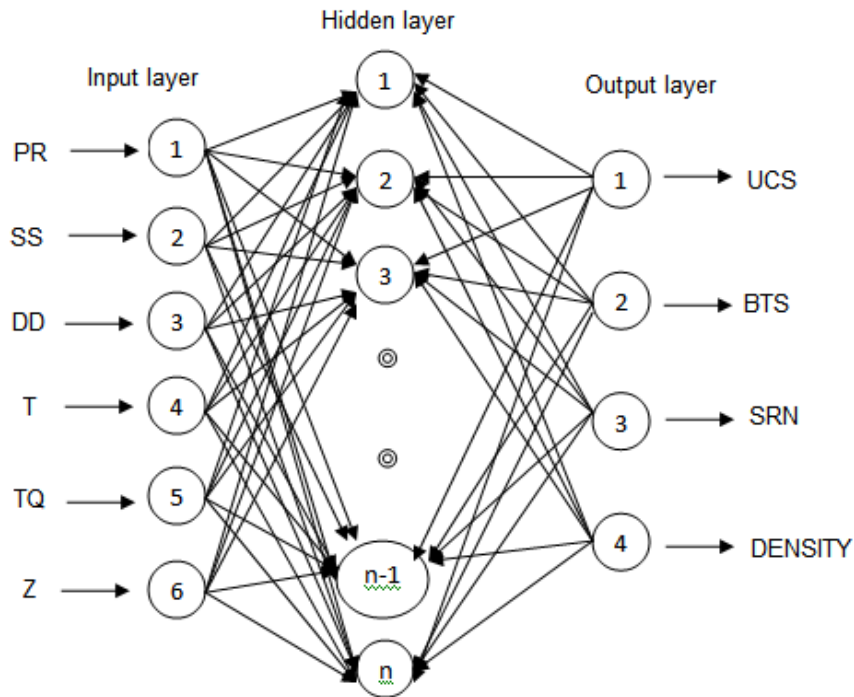


Fig.5.15 ANN model of the physico-mechanical properties of rocks

### 5.9.2 Development of ANN models for prediction of physico-mechanical properties.

In this study, 162 data sets obtained from six different sedimentary rocks are used to develop the ANN models. The MLPNN model is employed to predict the physico-mechanical properties of rocks during the rotary drilling process, as shown in Fig.5.11. The input layer consists of six input parameters: penetration rate (PR), spindle speed (SS) drill diameter (DD), thrust (T), torque (TQ), and vibration frequency (Z). The physico-mechanical properties of rocks such as UCS, BTS, SRN and density are embedded in the output layer.

Out of 162 data sets, training is assigned with 114 (70%) data sets, and for testing, 48 (30%) data sets were assigned. For the current ANN models, a popular learning algorithm known as feed-forward back-propagation was applied to testing and training data sets. The trial and error method is applied to fix the number of neurons in the hidden layer. In this system, 6 – 20 neurons were utilized with a single hidden layer. Logsig transfer function was used as a sigmoid function for the hidden layer (Rajesh et al.). Since the number of input parameters is equal to six, the simulation of

ANN models for predicting each rock property starts with six neurons. From the results, it was observed that error parameters such as RMSE and MAPE are less for predictions of each rock property when the 17th neuron used in the hidden layer of ANN network with Levenberg–Marquardt algorithm (trainlm) and logsig transfer function. Fig. 5.16, 5.17, and 5.18 show an example of the variation of VAF (%), RMSE (MPa), and MAPE (%), respectively, which produced during the prediction of UCS using a different number of neurons in the hidden layer. Since the VAF or  $R^2$  value is more and RMSE and MAPE are less at the 17th neuron, that neuron could be considered an optimum one and used in the hidden layer for better results.

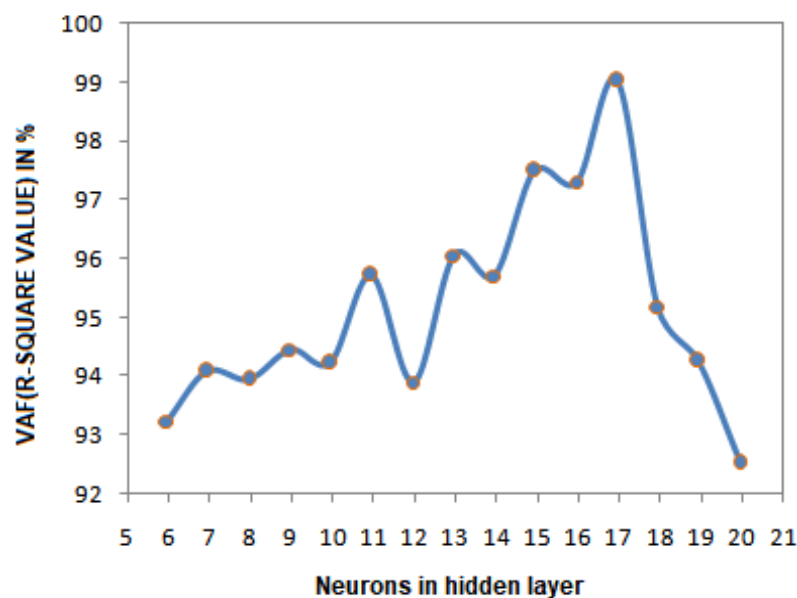


Fig. 5.16 Adaptation of VAF with number of neurons using trainlm algorithm (UCS)

Fig.5.19 Shows an example of R-value including training, testing, validation and overall, for the prediction of UCS with trainlm algorithm. The results of prediction performance of the algorithms, namely trainlm, trainrp, and trainscg, are shown in Table 5.18, 5.19, and 5.20. From the results, it could observe that the ANN network with the trainlm algorithm is showing the best performance compare to trainrp and trainscg algorithms.

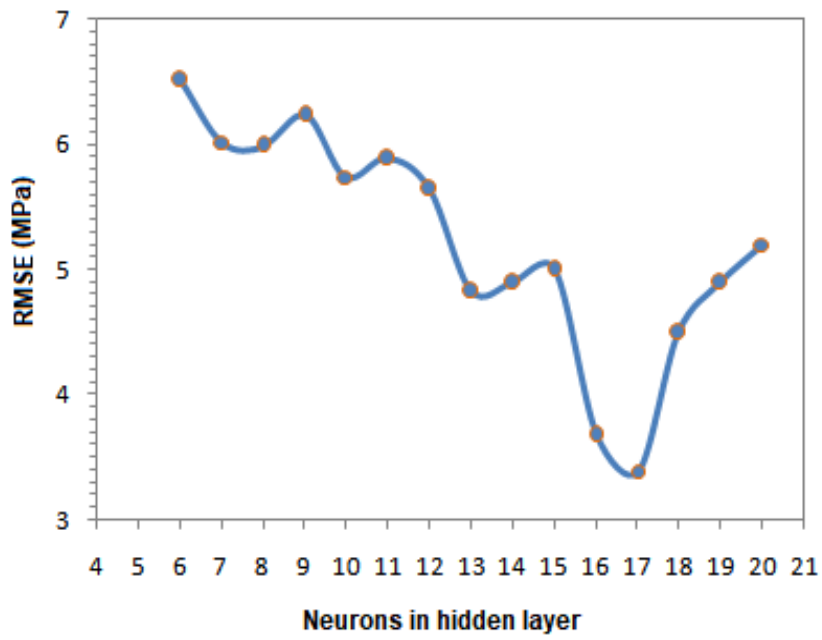


Fig. 5.17 Adaptation of RMSE with number of neurons using trainlm algorithm(UCS)

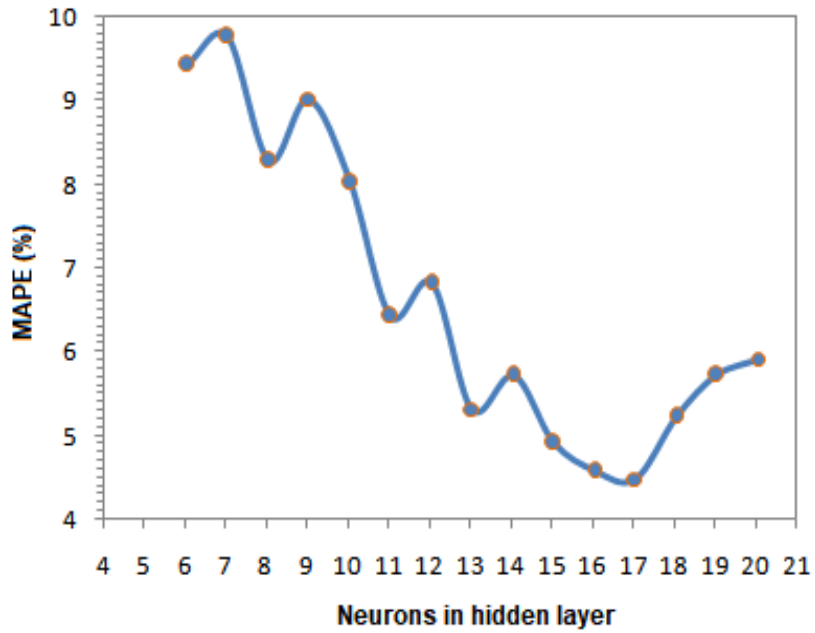


Fig.5.18 Adaptation of MAPE with number of neurons using trainlm algorithm (UCS)

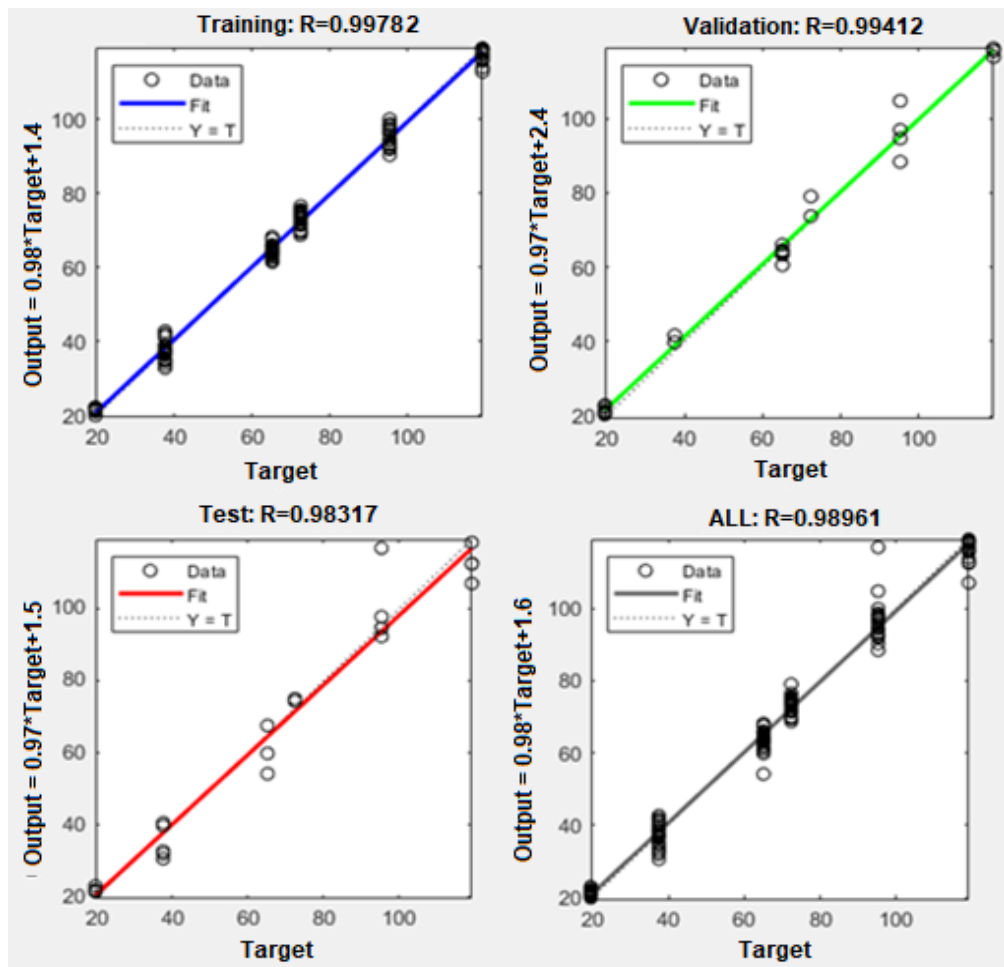


Fig.5.19 Example of prediction of UCS using ANN model (Trainlm)

Table 5.18 Performance of training and testing data using trainlm algorithm

Performance predictors	UCS	BTS	SRN	Density
<b>Trainlm</b>				
Training data				
R <sup>2</sup>	99.78	94.54	97.95	96.69
RMSE	3.2046	0.3464	1.9631	0.0395
MAPE	4.3219	5.3825	6.8963	1.0989
Testing data				
R <sup>2</sup>	98.31	93.82	97.69	96.02
RMSE	3.3148	0.3558	1.9502	0.0354
MAPE	4.4398	5.3205	6.2563	1.0561

Table 5.19 Performance of training and testing data using trainrp algorithm

Performance predictors	UCS	BTS	SRN	Density
<b>Trainrp</b>				
Training data				
R <sup>2</sup>	96.54	95.31	94.32	96.25
RMSE	5.1236	0.3612	1.9703	0.0379
MAPE	7.2145	5.4869	6.9023	6.0132
Testing data				
R <sup>2</sup>	93.12	94.21	92.02	94.09
RMSE	5.1932	0.3769	1.9931	0.0395
MAPE	6.9561	6.3214	7.2501	7.1208

Table 5.20 Performance of training and testing data using trainscg algorithm

Performance predictors	UCS	BTS	SRN	Density
<b>Trainscg</b>				
Training data				
R <sup>2</sup>	95.45	94.16	93.32	95.56
RMSE	5.9968	0.3932	1.9805	0.0399
MAPE	8.2148	6.1257	7.2563	7.0134
Testing data				
R <sup>2</sup>	92.59	93.98	91.684	92.78
RMSE	6.0231	0.4235	2.0348	0.0421
MAPE	8.9602	8.3218	7.3548	7.8564

### 5.9.3 Comparative Performance of Multiple Linear Regressions (MLR) and Artificial Neural Network (ANN) Model

In this section, the performance of the Type-II models, which were developed using the MLR and ANN model techniques, are compared based on the performance indices such as VAF or R<sup>2</sup> value, RMSE, and MAPE. The performance indices are computed from Eq.5.10, Eq.5.11, and Eq.5.12, respectively. The performance in terms of VAF or R<sup>2</sup> values with Type-II and ANN models is presented by bar chart as shown in Fig.5.20. The R<sup>2</sup> values of Type-II MLR model for UCS, BTS, SRN and density are 97.52%, 89.92%, 96.04%, and 93.71% respectively. Similarly, the R<sup>2</sup> values of the

ANN model using the testing data for UCS, BTS, SRN, and density are 98.85%, 93.82%, 97.69%, and 96.02%, respectively. It is observed that the  $R^2$  value of each rock property's prediction model using the ANN approach is higher than the MLR model, indicating that the ANN model could explain each response comparatively better than the MLR model.

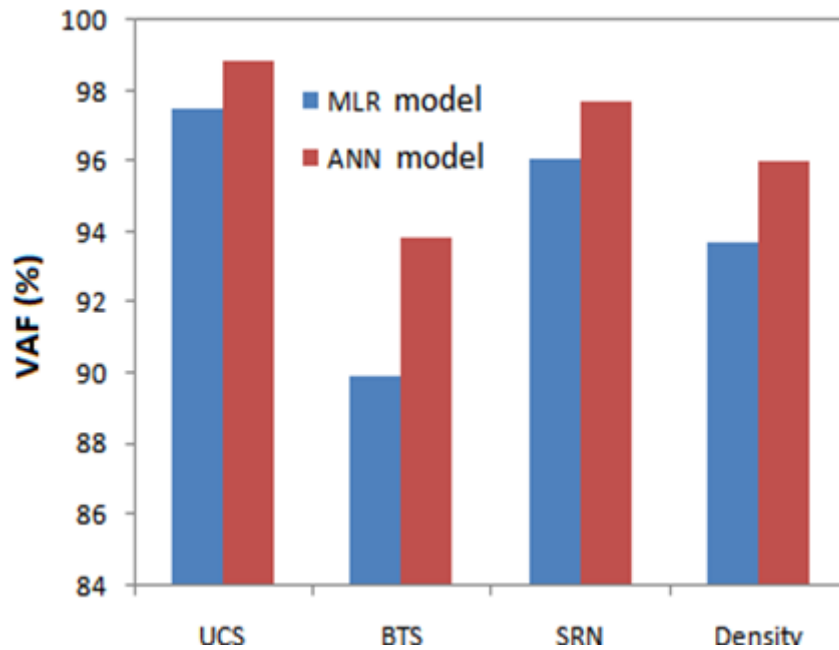


Fig.5.20 Comparison of MLR and ANN model for  $R^2$  (VAF)

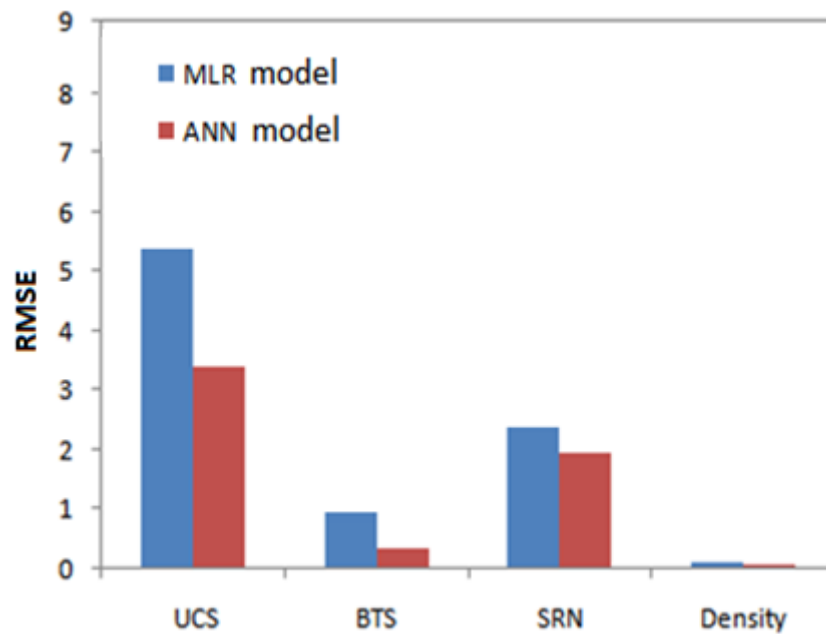


Fig.5.21 Comparison of MLR and ANN model for RMSE

Fig. 5.21 shows the comparative performance of the MLR and ANN model with their RMSE. The RMSE values of the MLR model for UCS, BTS, SRN, and density are 5.27, 0.87, 2.59, and 0.079, respectively. Similarly, the RMSE values of the ANN model for UCS, BTS, SRN, and density are 3.31, 0.35, 1.95, and 0.0354, respectively. In the ANN technique, the RMSE value for each rock property is comparatively less than the MLR model, indicating that the ANN model predicts the response with fewer roots means square error.

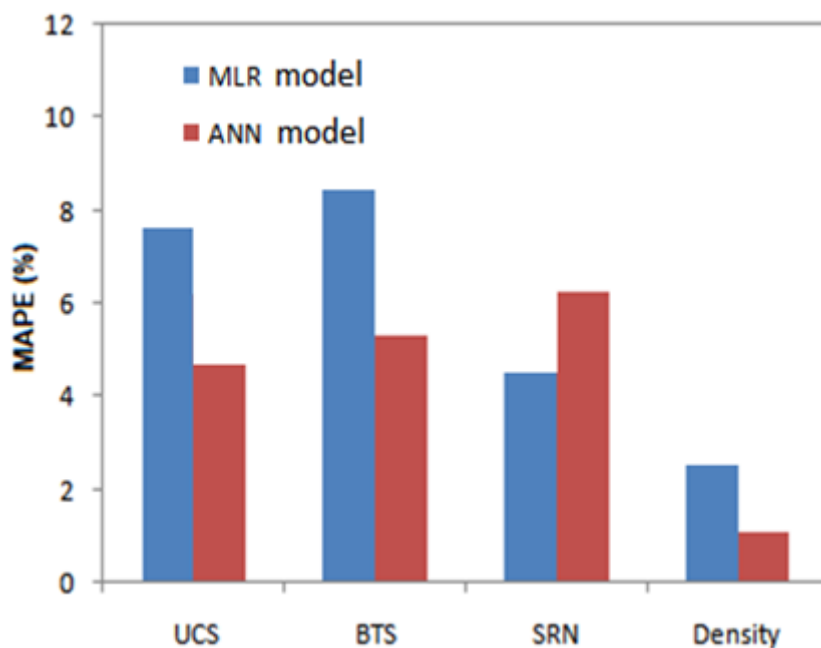


Fig.5.22 Comparison of MLR and ANN model for MAPE

Fig.5.22 shows the comparative performance of MLR and ANN approaches related to MAPE. Mean absolute percentage error or MAPE is the indicator of prediction accuracy of models. The MAPE values of the MLR model for UCS, BTS, SRN, and density are 7.74%, 8.18%, 4.63%, and 2.46%, respectively. Similarly, the ANN model's MAPE values for UCS, BTS, SRN, and density are 4.43%, 5.32%, 6.25%, and 1.05%, respectively. As compared to MLR, the ANN's MAPE values are less, indicating that the ANN model can predict the response with higher accuracy and lesser error.

Fig.5.23 shows the comparison of an error in percentage, produced during the prediction of each rock property using MLR and ANN techniques. The percentage error is calculated using the Eq.5.20.

$$\text{Percentage error (\%)} = (\text{RMSE}) / (\text{maximum value of DV}) \times 100 \quad (5.20)$$

For example, the percentage error for UCS using MLR model is computed as follows

$$\text{Percentage error (\%)} = (5.27 / 119.2) \times 100 = 4.42\%.$$

The percentage errors using the MLR model for UCS, BTS, SRN, and density are 4.42%, 10.01%, 4.38%, and 2.67%, respectively. Similarly, the percentage errors using the ANN model for UCS, BTS, SRN, and density are 2.84%, 3.97%, 3.2%, and 2.03%, respectively. The predictive model using the ANN technique could predict each rock property with less percentage error compared to MLR technique.

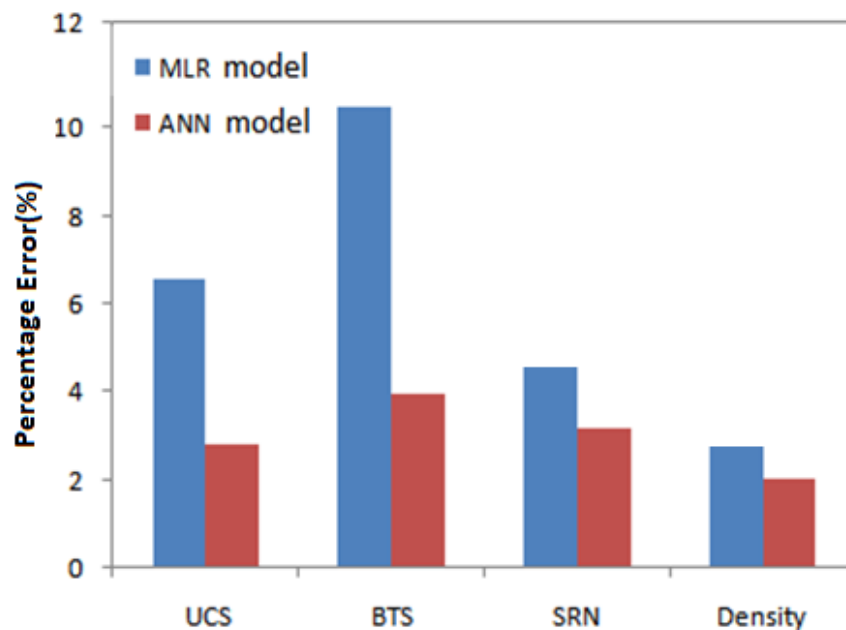


Fig.5.23 Comparison of MLR and ANN model for percentage error

### 5.10 Summary

A statistical model such as multiple regression and soft computing techniques such as the ANN models shows that both are capable and suited for geotechnical engineering problems.





# ***CHAPTER-6***

## CHAPTER 6

### 6. DRILLING SPECIFIC ENERGY AND ANALYSIS

#### 6.1 Introduction

Drilling Specific energy (DSE) is another idea for evaluating rock drillability (Yasar et al., 2011). The DSE could also be utilized as a tool for assessing drilling efficiency in a drilling operation. The utilization of DSE is mainly dependent upon the lithology of the drilling site. Therefore, DSE may also be an informative tool to understand the change in lithology.

Rock drilling is a costly process often used in many rock engineering projects, and the penetration rate is the prime concern of engineers. The estimation of DSE for different rock with different strength properties may help the driller choose the optimum value of drill operating parameters to have the maximum efficiency of drilling, i.e., penetration rate, and thus reduce the overconsumption of drilling energy.

#### 6.2 Computation of Drilling Specific Energy

The specific energy during rock drilling consists of two components, as shown in Eq.5.21. The first one is the energy required for the drill bit's indentation or axial movement, called thrust energy. Similarly, the second one is the energy required to cut or remove the material from the drilling hole's inner surface, called rotational energy. Based on this, Teale derived the DSE equation for rotary type rock drilling in 1965, as shown in Eq.5.22, and it is widely used for computation of DSE.

$$DSE = \text{Thrust energy} + \text{Rotaional energy}$$

$$DSE = E_T + E_R \quad (5.21)$$

$$DSE = \frac{F}{A} + \frac{2 \times \pi \times N \times T_q}{A \times PR} \quad (5.22)$$

Where,

DSE = Drilling Specific energy (J/m<sup>3</sup>)

F = Thrust acting on the bit (Newton)

A = Cross sectional area of hole in m<sup>2</sup>

N = Drill bit speed (r.p.s)

T<sub>q</sub> = Torque developed at bit rock interface corresponding to the applied thrust (N-m)

PR = Penetration rate (m/sec)

In this study, the DSE was calculated for each rock type using the 27 drill operating conditions comprising the combinations of thrust, torque, drill diameter, bit speed, and penetration rate. The average DSE was then calculated for each rock from 27 drill operating conditions, as shown in Table 6.1. It was observed that the average drilling specific energy was increasing as the physico-mechanical properties of rocks increased.

Table 6.1 Average specific energy of different physico-mechanical properties

Rock type	UCS(MPa)	BTS(MPa)	SRN	Density(gm/cc)	Average DSE (MJ/m <sup>3</sup> )
Shale	19.6	1.6	23	2.0521	24.40
Sandstone-1	37.5	3.4	42	2.2587	28.78
Sandstone-2	65.1	4.2	49	2.5848	35.68
Sandstone-3	72.4	7.5	51	2.5930	36.09
Limestone-1	95.3	8.1	56	2.6589	38.40
Limestone-2	119.2	8.7	59	2.9542	42.12

### 6.3 Correlation of Drilling Specific Energy (DSE) with Rock Properties

In this section, the analysis of drilling specific energy concerning the considered physico-mechanical properties of rocks has been carried out. The relationships between specific energy and UCS, BTS, SRN, and density were investigated using a simple linear regression method shown in Figs. 6.1, 6.2, 6.3 and 6.4, respectively. The

results showed that UCS correlates highly with specific energy, with  $R^2 = 89.9\%$  ( $R = 0.948$ ) (Kolapo et al. 2020). The next highest correlation with specific energy is density, with  $R^2 = 82.6\%$  ( $R = 0.908$ ). BTS is correlating with specific energy, with  $R^2 = 79.6\%$  ( $R = 0.892$ ). Among several rock properties, SRN is comparatively weak correlating with specific energy, with  $R^2 = 73.95\%$  ( $R = 0.859$ ).

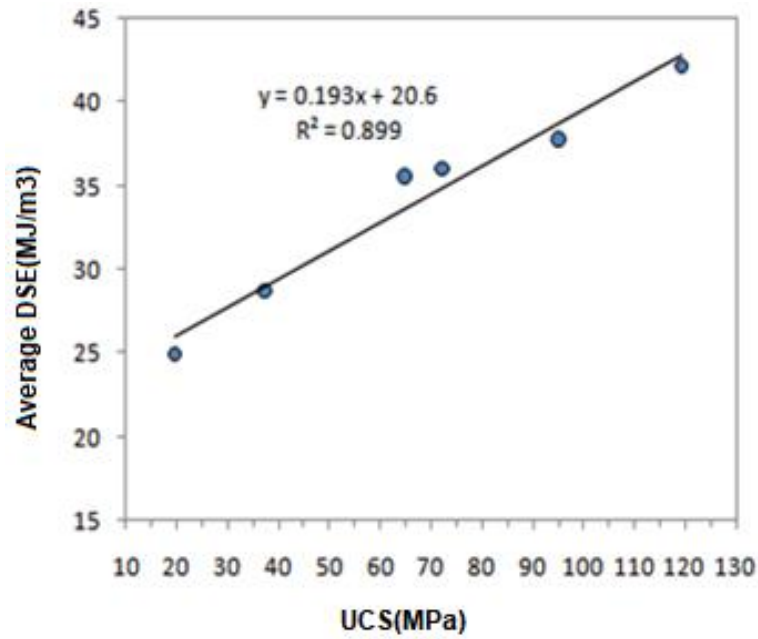


Fig.6.1 Correlation of specific energy with UCS

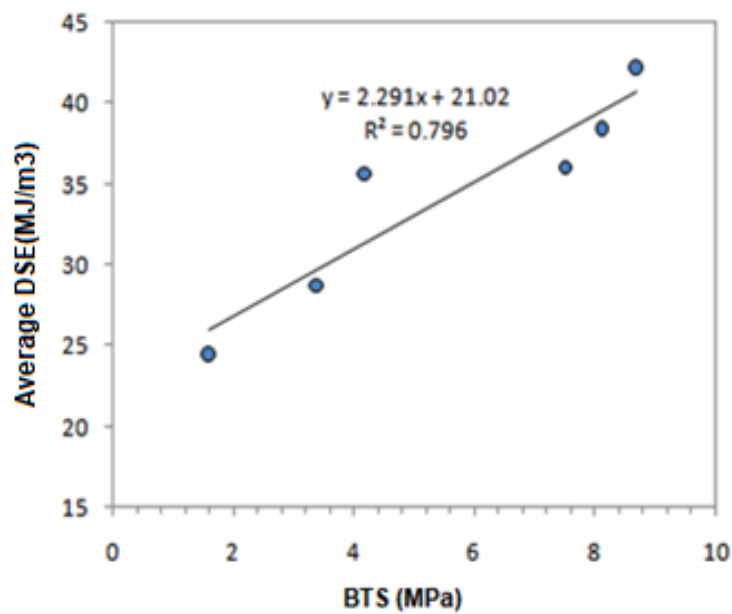


Fig.6.2 Correlation of specific energy with BTS

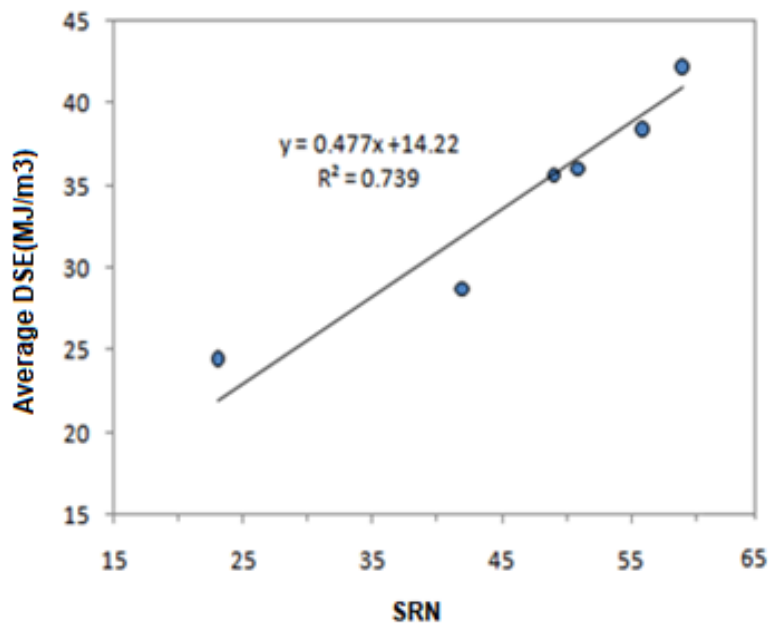


Fig.6.3 Correlation of specific energy with SRN

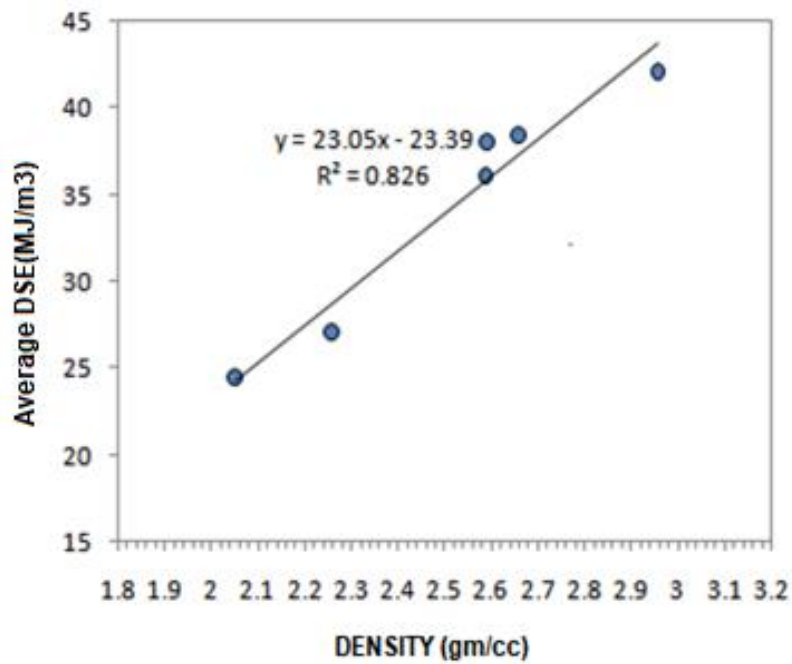


Fig.6.4 Correlation of specific energy with density

#### 6.4 Influence of Weight on Bit or Drilling Thrust on DSE

The influence of thrust on specific energy for shale, sandstone-1, sandstone-2, sandstone-3, limestone-1, and limestone-2 with UCS 19.6 MPa, 37.5MPa, 65.1 MPa,

72.4MPa, 95.3 MPa, and 119.2 MPa, respectively, is shown in Figs.6.5 to 6.10. DSE decreases from 29.63 to 12.8 MJ/m<sup>3</sup> during shale rock drilling using different thrusts ranging from 345 – 479N, at 400 r.p.m. Similarly, during the drilling of sandstone-1, sandstone-2, sandstone-3, limestone-1, and limestone-2, the DSE is decreasing in the range of 32.15 – 14.40 MJ/m<sup>3</sup>, 37.04–19.2 MJ/m<sup>3</sup>, 38.12–20.80 MJ/m<sup>3</sup>, 44.45–23.1 MJ/m<sup>3</sup>, and 47.3-24.3 MJ/m<sup>3</sup>, as the thrust increasing in the range of 396 – 550 N, 514 – 603N, 534 – 635 N, 582 – 679 N, and 634 – 702 N, respectively. From the data analysis, it was observed that the trend of specific energy with increased drill thrust was the same at a different speed.

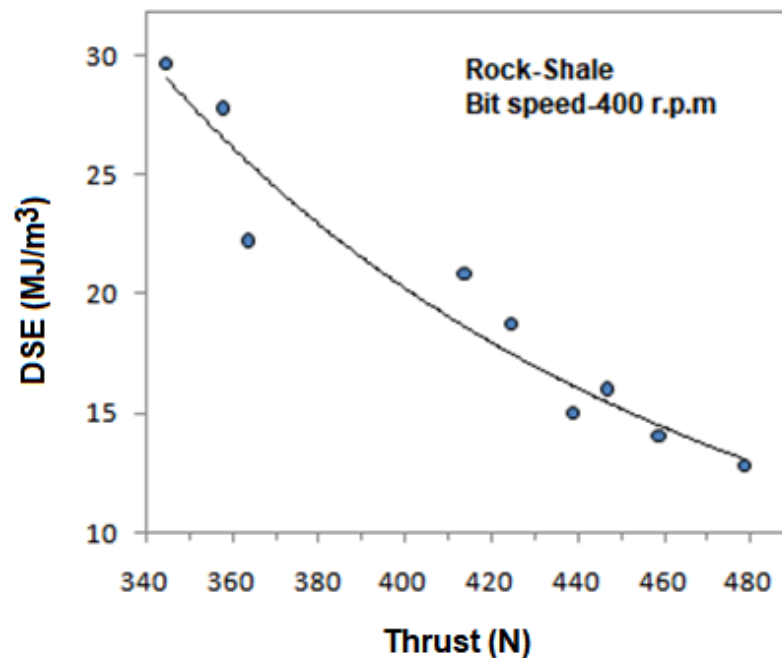


Fig. 6.5 Influence of thrust on specific energy during the drilling of shale

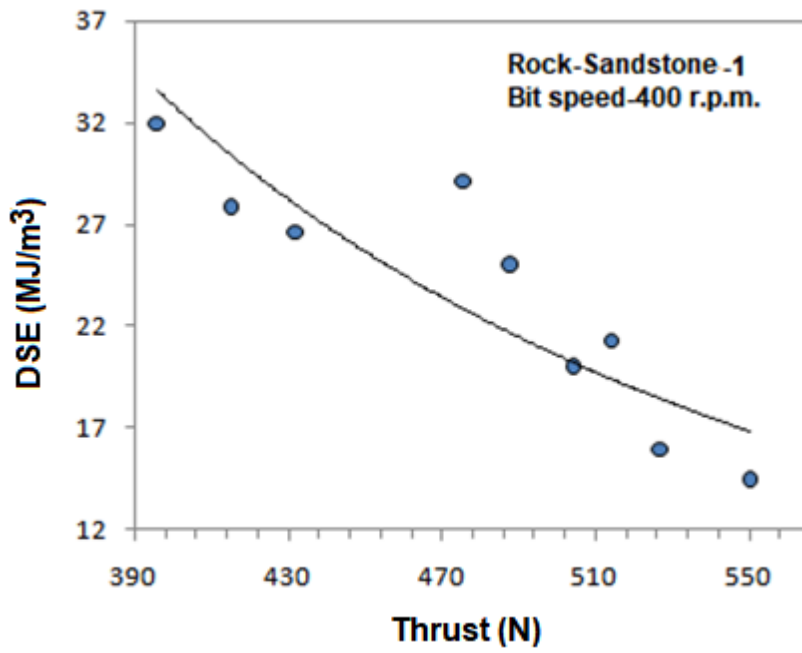


Fig. 6.6 Influence of thrust on specific energy during the drilling of sandstone-1

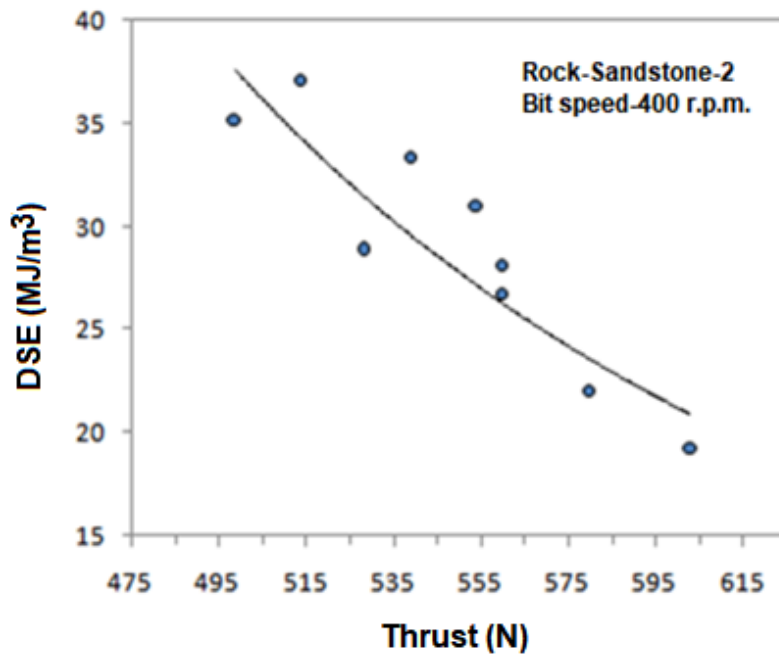


Fig. 6.7 Influence of thrust on specific energy during the drilling of sandstone-2



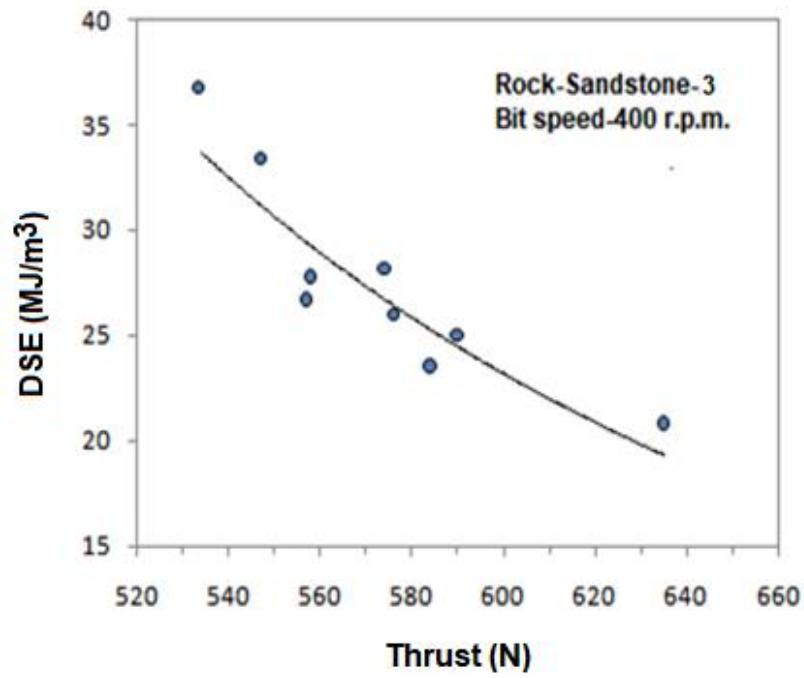


Fig. 6.8 Influence of thrust on specific energy during the drilling of sandstone-3

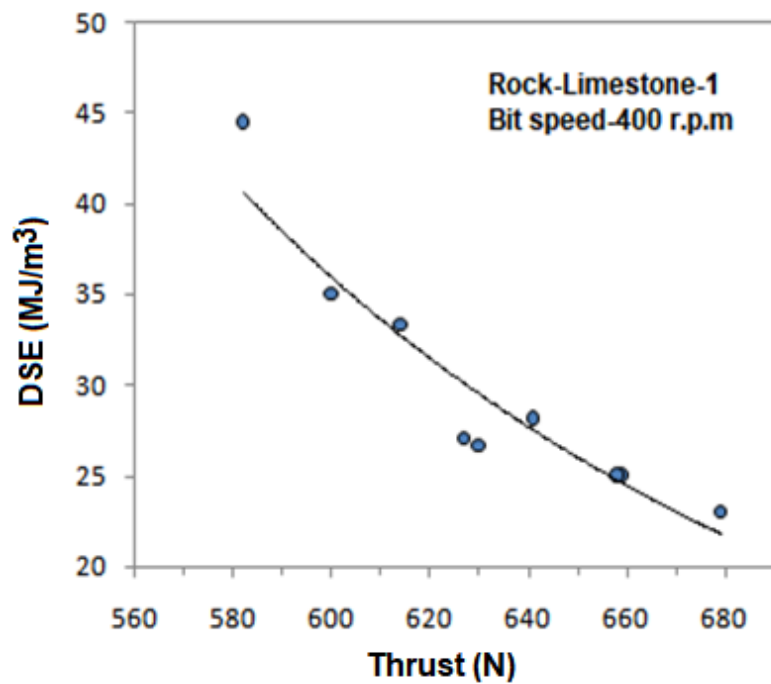


Fig. 6.9 Influence of thrust on specific energy during the drilling of limestone-1

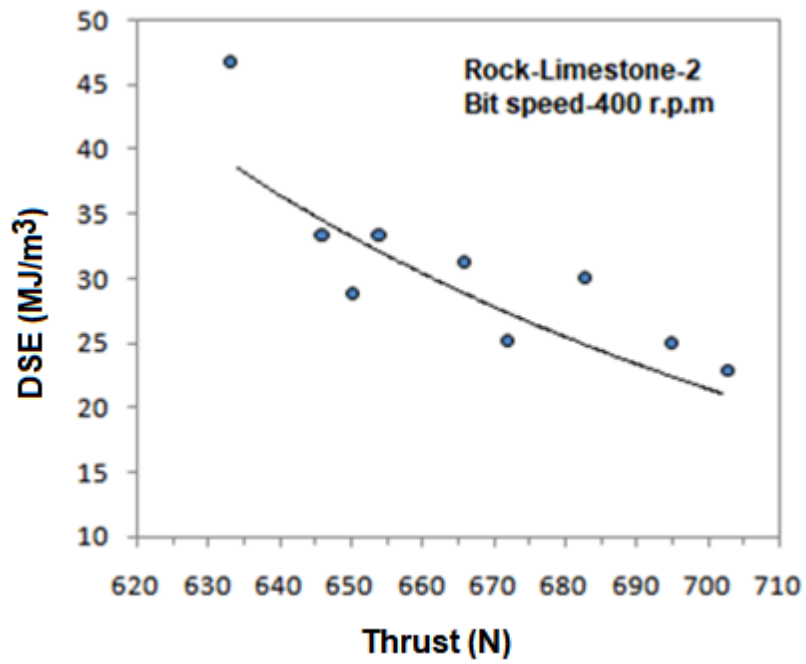


Fig. 6.10 Influence of thrust on specific energy during the drilling of limestone-2

# ***CHAPTER-7***

## CHAPTER 7

### CONCLUSIONS AND SCOPE FOR FUTURE WORK

#### 7.1 Conclusions

In the present experimental investigation, extensive full-scale rotary drilling tests were carried out for six different sedimentary rocks using the CNC vertical milling center. Experimental techniques have been developed to measure the drilling responses, such as thrust acting, the torque developed at the bit-rock interface, and vibration frequency induced at the drill head during the drilling of rocks carried out at different combinations of drill operating parameters. The data collected during the drilling process was used to develop the model predicting physico-mechanical properties of rocks. The prediction performance of the model was checked using standard prediction indices. Besides, the correlation of drilling specific energy with rock properties is analyzed. The conclusions drawn from the analysis of experimental results are as follows:

1. During the drilling of shale, sandstone-1, sandstone-2, sandstone-3, limestone-1, and limestone-2, as the drill bit's penetration rate is varied from 3mm/min to 5mm/min, the change of mean thrust acting at the bit-rock interface increased by 6.18%, 8.19%, 8.23%, 8.85%, 9.31%, and 11.20%, respectively. Similarly, the change in mean torque developed at the bit-rock interface increased by 11.47%, 6.83%, 9.49%, 6.96%, 10.40%, and 6.78%, respectively. Therefore, it is concluded that both thrust and torque increase for a particular rock drilling with the increase of penetration rate.

From the shale to limestone-2 drilling, the change of mean thrust is increased by 55.91%, 59.27%, and 63.29% at a penetration rate of 3mm/min, 4mm/min, and 5mm/min, respectively. Similarly, the change in mean torque is increased by

102.45%, 93.67%, and 93.93% with 3mm/min, 4mm/min, and 5mm/min, respectively. Therefore, it is concluded that both the drilling thrust and torque increase with the increase of rock strength at a particular penetration rate.

2. During the drilling of shale, sandstone-1, sandstone-2, sandstone-3, limestone-1, and limestone-2, as spindle speed developed from 400 r.p.m. to 600 r.p.m., the change in mean thrust acting at bit-rock interface decreased by 16.29%, 19.50%, 18.61%, 19.16%, 14.07%, and 17.01%, respectively. Similarly, the change in mean torque developed at the bit-rock interface decreased by 23.81%, 18.16%, 16.89%, 6.69%, 9.36%, and 11.54%, respectively. Therefore, it is concluded that as the spindle speed is increasing, the drilling thrust and torque would significantly decrease for a particular rock drilling.

From shale to limestone-2 drilling, the change in mean thrust increases by 61.12%, 63.18%, and 60.45% at a spindle speed of 400 r.p.m., 500 r.p.m., and 600 r.p.m., respectively. Similarly, the change in mean torque increases by 67.41%, 78.27%, and 85.83% at a speed of 400 r.p.m., 500 r.p.m., and 600 r.p.m., respectively. Therefore, it is concluded that the drilling thrust and torque increase at a particular speed as the drilling rock strength increases.

3. During the drilling of shale, sandstone-1, sandstone-2, sandstone-3, limestone-1, and limestone-2, as the drill bit's diameter is changed from 12 mm to 20 mm, the change in mean thrust acting at the bit-rock interface increased by 22.32%, 24.63%, 25.50%, 26.08%, 23.63%, and 25.45%, respectively. Similarly, the change in mean torque developed at the bit-rock interface increased by 73.74%, 46.75%, 70.86%, 58.84%, 55.10%, and 69.25%, respectively. Therefore, it was concluded that both drilling thrust and torque increase for a particular rock drilling with the increase of drill diameter.

From the shale to limestone-2 drilling, the change in mean thrust is increased by 68.19%, 72.23%, and 72.51% at drill diameter of 12 mm, 16 mm, and 20 mm, respectively. Similarly, the change in mean torque is increased by 91.52%, 87.16%, and 86.56% at drill diameter of 12 mm, 16 mm, and 20 mm, respectively. Therefore, it is concluded that both the drilling thrust and torque increase at a particular drill diameter as the drilling rock strength increases.

4. During the drilling of shale, sandstone-1, sandstone-2, sandstone-3, limestone-1, and limestone-2, as spindle speed increased from 400 r.p.m. to 600 r.p.m, the change in mean vibration frequency induced at the drill head increased by 65.54%, 64.95%, 64.07%, 63.50%, 62.83%, and 62.64%, respectively. Similarly, from the shale to limestone-2 drilling, the change in mean vibration frequency at drill head is increased by 3.65%, 3.05%, and 1.84% at a spindle speed of 400 r.p.m., 500 r.p.m., and 600 r.p.m, respectively. Therefore, it is concluded that the vibration frequency is highly responsive to spindle speed rather than the rock strength.
5. During the drilling of shale, sandstone-1, sandstone-2, sandstone-3, limestone-1, and limestone-2, as drill diameter increased from 12mm to 20mm, the change in mean bit-pressure induced at the bit-rock is decreased by 112.5%, 115.38%, 143.78%, 164.16%, 155.35%, and 170.35%, respectively. Therefore it was concluded that bit-pressure decreases as the drill bit diameter increases during a particular rock drilling. Similarly, from the shale to limestone-2 drilling, the change in mean bit-pressure at bit-rock interface is increased by 85.15%, 52.06%, and 41.32% at a drill diameter of 12 mm, 16mm and 20mm, respectively.
6. Compared to Type – I models developed with multiple regression models, Type-II models developed with a second-order multiple regression could increase the explanation of variance ( $R^2$ ) in UCS, BTS, SRN, and density by 3.03%, 1.8%, 8.12%, and 1.65%, respectively.
7. Compared to Type – I models, Type-II models could decrease the NRSME in UCS, BTS, SRN, and density by 2.58%, 0.56%, 4.3%, and 3.17%, respectively.
8. Similarly, compared to Type – I, Type-II models could decrease the MAPE in UCS, BTS, SRN, and density by 1.77%, 1.4%, 2.72%, and 0.24%.
9. In ANOVA, generated for UCS, BTS, SRN, and density, the adjusted sum of square (Adj.SS) and F-value for thrust are higher than torque and vibration frequency. Therefore it was concluded that the thrust is highly responsive to the drilling of different rocks.

10. Cross-correlation of drilling responses with strength properties such as UCS indicated that the thrust acting and torque developed between bit-rock interface have strong ( $R = 0.844$ ) and moderate correlation strength ( $R = 0.580$ ), respectively, with UCS. However, the vibration frequency induced at the drill head has very weak correlation strength ( $R = 0.051$ ) with UCS.

11. The strength of the relationship between thrust produced and torque developed at the bit-rock interface is moderate ( $R = 0.648$ ).

12. Validation of both Type-I and Type-II models for vital rock property such as UCS indicated that both models could predict the response within the acceptable error, i.e. below 15%. However, the Type-II may be quite feasible than the Type-I, as it has less complexity, high statistical significance, and the overall cost is also low.

13. Compared to Type-II models developed with multiple linear regression, the ANN models could decrease NRMSE value by 1.97%, 7.38%, 1.74%, and 3.48% for UCS, BTS, SRN, density, respectively. Similarly, the MAPE is decreased by 3.42%, 2.8%, 2.26%, and 1.39%. Therefore it is concluded that the ANN models are superior to regression models.

14. Compared to other algorithms used in ANN models, the ANN models developed for each rock property with Levenberg Marquardt (trainlm) algorithm, with 17th neuron (6-17-4), could predict the dependent variables close to the actual values. Therefore, it was concluded that Levenberg Marquardt (trainlm) algorithm may be useful for engineering geology problems.

15. During the drilling of shale (UCS = 19.6 MPa), sandstone-1 (UCS = 37.5 MPa), sandstone-2 (UCS = 65.1 MPa), sandstone-3 (UCS = 72.4 MPa), limestone-1 (UCS = 95.3 MPa), and limestone-2 (UCS = 119.2 MPa) with different drill operating parameters, the average drilling specific energy was 24.40 MJ/m<sup>3</sup>, 28.78 MJ/m<sup>3</sup>, 35.68 MJ/m<sup>3</sup>, 36.09 MJ/m<sup>3</sup>, 38.40 MJ/m<sup>3</sup>, and 42.12 MJ/m<sup>3</sup>, respectively. Therefore, it was concluded that the drilling specific energy increases as the UCS and rock properties increase.

16. The relationship of drilling specific energy with rock properties such as UCS, BTS, SRN, and density was found good as they have R-values of 0.94, 0.89, 0.85, and 0.90, respectively.

## **7.2 Scope for Future Work**

1. In the present experimental investigation, sedimentary rocks are used. In future work, other types of rocks such as metamorphic and igneous can be used to check the reliability of this method.

2. In the present work, CNC vertical machining center is used for drilling operations. Since the machine's cost is very high, it is better to develop a low-cost conventional drilling setup with features like loading arrangement (drilling thrust) and varying the bit speed to get the different penetration rates. Then it can also be used as a drilling response along with others.

3. In the present study, the soft computing technique such as ANN is used to predict rock properties. However, other soft computing techniques like fuzzy inference can also be used to check prediction of this approach.





# ***REFERENCES***

## REFERENCES

- Abbas, C.A., Huang, C., Wang, J. (2020) “Machinability investigations on high-speed drilling of aluminum reinforced with silicon carbide metal matrix composites.” *Int J Adv Manuf. Technol.* 108, 1601–1611.
- Adebayo and Bello (2011) “Property Analysis for Correlation of Specific Energy with Penetration Rate and Bit Wear Rate.” *Advanced Materials Research*, 367, 547-553.
- Adebayo B., Mukoya J.G.M. (2019) “Rock properties and machine parameters evaluation at Rössing Uranium Mine for optimum drill performance.” *Journal of the Southern African Institute of Mining and Metallurgy*, 119(5), 459-464.
- An, Q., Ming, W., Cai, X., Chen, M. (2015) “Study on the cutting mechanics characteristics of high-strength UD-CFRP laminates based on orthogonal cutting method.” *Compos Struct* 131, 374–383.
- ASTM D4543-08 (2008) “Standard Practices for Preparing Rock Core as Cylindrical Test Specimens and Verifying Conformance to Dimensional and Shape Tolerances”, *American Society for Testing and Materials*, 100 Barr Harbor Dr., West Conshohocken, PA 19248.
- ASTM Standards 4.08 (1984) “ASTM Standard test method for unconfined compressive strength of intact rock core specimens”, *Soil and Rock, Building Stones: Annual Book of*, ASTM, Philadelphia, Pennsylvania.
- Aydin, A. (2009) “ISRM suggested method for determination of Schmidt hammer rebound hardness: revised version.” *International Journal of Rock Mechanics and Mining Sciences*, 46, 627–634.
- Bakar, M.Z.A., Butt I.A., Majeed Y. (2018) “Penetration rate and specific energy prediction of rotary–percussive drills using drill cuttings and engineering properties of selected rock units.” *Journal of Mining Science*, 54(2), 270–284.

Balci, C., Demircin, M.A., Copur, H., Tuncdemir, H. (2004) “Estimation of optimum specific energy based on rock properties for assessment of road header performance.” *The Journal of the South African Institute of Mining and Metallurgy*, 104(11), 633-642.

Basarir, H. (2019). “Prediction of rock mass P wave velocity using blasthole drilling information.” *International Journal of Mining, Reclamation and Environment*, 33(1), 61-74.

Basarir, H., & Karpuz, C. (2016). “Preliminary estimation of rock mass strength using diamond bit drilling operational parameters.” *International Journal of Mining, Reclamation and Environment*, 30(2), 145-164.

Basarir, H., Tutluoglu, L., Karpuz, C. (2014). “Penetration rate prediction for diamond bit drilling by adaptive neuro-fuzzy inference system and multiple regressions.” *Engineering Geology*, 173, 1-9.

Basarir, H., Tutluoglu, L., Karpuz, C. (2014). “Penetration rate prediction for diamond bit drilling by adaptive neuro-fuzzy inference system and multiple regressions.” *Engineering Geology*, 173, 1-9.

Benesty, J., Chen, J., Huang, Y., & Cohen, I. (2009). Pearson correlation coefficient. In *Noise reduction in speech processing* (pp. 37–40). Springer.

Bieniawski, Z.T. 1976. Rock mass classification in rock engineering. In *Exploration for rock engineering, proc. of the symp.*, (ed. Z.T. Bieniawski) 1, 97-106. Cape Town: Balkema.

Bhatnagar A., Khandelwal M., Rao K.U.M. (2011) “Laboratory investigations for the role of flushing media in diamond drilling of marble”. *Rock mechanics and rock engineering*, 44, 349-356.

Bradford, I. D. R., Fuller, J., Thompson, P. J., & Walsgrove, T. R. (1998, January). Benefits of assessing the solids production risk in a North Sea reservoir using elastoplastic modelling. In *SPE/ISRM rock mechanics in petroleum engineering*. Society of Petroleum Engineers.

- Broch, E., and Franklin, J. A., (1972). "The point-load strength test." *Int. J. Rock Mech. Min. Sci.*, 9, 669--697.
- Brown, E. T. (1981). Suggested methods for determining the uniaxial compressive strength and deformability of rock materials. *Rock Characterisation Testing and Monitoring—ISRM Suggested Methods*.
- Brown, E. T., ET, B. (1978). "Instrumented drilling as an aid to site investigations." *Proc.3<sup>rd</sup> Int. Congr., Int. Assoc., Eng. Geo. Section IV.1*, 21-28, Madrid.
- Brown, E.T., Carter, P., Robertson, W. (1984) "Experience with a Prototype Instrumented Drilling Rig." *Geo-drilling*, 24, 10–14.
- Carmichael, R. S. (Ed.). (2017). *Handbook of Physical Properties of Rocks* (1982): Volume II. CRC press.
- Ceryan, N., Okkan U., Kesimal, A. (2012) "Prediction of unconfined compressive strength of carbonate rocks using artificial neural networks", *Environ. Earth Sci.*, 68(3), 807-819.
- Ceryan, N., Okkan, U., Kesimal, A. (2013). "Prediction of unconfined compressive strength of carbonate rocks using artificial neural networks." *Environmental earth sciences*, 68(3), 807-819.
- Clark, G.B. (1982). *Principles of rock drilling and bit-wear, Part1*. Colo. School of Mines Quarterly, 77.
- Cooper, C., Doktan, M., Dean12, R. (2004). "Monitoring while drilling and rock mass recognition." In CRC Min. Conf. (Vol. 400, pp. 1-12).
- Davarpanah, A., Zarei, M., Mehdi-Nassabeh, S. M. (2016). "Assessment of Mechanical Specific Energy Aimed at Improving Drilling Inefficiencies and Minimize Wellbore Instability." *Journal of Petroleum and Environmental Biotechnology*, 7, 309.
- Dehghan, S., Sattari, G. H., Chelgani, S. C., Aliabadi, M. A. (2010). "Prediction of uniaxial compressive strength and modulus of elasticity for Travertine samples using

regression and artificial neural networks.” *Mining Science and Technology (China)*, 20(1), 41-46.

Erosy A., Atici, U. (2004) “Performance characteristics of circular diamond saws in cutting different types of rocks”, *Diamond and related materials*, 13, 22-37.

Erosy, A., and Waller, M. (1995) “Prediction of drill-bit performance using multivariable linear regression analysis.” *Trans.Inst.Min.Metall, Sect. A*, 104, 101-114.

Ferentinou, M., Fakir, M. (2017) “An ANN Approach for the Prediction of Uniaxial Compressive Strength, of Some Sedimentary and Igneous Rocks in Eastern KwaZulu-Natal”, *Symposium of the International Society for Rock Mechanic, Procedia Engineering*, 191, 1117 – 1125.

Finfinger G (2003) “A methodology for determining the character of mine roof rocks”, PhD Dissertation, Dept. of Mining Engineering, West Virginia Univ., Morgantown, W. Va.

Ghritlahre, H. K., and Prasad, R. K. (2018). “Investigation on heat transfer characteristics of roughened solar air heater using ANN technique.” *International Journal of Heat and Technology*, 36(1), 102-110.

Gokceoglu, C., Zorlu, K. (2004). “A fuzzy model to predict the uniaxial compressive strength and the modulus of elasticity of a problematic rock.” *Engineering Applications of Artificial Intelligence*, 17(1), 61-72.

Gokceoglu. (2002). “A fuzzy triangular chart to predict the uniaxial compressive strength of the Ankara agglomerates from their petrographic composition”. *Eng. Geol.*, 66, 39-51.

Gurocak, Z., Solanki, P., Alemdag, S., Zaman, M. M. (2012) “New Considerations for Empirical Estimation of Tensile Strength of Rocks”, *Engineering Geology*, 145, 1 – 8.

- Hagan, T.N, Reid, I.W. (1983). "Performance monitoring of production blasthole drills – a means of increasing blasting efficiency." *Second International Surface Mining and Quarrying Symposium*, 173 – 179.
- Hartman, H.L., and Mutmanský, J.M. (2002) *Introductory mining engineering*. John Wiley and Sons, New York, USA.
- Haykin S (1999) *Neural networks*, 2nd edn. Prentice-Hall, Englewood Cliffs.
- He, M., Li, N., Zhu, J., and Chen, Y. (2020). "Advanced prediction for field strength parameters of rock using drilling operational data from impregnated diamond bit." *Journal of Petroleum Science and Engineering*, 187, 106847.
- Hojdar, J. (1987). Open-pit mining of lignite in Czechoslovakia. *Continuous Surf. Min.:(United Kingdom)*, 1(1/3).
- Hornik, K., Stinchcombe, M., White, H. (1989). "Multilayer feed forward networks are universal approximators." *Neural networks*, 2(5), 359-366.
- Horsrud, P. (2001). Estimating mechanical properties of shale from empirical correlations. *SPE Drilling & Completion*, 16(02), 68-73.
- Howarth, D.F., Adamson, W.R., Berndt, J.R. (1986) "Correlation of model tunnel boring and drilling machine performances with rock properties." *Int J Rock Mech Min Sci.* 23, 171–175.
- Huang, S.L., Wang, Z.W., (1997) "The mechanics of diamond core drilling of rocks." *International Journal of Rock Mechanics and Mining Sciences*, 34, 3-4.
- İnce, İ., Bozdağ, A., Fener, M., and Kahraman, S. (2019). "Estimation of uniaxial compressive strength of pyroclastic rocks (Cappadocia, Turkey) by gene expression programming." *Arabian Journal of Geosciences*, 12(24), 1-13.
- ISRM (1973) "Suggested method for determining the point-load strength index". *ISRM Committee on Laboratory Tests, Document*, 1, 8-12.
- Itakura, K., Goto, T., Yoshida, Y., Tomita, S., Iguchi, S., Ichihara, Y., Mastalir, P. (2008) "Portable intelligent drilling machine for visualizing roof-rock geostructure." *Proceedings of Aachen international mining symposium*, Aachen, 597–609.

Itakura, K., Sato, K., Deguchi, G., Ichihara, Y., Matsumoto, H. (2001) “Visualization of geostructure by mechanical data logging of rock bolt drilling and its accuracy”. *Proceedings of 20th international conference on ground control in mining*. Lakeview Resort and Conference Center, Morgantown, 184–190.

Itakura, K., Sato, K., Deguchi, G., Ichihara, Y., Matsumoto, H., Eguchi, H. (1997) “Development of a roof-logging system by rock bolt drilling.” *Trans. Inst. Min. Metall. Sect. A Min.*, 106, A118–A12.

Kahraman, S. (2002) “Correlation of TBM and drilling machine performance with rock brittleness.” *Eng. Geol.*, 65, 269–283.

Kahraman, S. (2003) “Performance analysis of drilling machines using rock modulus ratio.”, *South African Institute of Mining and Metallurgy*, 103(8), 515-522.

Kahraman, S. A. İ. R. (2016). Estimating the penetration rate in diamond drilling in laboratory works using the regression and artificial neural network analysis. *Neural Processing Letters*, 43(2), 523-535.

Kahraman, S., Altun, H., Tezekici, B. S., Fener M.(2006) “Sawability prediction of carbonate rocks from shear strength parameters using artificial neural networks”, *International Journal of Rock Mechanics & Mining Sciences*, 43, 157–164.

Kahraman, S., Altun, H., Tezekici, BS., Fener M. (2006) “Estimating the Penetration Rate in Diamond Drilling in Laboratory Works Using the Regression and Artificial Neural Network Analysis.” *International Journal of Rock Mechanics & Mining Sciences*, 43, 157–164.

Kahraman, S., Balci, C., Yazici, C., Bilgin, N. (2000) “Prediction of the penetration rate of rotary blast hole drills using a new drillability index.” *International journal of rock mechanics and mining sciences*, 37(5), 729-743.

Kahraman, S., Bilgin, N., Feridunoglu, C. (2003) “Dominant rock properties affecting the penetration rate of percussive drills.” *International Journal of Rock Mechanics & Mining Sciences*, 40, 711–723.



- Kahraman, S., Gunaydin, O.(2008) “Indentation hardness test to estimate the Sawability of carbonate rocks.”, *Bull Eng geol Environ.* 67, 507-511.
- Kalantari, S., Hashemolhosseini, H., Baghbanan, A. (2018) “Estimating rock strength parameters using drilling data.” *International Journal of Rock Mechanics and Mining Sciences*, 104, 45-52.
- Karpuz, C., Pasamehmetoglu, A.G, Dincer, T., Muftuoglu, Y. (1990). “Drillability studies on the rotary blasthole drilling of lignite overburden series.” *Int. J. Surface Min.*, 4, 89-93.
- Kawasaki, S., Tanimoto, C., Koizumi, K., and Ishikawa, M. (2002). “An attempt to estimate mechanical properties of rocks using the Equotip hardness tester.” *Journal of the Japan Society of Engineering Geology*, 43(4), 244-248.
- Kawasaki, S., Yoshida, M., Tanimoto, C., and Masuya, T. (2000). "The development of property evaluation method for rock materials based on the simple rebound hardness test investigations on the effects of test conditions and fundamental properties." *Journal of the Japan Society of Engineering Geology* 41(4), 230-241.
- Kayabali, K., and Selcuk, L. (2010). “Nail penetration test for determining the uniaxial compressive strength of rock”. *International Journal of Rock Mechanics and Mining Sciences*, 47(2), 265-271.
- Khandelwal, M., Singh, T.N. (2009) “Correlating static properties of coal measures rocks with p-wave velocity.” *Int. J. Coal. Geol.* 79, 55–60.
- Khorzoughi, M. B., and Hall, R. (2016). “Processing of measurement while drilling data for rock mass characterization.” *International journal of mining science and technology*, 26(6), 989-994.
- Khoshouei, M., and Bagherpour, R. (2020). “Predicting the Geomechanical Properties of Hard Rocks Using Analysis of the Acoustic and Vibration Signals during the Drilling Operation.” *Geotechnical and Geological Engineering*, 1-13.

King, R. L., Hicks, M. A., Signer, S. P. (1993) "Using unsupervised learning for feature detection in a coal mine roof". *Engineering application of artificial intelligence*, 6(6), 565 – 573.

Kivade, S.B, Murthy, C.H.S.N., Vardhan, H. (2015) "ANN Models for Prediction of Sound and Penetration Rate in Percussive Drilling." *J. Inst. Eng. India Ser. D*, 96(2), 93–103.

Kivade, S.B, Murthy, C.H.S.N., Vardhan, H. (2015) "Experimental investigation on penetration rate of percussive drill." *Procedia earth and planetary science*, 11, 89-99.

Kolapo, P. (2020). "Investigating the effects of mechanical properties of rocks on specific energy and penetration rate of borehole drilling." *Geotechnical and Geological Engineering*, 1-12, <https://doi.org/10.1007/s10706-020-01577-y>.

Kumar, B. R., Vardhan, H., & Govindaraj, M. (2012). "Prediction of uniaxial compressive strength, tensile strength and porosity of sedimentary rocks using sound level produced during rotary drilling." *Rock mechanics & rock engineering*, 44(5), 613-620.

Kumar, B. R., Vardhan, H., and Govindaraj, M. (2011). "Sound level produced during rock drilling vis-à-vis rock properties." *Engineering geology*, 123(4), 333-337.

Kumar, B. R., Vardhan, H., Govindaraj, M., and Saraswathi, S. P. (2013a). "Artificial neural network model for prediction of rock properties from sound level produced during drilling." *Geomechanics and Geoengineering*, 8(1), 53-61.

Kumar, B. R., Vardhan, H., Govindaraj, M., and Vijay, G. S. (2013b). "Regression analysis and ANN models to predict rock properties from sound levels produced during drilling." *International Journal of Rock Mechanics and Mining Sciences*, 58, 61-72.

Kumar, C. V., Vardhan, H., and Murthy, C. S. (2019). "Quantification of rock properties using frequency analysis during diamond core drilling operations." *Journal of the Institution of Engineers (India): Series D*, 100(1), 67-81.

- Kumar, C. V., Vardhan, H., Murthy, C. S., and Karmakar, N. C. (2019) “Estimating rock properties using sound signal dominant frequencies during diamond core drilling operations.” *Journal of Rock Mechanics and Geotechnical Engineering*, 11(4), 850-859.
- Kumar, C. V., Vardhan, H., and Murthy, C. S. (2020). “Multiple regression model for prediction of rock properties using acoustic frequency during core drilling operations.” *Geomechanics and Geoengineering*, 15(4), 297-312.
- Lacharite, N. (1960). “A study to correlate the shearing, bending and compression properties of rock.” *Fuels and Min Pract Div, Mines Branch, Can Dept Mines and Tech Surv, Ottawa, IR, 60*.
- Lama, R. D., and Vutukuri, V. S. (1978). “Handbook on mechanical properties of rocks-testing techniques and results.” Vol. 3, No. 2.
- Leighton, J. C. (1982). “Development of a correlation between rotary drill performance and controlled blasting powder factors, Doctoral dissertation.” University of British Columbia.
- Leighton, J. C. (1983). “Correlating Rotary Drill Performance to Powder Factors for Improved Blasting Control.” *36th Cdn. In Geotech. Conf.*, Vancouver, BC, 4-10.
- Li, Z., Itakura, K. (2011a) “Fundamental research on drilling processes using drag bits.” *Adv. Mater. Res.* 243–249, 3612–3617.
- Li, Z., Itakura, K. (2011b) “Prediction of rock strength from mechanical data of drilling.” *Eskikaya S (editor), 22nd world mining congress and expo*, 407–412.
- Li, Z., Itakura, K. I., and Ma, Y. (2014). “Survey of measurement-while-drilling technology for small-diameter drilling machines.” *Electronic Journal of Geotechnical Engineering*, 19(2), 10267-10282.
- Li, Z., K. and Itakura, K., I. (2012) “An analytical drilling model of drag bits for evaluation of rock strength”, *Soils and Foundations*, 52 (2), 216-227.

Lopez, C., Lopez, E., Javier, F. (1995) "Drilling and Blasting of Rocks"; *CRC Press*: Boca Raton, FL, USA.

Lucifora, D. and Rafezim, H. (2013) "State of the art review: monitoring-while-drilling for mining applications." *Proceedings of the World Mining Congress (WMC)*, Montreal, QC, Canada, 11-15.

Luo, Y., Peng, S., Mirabile, B., Finfinger, G and Wilson. (2002). "Estimating rock strengths using drilling parameters during roof bolting operations-progress report." *Proceedings of 21<sup>st</sup> international conference on ground control in mining*. Morgantown, WV: West Virginia University, pp.288-293.

Majdi, A., Rezaei M. (2013) "Prediction of unconfined compressive strength of rock surrounding a roadway using artificial neural network." *Neural Computer & Applic.*, 23, 381–389.

Mazanti BB, Sowers GF. (1965) "Laboratory testing of rock strength." *Proceedings of the International Symposium on Testing Techniques for Rock Mechanics*. Seattle, Washington,. p. 207–27.

Minaeian, B., Ahangari, K. (2013) "Estimating uniaxial compressive strength based on P-wave and Schmidt hammer rebound using statistical method." *Arab. J. Geosci.* 6, 1925–193.

Minaeian, B., Ahangari, K. (2013) "Estimation of uniaxial compressive strength based on P-wave and Schmidt hammer rebound using statistical method"., *Arab. J. Geosci.*, 6, 1925-1931.

Mohamad, E. T., Armaghani, D. J., Momeni, E., & Abad, S. V. A. N. K. (2015). "Prediction of the unconfined compressive strength of soft rocks: a PSO-based ANN approach." *Bulletin of Engineering Geology and the Environment*, 74(3), 745-757.

Mohammadi, B., Ramezanzadeh, A. and Tokhmechi, B. (2017). "Studying empirical correlation between drilling specific energy and geo-mechanical parameters in an oil field in SW Iran." *Journal of Mining and Environment*, 8(3), 393-401.

- Momeni, E., Nazir, R., Jahed, Armaghani, D., Maizir, H. (2014) “Prediction of pile bearing capacity using a hybrid genetic algorithm-based ANN.” *Measurement* 57, 122–131.
- Moronkeji, D., Villegas, R., Shouse, R., and Prasad, U. (2017). “Rock strength prediction during coring operation.” *International Symposium of the Society of Core Analysts*, Vienna, Austria, 27.
- Moulenkamp, F., Grima, M. A. (1999) “Application of neural networks for the prediction of the unconfined compressive strength (UCS) from Equotip hardness.” *Int J Rock Mech Min Sci* 36(1), 29–39.
- Ojo, O. and Olaleye, B.M. 2002. “Strength characteristics of two Nigerian rocks.” *Global Journal of Pure and Applied Sciences*, 8(4), 543-52.
- Paone, J., Bruce, W. E, Virciglio, P.R. (1969) “Drillability studies-statistical regression analysis of diamond drilling.” U.S. *Department of the interior, Bureau of Mines, RI-6880*, 29.
- Peng, S.S, Tang, D.X, Mirabile, B., Luo, Y., Wilson, G. (2003) “Mine roof geology information system (MRGIS).” *Peng SS et al (eds) Proceedings of 22nd international conference on ground control in mining*, Morgantown, pp 127–135.
- Peng, S.S., Sasaoka, T., Tang, D., Luo, Y., Wilson, G. (2005b) “Mine roof geology information system—a method for quantitative void/fracture detection and estimation of rock strength for underground mine”. *Coal Age*, 44–49.
- Peng, S.S., Tang, D., Sasaoka, T., Luo, Y., Finfinger, G., Wilson, G. (2005a) “A method for quantitative void/fracture detection and estimation of rock strength for underground mine roof.” *Proceedings of 24th international conference on ground control in mining*, West Virginia Univ., Morgantown, W. Va., 195–197.
- Prasad, U. (2018) “Mechanical Specific Energy (MSE) in Coring: A Tool to Understand the Drilling Mechanism and Coring Parameters Optimization for Improved Core Recovery.” *AAPG International Conference and Exhibition*.

Proceq, S.A. (1977a) “Operating instructions concrete test hammer types N and NR.” Zurich, Switzerland.

Proceq, S.A. (1977b) “Equotip operations instructions,” 5th edn. PROCEQSA Zurich, Switzerland

Rabbani, E., Sharif, F., Koolivand, Salooki, M., Moradzadeh, A. (2012) “Application of neural network technique for prediction of uniaxial compressive strength using reservoir formation properties.” *Int J Rock Mech Min Sci.* 56, 100–111

Rafiq, M.Y., Bugmann, G, and Easter Brook, DJ (2001) “Neural network design for engineering applications.” *Comput.struct.*79, 1541-1552.

Rao, K.U.M., Bhatnagar, A., Misra, B. (1998) “Principles of Rock Drilling.” A.A.Balkema. Rotterdam.

Rao, K.U.M., Bhatnagar, A., Misra, B. (2002) “Laboratory investigations on rotary diamond drilling.” *Geotechnical & Geological Engineering*, 20, 1-16.

Reddish, D. J. and Yasar, E. (1997) “A new portable rock strength index test based on specific energy of drilling.” *Int. J. Rock Mech. & Min. Sci.* 33, 5, 543-548.

Rezaei, M., Majdi A., Monjezi, M. (2012) “An intelligent approach to predict unconfined compressive strength of rock surrounding access tunnels in long wall coal mining.” *Neural Comput Appl* 24(1), 233–241.

Romeo, G., Mele, F and Morelli, A (1995) “Neural networks and discrimination of seismic signals, *Comput.Geosci*, 21(2), 279-288.

Rostami, J., Kahraman, S., Naeimipour, A., & Collins, C. (2015). “Rock characterization while drilling and application of roof bolter drilling data for evaluation of ground conditions.” *Journal of Rock Mechanics and Geotechnical Engineering*, 7(3), 273-281.

Roy, S., Adhikari, G. R. (2007) “Worker Noise exposures from Diesel and Electric Surface Coal Mining Machinery” *Noise Control Engineering Journal*, 55(5), 434 – 437.

- Sabatini, P. J. (2002). Evaluation of soil and rock properties. *US Department of Transportation*, Office of Bridge Technology, Federal Highway Administration.
- Sarkar, K., Tiwary, A., Singh, T.N. (2010) Estimation of strength parameters of rock using artificial neural networks. *Bull Eng Geol Environ* 69, 599–606.
- Schmidt, E. (1951). A non destructive concrete tester. *Concrete*, 59, 34-35.
- Schunnesson, H. (1996). “RQD predictions based on drill performance parameters.” *Tunnelling and Underground Space Technology*, 11(3), 345-351.
- Schunnesson, H. “Drill process monitoring in percussive drilling: A multivariate approach to data analysis.” Licentiate Thesis, University of Technology, Lulea, Sweden, 1990.
- Scoble, M. J. and Peck, J. (1987) “A technique for ground characterization using automated production drill monitoring.” *International Journal of Surface Mining, Reclamation and Environment*, 1, 1, 41-54.
- Scoble, M. J., Peck, J., Hendricks, C. (1989) “Correlation between rotary drill performance parameters and borehole geophysical logging.” *Min. Sci. Technol.*, 8, 301–312.
- Shankar, V.K., Kunar, B.M., Murthy, C.S. (2020). “Measurement of bit-rock interface temperature and wear rate of the tungsten carbide drill bit during rotary drilling”. *Friction* 8, 1073–1082.
- Singh, T.N., Kanchan, R., Saigal, K., Verma, A.K. (2004) “Prediction of P-wave velocity and anisotropic properties of rock using artificial neural networks technique.” *J Sci Ind Res* 63(1), 32–38.
- Singh, V.K., Singh, D., Singh, T.N. (2001) “Prediction of strength properties of some schistose rocks from petrographic properties using artificial neural networks.”, *International Journal of Rock Mechanics and Mining Sciences*, 38(2), 269-284.
- Sonmez, H., Gokceoglu, C., Nefeslioglu, H.A., Kayabasi, A. (2006) “Estimation of rock modulus: for intact rocks with an artificial neural network and for rock masses with a new empirical equation.” *Int J Rock Mech Min Sci*, 43, 224–235.

Stacey, T.R. (1980) “A simple device for the direct shears strength testing of intact rock.” *J South African Inst Min Metall*; 80(3), 129–30.

Stoxreiter, T., Portwood, G., Gerbaud, L., Seibel, O., Essl, S., Plank, J. and Hofstätter, H. (2019). “Full-scale experimental investigation of the performance of a jet-assisted rotary drilling system in crystalline rock.” *International Journal of Rock Mechanics and Mining Sciences*, 115, 87-98.

Sulukcu, S., and Ulusay, R. (2001). “Evaluation of the block punch index test with particular reference to the size effect, failure mechanism and its effectiveness in predicting rock strength”. *International Journal of Rock Mechanics and Mining Sciences*, 38(8), 1091-1111.

Szlavin, J. (1974) “Relationships between some physical properties of rock determined by laboratory tests.” In *International Journal of Rock Mechanics and Mining Sciences & Geomechanics Abstracts*, 11(2), 57-66.

Szwedzicki, T. (1998). “Indentation hardness testing of rock.” *International Journal of Rock Mechanics and Mining Sciences*, 35(6), 825-829.

Tang, D. X., Peng, S. S., Luo, Y., & Wilson, G. (2004). “Void prediction in mine roof geology information system (MRGIS).” *Transactions-society for mining metallurgy and exploration incorporated*, 316, 171.

Tang, X. (2006) “Development of real time roof geology detection system using drilling parameters during roof bolting operation.” PhD Dissertation, Dept. of Mining Engineering, College of Engineering and Mineral Resources, West Virginia University.

Teale R. (1965) “The Concept of Specific Energy in Rock Drilling.” *International Journal of Rock Mechanics and Mining Sciences*, 2. 57-73. Pergamon Press 1965. Printed in Great Britain.

Telgarsky, R. (2013). “Dominant frequency extraction.” *arXiv preprint arXiv:1306.0103*.



Tiryaki, B. (2008) "Predicting intact rock strength for mechanical excavation using multivariate statistics, artificial neural networks, and regression trees." *Eng. Geol.* 99, 51–60.

Tiryaki, B., Dikmen, A.C. (2006) "Effects of rock properties on specific cutting energy in linear cutting of sandstones by picks." *Rock Mech. Rock Eng.* 39 (2), 89–120.

Ulusay R., Hudson J.A. (2007) "The complete ISRM suggested methods for rock characterization, testing and monitoring: 1974–2006." *International Society for Rock Mechanics (ISRM)*.

Ulusay, R, Gokceoglu, Sulukcu, C. (2001). "Draft ISRM suggested method for determining block punch strength index (BPI)." *International journal of rock mechanics and mining sciences*, 38(2001), 1113-1119.

Ulusay, R. (Ed.). (2014). *The ISRM suggested methods for rock characterization, testing and monitoring: 2007-2014*. Springer.

Verwaal, W., and A. Mulder (1993) "Estimating rock strength with the Equotip hardness tester." *International Journal of Rock Mechanics and Mining Sciences and Geomechanics Abstracts*, 30(6), 659-662.

Wong, T. F., David, C., and Zhu, W. (1997). "The transition from brittle faulting to cataclastic flow in porous sandstones: Mechanical deformation." *Journal of Geophysical Research: Solid Earth*, 102(B2), 3009-3025.

Yagiz, S., Gokceoglu, C., Sezer, E., Iplikci, S. (2009) "Application of two non-linear prediction tools to the estimation of tunnel boring machine performance." *Eng Appl Artif Intell* 22(4), 808–814.

Yagiz, S., Sezer, E.A., Gokceoglu, C. (2012) "Artificial neural networks and nonlinear regression techniques to assess the influence of slake durability cycles on the prediction of uniaxial compressive strength and modulus of elasticity for carbonate rocks." *Int J Numer Anal Methods* 36, 1636–1650.

Yarali, O., Soyer, E. (2013) "Assesment of relationship between drilling rate and mechanical properties of rocks." *Tunn. Undergr. Sp. Technol.* 33, 46–53.

Yari, M., Bagherpour, R. (2018 a). "Implementing acoustic frequency analysis for development the novel model of determining geomechanical features of igneous rocks using rotary drilling device." *Geotechnical and Geological Engineering*, 36(3), 1805-1816.

Yari, M., Bagherpour, R. (2018 b). "Investigating an innovative model for dimensional sedimentary rocks characterization using acoustic frequencies analysis during drilling." *The Mining-Geology-Petroleum Engineering Bulletin*, 33(2), 17-25.

Yasar, E., Ranjit, P.G., Viète, D.R. (2011) "An experimental investigation into the drilling and physico-mechanical properties of a rock-like brittle material." *Journal of petroleum science and engineering*, 76, 185-193.

Yaşar, E., Ranjith, P. G., and Viète, D. R. (2011). "An experimental investigation into the drilling and physico-mechanical properties of a rock-like brittle material." *Journal of Petroleum Science and Engineering*, 76(3-4), 185-193.

Yenice, H. (2019). "Determination of Drilling Rate Index Based on Rock Strength Using Regression Analysis." *Anais da Academia Brasileira de Ciências*, 91(3).

Yilmaz, I., Yuksek, A.G. (2008) "An example of artificial neural network (ANN) application for indirect estimation of rock parameters." *Rock Mech Rock Eng* 41(5), 781–795.

Yilmaz, I., Yuksek, A.G. (2009) "Prediction of the strength and elasticity modulus of gypsum using multiple regression, ANN, and ANFIS models." *Int J Rock Mech Min Sci* , 46(4), 803–810.

Zarin, P, H., (2014). "Application of artificial intelligence hybrid models in improving formation absolute permeability predictions from well log data." *Petroleum University of Technology, Ahvaz*.

Zhang, L. (2005) "Engineering properties of rocks." Elsevier Ltd, Amsterdam

Zorlu, K., Gokceoglu, C., Ocakoglu, F., Nefeslioglu, H.A., Acikalin, S. (2008). "Prediction of uniaxial compressive strength of sandstones using petrography-based models." *Eng. Geol.* 96(3), 141-158.







# ***ANNEXURE***

## ANNEXURE-I

TABLE 1.1 Drilling responses measured considering various drill operating parameters during the drilling of shale

PR (mm/min)	SS (r.p.m.)	DD (mm)	T (N)	TQ (N-m)	Z (Hz)
3	400	12	345	4	327
4	400	12	358	5	327
5	400	12	364	5	328
3	500	12	324	4	425
4	500	12	332	3	425
5	500	12	336	4	426
3	600	12	294	3	542
4	600	12	298	3	542
5	600	12	300	3	543
3	400	16	414	5	328
4	400	16	425	6	328
5	400	16	439	6	329
3	500	16	386	5	425
4	500	16	405	5	425
5	500	16	412	5	427
3	600	16	352	5	542
4	600	16	387	5	542
5	600	16	378	5	543
3	400	20	447	6	329
4	400	20	459	7	329
5	400	20	479	8	329
3	500	20	409	6	428
4	500	20	431	7	429
5	500	20	435	7	430
3	600	20	380	6	544
4	600	20	405	6	543
5	600	20	412	6	545



TABLE 1.2 Drilling responses measured considering various drill operating parameters during the drilling of sandstone-1

PR (mm/min)	SS (r.p.m.)	DD (mm)	T (N)	TQ (N-m)	Z (Hz)
3	400	12	396	4	330
4	400	12	415	5	330
5	400	12	432	6	331
3	500	12	372	4	428
4	500	12	381	5	428
5	500	12	392	5	429
3	600	12	338	6	545
4	600	12	342	6	545
5	600	12	361	6	546
3	400	16	476	7	331
4	400	16	488	8	331
5	400	16	504	8	332
3	500	16	443	7	428
4	500	16	465	7	428
5	500	16	484	6	430
3	600	16	404	7	545
4	600	16	445	7	545
5	600	16	468	7	546
3	400	20	514	8	332
4	400	20	527	8	332
5	400	20	550	9	332
3	500	20	470	8	431
4	500	20	495	8	432
5	500	20	500	8	433
3	600	20	437	7	547
4	600	20	465	6	546
5	600	20	473	7	548

TABLE 1.3 Drilling responses measured considering various drill operating parameters during the drilling of sandstone-2

PR (mm/min)	SS (r.p.m.)	DD (mm)	T (N)	TQ (N-m)	Z (Hz)
3	400	12	514	5	333
4	400	12	539	6	333
5	400	12	554	8	334
3	500	12	483	5	431
4	500	12	491	6	431
5	500	12	512	6	432
3	600	12	439	8	548
4	600	12	435	7	548
5	600	12	469	4	549
3	400	16	499	8	334
4	400	16	560	9	334
5	400	16	529	11	335
3	500	16	465	10	431
4	500	16	488	10	431
5	500	16	532	9	433
3	600	16	424	10	548
4	600	16	466	9	548
5	600	16	486	9	549
3	400	20	560	10	335
4	400	20	580	11	335
5	400	20	603	12	335
3	500	20	526	11	434
4	500	20	535	10	435
5	500	20	548	11	436
3	600	20	465	10	550
4	600	20	474	9	549
5	600	20	502	10	551

TABLE 1.4 Drilling responses measured considering various drill operating parameters during the drilling of sandstone-3

PR (mm/min)	SS (r.p.m.)	DD (mm)	T (N)	TQ (N-m)	Z (Hz)
3	400	12	534	5	336
4	400	12	558	5	336
5	400	12	576	8	337
3	500	12	502	5	434
4	500	12	525	5	434
5	500	12	545	6	435
3	600	12	456	8	551
4	600	12	470	7	551
5	600	12	487	7	552
3	400	16	547	8	337
4	400	16	574	9	337
5	400	16	590	10	338
3	500	16	514	9	434
4	500	16	535	10	434
5	500	16	560	9	436
3	600	16	467	10	551
4	600	16	463	9	551
5	600	16	499	9	552
3	400	20	557	10	338
4	400	20	584	11	338
5	400	20	635	13	338
3	500	20	524	10	437
4	500	20	532	10	438
5	500	20	578	8	439
3	600	20	476	8	553
4	600	20	498	9	552
5	600	20	512	10	553

TABLE 1.5 Drilling responses measured considering various drill operating parameters during the drilling of limestone-1

PR (mm/min)	SS (r.p.m.)	DD (mm)	T (N)	TQ (N-m)	Z (Hz)
3	400	12	582	6	338
4	400	12	600	5	338
5	400	12	627	8	339
3	500	12	543	5	436
4	500	12	572	5	436
5	500	12	594	6	437
3	600	12	485	8	553
4	600	12	512	8	553
5	600	12	530	9	554
3	400	16	614	8	339
4	400	16	641	9	339
5	400	16	659	10	340
3	500	16	577	9	436
4	500	16	603	11	436
5	500	16	621	10	438
3	600	16	524	10	553
4	600	16	540	9	553
5	600	16	550	9	554
3	400	20	630	10	340
4	400	20	658	11	340
5	400	20	679	15	340
3	500	20	592	10	439
4	500	20	619	11	440
5	500	20	664	8	441
3	600	20	538	8	555
4	600	20	554	10	554
5	600	20	574	10	555

TABLE 1.6 Drilling responses measured considering various drill operating parameters during the drilling of limestone-2

PR (mm/min)	SS (r.p.m.)	DD (mm)	T (N)	TQ (N-m)	Z (Hz)
3	400	12	634	6	342
4	400	12	654	6	340
5	400	12	683	9	341
3	500	12	591	6	438
4	500	12	612	5	438
5	500	12	647	6	439
3	600	12	528	9	555
4	600	12	558	7	555
5	600	12	577	9	556
3	400	16	646	8	341
4	400	16	666	10	341
5	400	16	695	10	342
3	500	16	602	9	438
4	500	16	634	12	438
5	500	16	659	11	440
3	600	16	523	10	555
4	600	16	568	9	555
5	600	16	588	9	556
3	400	20	651	10	342
4	400	20	672	11	342
5	400	20	702	17	342
3	500	20	608	16	441
4	500	20	640	17	442
5	500	20	665	12	443
3	600	20	543	15	557
4	600	20	564	13	556
5	600	20	593	12	559

***LIST OF  
PUBLICATIONS***

## LIST OF PUBLICATIONS BASED ON PH.D. RESEARCH WORK

### Journals

1. **Lakshminarayana, C.R.**, Tripathi, A.K. & Pal, S.K. (2021) “Experimental investigation on potential use of drilling parameters to quantify rock strength.” *International journal of Geo-engineering* (**Springer - SCOPUS – Accepted**).
2. **Lakshminarayana, C.R.**, Tripathi, A.K. & Pal, S.K. (2020). “Rock strength characterization using measurement while drilling technique.” *Indian Geotech J* 50, 994–1005. <https://doi.org/10.1007/s40098-020-00441-3> (**Springer-SCOPUS**).
3. **Lakshminarayana, C.R.**, Tripathi, A.K. & Pal, S.K. (2020) “Prediction of Mechanical Properties of Sedimentary Type Rocks Using Rotary Drilling Parameters.” *Geotech Geol Eng* 38, 4863–4876. <https://doi.org/10.1007/s10706-020-01332-3> (**Springer - SCOPUS**).
4. **Lakshminarayana, C.R.**, Tripathi, A.K. & Pal, S.K. (2019). “Estimation of Rock Strength Properties Using Selected Mechanical Parameters Obtained During the Rotary Drilling.” *J. Inst. Eng. India Ser. D.* 100, 177–186. <https://doi.org/10.1007/s40033-019-00197-y> (**Springer - SCOPUS**).

### Conferences

1. **Lakshminarayana, C.R.**, Tripathi, A.K. & Pal, S.K., presented & published a research paper entitled “Quantification of Rock Strength Using the Mechanical Drilling Parameters” , in the International Conference on Emerging Trends in Engineering (ICETE19), organised by University college of Engineering, Osmania University, Hyderabad from 22nd to 23rd March 2019. (**Springer**).
2. **Lakshminarayana, C.R.**, Tripathi, A.K. & Pal, S.K., presented & published a research paper entitled “MWD technique to estimate the uniaxial compressive strength of rock” in the International Conference on emerging Research in Civil Mechanical and Aeronautical Engineering (ERCAM2019), organised by NMIT, Bengaluru from 24th to 26th July 2019, (**AIP Conference Proceedings-Scopus indexed**).





# ***BIO-DATA***

## BIO-DATA

1. Name : Lakshminarayana C.R.
2. Father's Name : Ramaiah K.R.
3. Date of Birth : 23-03-1977
4. Nationality : Indian
5. Marital Status : Married
6. Present Position : Research Scholar
7. Address for Communication : # 354,1<sup>St</sup> Cross  
Shankerpura  
Chickmagalur district  
Chickmagalur-577101  
Karnataka  
India
8. Mobile : +91-8073208137
9. E-mail : crlaks042@gmail.com
10. Academic qualifications :

Degree	University/board	Year
M.Tech (Mechanical Engineering)	V.T.U., Karnataka	2014
B.E. (Mechanical Engineering)	Mysore University, Karnataka	2004

